RESIDENTIAL BATTERY ENERGY STORAGE SYSTEMS FOR RENEWABLE ENERGY INTEGRATION AND PEAK SHAVING

by

Jason Claude Ryan Leadbetter

Submitted in partial fulfilment of the requirements
for the degree of Master of Applied Science

at

Dalhousie University
Halifax, Nova Scotia
August 2012

DALHOUSIE UNIVERSITY

DEPARTMENT OF MECHANICAL ENGINEERING

The undersigned hereby certify that they have read and recommend to the Faculty of Graduate Studies for acceptance a thesis entitled "RESIDENTIAL BATTERY ENERGY STORAGE SYSTEMS FOR RENEWABLE ENERGY INTEGRATION AND PEAK SHAVING" by Jason Claude Ryan Leadbetter in partial fulfilment of the requirements for the degree of Master of Applied Science.

Dated: August 14, 2012

Supervisor: _____

Readers: _____

_____

DALHOUSIE UNIVERSITY

DATE: August 14, 2012

AUTHOR: Jason Claude Ryan Leadbetter

TITLE: RESIDENTIAL BATTERY ENERGY STORAGE SYSTEMS FOR RENEWABLE ENERGY INTEGRATION AND PEAK SHAVING

DEPARTMENT OR SCHOOL: Mechanical Engineering

DEGREE: MASc CONVOCATION: October YEAR: 2012

_____

Signature of Author

Table of Contents

List of Tables

List of Figures

Abstract

Renewable energy integration will become a significant issue as renewable penetration levels increase, and will require new generation support infrastructure; Energy storage provides one solution to this issue. Specifically, battery technologies offer a wide range of energy and power output abilities, making them ideal for a variety of integration applications. Distributed energy storage on distribution grids may be required in many areas of Canada where renewables will be installed. Peak shaving using distributed small (residential) energy storage can provide a reduction in peak loads and help renewable energy integration. To this end, a peak shaving model was developed for typical houses in several regions in Canada which provided sizing and performance results. An experimental battery bank and cycling apparatus was designed and constructed using these sizing results. This battery bank and cycling apparatus was then used to calibrate and validate a lithium iron phosphate battery energy storage system model.

List of Abbreviations and Symbols Used

Abbreviations

AGM – Absorbed Glass Mat (lead acid battery type)
AL – Appliances and Lighting
BESS – Battery Energy Storage System
CAES – Compressed Air Energy Storage
CC/CV – Constant Current/Constant Voltage (battery charge profile)
CHREM – Canadian Hybrid Residential End-Use Energy and GHG Emissions Model
DHW – Domestic Hot Water
DOD – Depth of Discharge (1-SOC)
E/P – Energy to Power ratio
EDLC – Electric Double Layer Capacitor
ESA – Electricity Storage Association
FACTS – Flexible AC Transmission System (devices)
FW – Flywheel (energy storage technology)
LFP – Lithium Iron Phosphate (Battery)
Li-ion – Lithium Ion (battery)
NA-S – Sodium Sulfur (battery)
Pb-A – Lead Acid (battery)
PHS – Pumped Hydro Storage
SC – Space Cooling
SH – Space Heating
SOC – State of Charge
VRB – Vanadium Redox Battery
VRLA – Valve Regulated Lead Acid (battery)

Symbols

α – SOC scaling factor used in the developed battery model
η – One-way system efficiency
E_B –Stored energy remaining in the battery
P_H – House electricity demand (power)
P_G – Grid demand (power)
P_{Inv} – Inverter output power
$P_{Inv,Max}$ – Inverter maximum power output
$P_{G,Limit}$ – Grid demand limit (power)
t – time of day
Δt – time-step length

Acknowledgements

I would first like to thank my supervisor Dr. Lukas Swan. It is with his support, expertise, enthusiasm, and limitless motivation that I have gained so much through these years of my Master's degree. Such drive for knowledge and progress in both research and real-world change is rare and truly inspiring. He not only offered excellent academic guidance, but also provided me countless opportunities to grow as a both an engineer and a person. Lukas also provided me with funding during the first year of my program when I had not yet received my NSERC grant. I will be forever thankful of the opportunity to work with Lukas, and look forward to applying all that he has taught me. I am truly grateful for the support Lukas has given me and the skills I have gained from working with him.

Several companies provided materials in support of this research. Both ZENN Motor Company and Surrette Battery Company provided batteries in support of this research. DHS Engineering provided several items come of which included chargers and a motor controller. The electrical Engineering Department at Dalhousie also provided equipment in support of my research. Without the support of these groups, my research would not have been possible, and for their support I am very grateful. To my supervisory committee, I am thankful for your advice, consideration, and expertise.

I would also like to thank all of those in the Mechanical Engineering department who have helped me along the way including Ted Hubbard, Darrell Doman, Jon Macdonald, Peter Jones, Mark MacDonald, Albert Murphy, Angus MacPherson, Morgyn MacLeod, Sandra Pereira, and Michelle Avery. Thanks to Nathaniel Pierre from the University of Delaware for the assistance he provided with MatLab coding.

I would like to thank the Natural Sciences and Engineering Research Council of Canada for funding of my research through a CGS-M grant.

CHAPTER 1 INTRODUCTION

1.1 ELECTRICITY DEMAND AND RENEWABLE INTEGRATION

The operation of electricity grids requires generating resources capable of supporting rapid short term variations (sub-second to seconds), medium term semi-predictable variations (minutes to hours), long-term (hours to days) trends, and seasonal variations [1]. Addressing these rapid and medium term variations can be difficult and requires the use of fast-responding generators such as natural gas turbines. These variations can be very large on an individual basis; however, through aggregation of demands the fluctuations become less frequent and are of lesser magnitude. An example of this is shown in Figure 1 where a single house demand is plotted against the demand of the entire NS electricity grid.

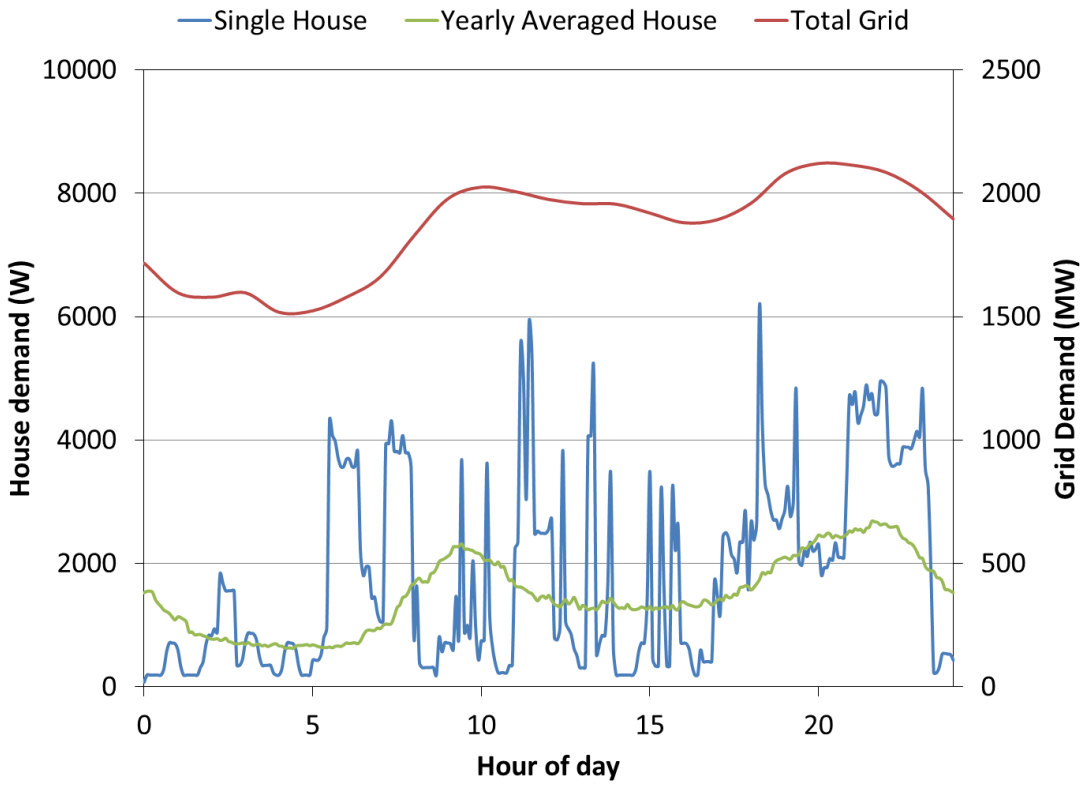

Figure 1: Simulated house demand (Jan 1, single house), Simulated annual average hourly house demand, and total grid demand (Nova Scotia grid load Jan 1, 2011 from: [2]**)**

The total grid demand is obviously smoother, however the variations in demand are not entirely eliminated. The house yearly averaged profile is also included in this plot to demonstrate that the average residential peaks correspond with the two daily peaking events in the electricity grid. Nearly 32% of all electricity consumed in Canada is consumed by the residential sector [3]. The concurrent peaks of the house yearly averaged profile and the large percentage of electricity consumed suggest that residential peak loads are a large contributor to overall peak loads. Despite the averaging effects of aggregating many houses together, building occupant behavior and heating/cooling requirements will always lead to periods of the day when demand is much higher than other times of the day. It is also of note that the total grid load plotted in Figure 1 is an hourly average grid load value; higher resolution data would show results similar to those in Figure 2.

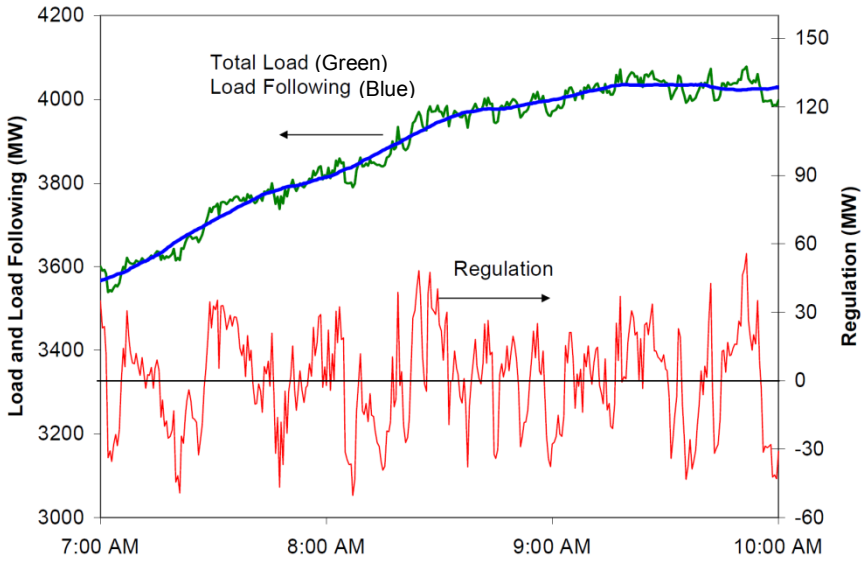

Figure 2: Rapid variation in grid demand [4]

The process of dealing with the rapid fluctuations in Figure 2 is referred to as regulation and is handled by fast responding generators operating at partial load.

With the global push towards increased levels of renewable energy resources [5-7], the impact these resources have on electricity grid must be considered. The generation

profiles of individual renewable resources as well as the aggregate generation corresponding to equal capacity combinations of each resource are plotted in Figure 3.

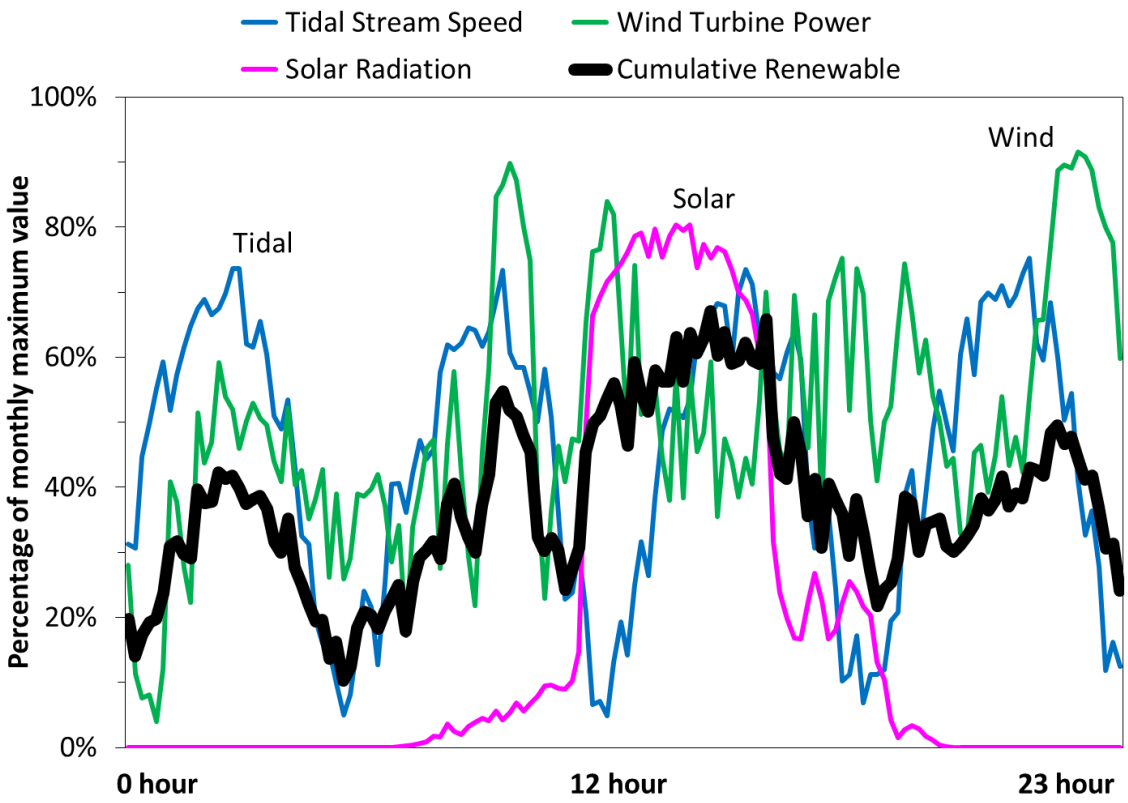

Figure 3: Example single day renewable generation profiles (equal installed capacity scenario simulation)

Again, aggregation makes the profiles somewhat more smoothed and more predictable. Unfortunately, the generation profile still displays both large swings in output levels and short-term rapid fluctuations. It is these increased variation levels that create operational issues for the existing electricity grids. Historically, stable operation of the electricity grid was accomplished through the use of regulation generators, spinning reserves, supplemental reserves, and replacement reserves [4, 8]. As more and more intermittent renewable energy resources are added to the electricity grid, issues will arise that historical grid control methods can no longer address and thus alternatives must be considered [1]. At low penetration levels of intermittent renewable energy resources (wind, solar, tidal) the impact is not significant, and creates very little additional cost. As

penetration levels increase, integration costs increase due to additional need for spinning reserves, supplemental reserves, and additional infrastructure [9].

There are several possible solutions to the issues arising from renewable energy integration, many of which can be used in combination with one another to reduce overall integration costs and minimize operational difficulties [10]. A first solution is to limit installation of intermittent renewable resources. Obviously this is not viable considering the need for renewable energy sources and the present trends in renewable installations. At high levels of penetration spinning reserve become highly inefficient and costly, and renewable resources must be curtailed to prevent grid stability and equipment limitation issues [1]. A second solution is thus to install a large number of the intermittent generation sources, and curtail the output of the generators through blade pitching (wind/tidal) or panel disconnection (solar); however such action is very unfavorable in terms of economics [1] and would require central operator control of wind, solar, and tidal fields. Demand side management is a third possible solution that has been studied in many regions [11-14]. Unfortunately, demand-side management using heating/appliance load scheduling can only modify demand so much before it begins to negatively impact operation of the systems in houses and commercial buildings and directly affect the occupants.

As an alternative solution, bi-directional energy storage may be used to provide these grid support services. Energy storage does not require fossil fuel use during operation, limit renewable uptake, or negatively impact operation of homes or businesses.

1.2 Energy Storage for Renewable Integration and Grid Support

Energy storage is already in use in many electricity grids. Nearly all present energy storage capacity consists of pumped hydro storage stations [15]. These require vast storage areas, specific geographical features, and large capital investment. As a result, they are located centrally and connect directly to high capacity, high-voltage transmission infrastructure. Small distribution grids and weak transmission lines do not directly benefit from these large, central storage facilities, particularly when the intermittent generators

are installed near the end of the line on such distribution grids. To address these issues, smaller distributed storage systems are required [16, 17].

There are a variety of energy storage technology options available including numerous battery chemistries, flywheels, compressed air, hydrogen, and capacitors. Batteries are the focus of this thesis, primarily because they cover a large range of power and energy storage capabilities, are unconstrained by geography, suffer low parasitic losses, are reasonably efficiency, can be distributed across the grid, are mature (in some cases), and are modular and scalable [18-20]. The other technologies lack one or more of these characteristics that are crucial for distributed deployment within buildings, and therefore were not selected as the main topic of this thesis.

Peak shaving is one example of a grid support service that can be provided using energy storage systems and is the focus of this thesis. The goal of peak shaving is to reduce peak electricity grid demand in order to operate the electricity grid in a more efficient, and controlled manner. Figure 4 shows an exaggerated result of peak shaving on overall electricity grid load where the overnight hours load is increased and the daytime peaks are reduced.

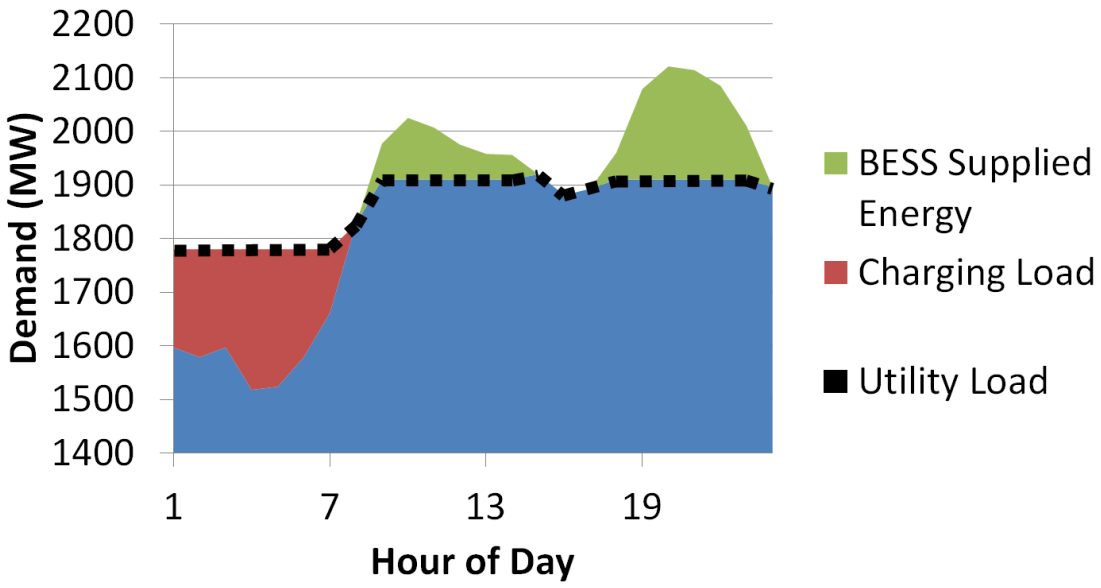

Figure 4: Peak Shaving Operation

1.3 RESEARCH OBJECTIVES

Given the developing need for distributed energy storage [16, 17], the sector targeted for this research is the residential sector. Residential demand is nearly ubiquitous across the electricity grid making it an excellent target for distributed energy storage systems. Many weak distribution grids exist purely to service the sprawling rural communities throughout Canada, and these are the areas that will require the most grid support to enable the installation of intermittent renewable resources. With the recent introduction of feed-in-tariffs in many areas [21, 22], government is actively encouraging the development of intermittent renewable resources on a community scale basis, which will only accelerate the need for integration technologies. The residential sector is also largely responsible for the uncontrollable peak loads due to heating, cooling, and appliances, and is charged on the basis of energy, not demand [23]. This thesis is divided into several chapters. The first half discusses the need for energy storage, the available storage technologies, and the technology applications and new modeling/simulation work. The later half describes the experimental work conducted including calibration and validation of a battery model that is used with the model presented in the earlier chapters.

Chapter 2 presents a comprehensive literature review examining over 90 battery and renewable integration studies to determine the most appropriate battery technologies for various uses and services required to enable renewable integration. The chapter first deals with the nature of electricity grids and renewable resources. The range of applications of batteries and the advantages of the various battery and non-battery energy storage technologies are discussed in detail. A thorough examination of the characteristics of various battery technologies, their present state of development, existing installations, and active research areas are presented. Based on these discussions, recommendations are made as to appropriate applications for the major battery types.

Chapter 3 presents an energy storage scoping study to determine the capacity, power, and cycle life required for building energy storage for peak shaving applications. The use of peak shaving systems distributed across many homes can help reduce overall peak grid demand. Peak demand periods are the highest operating cost periods for electricity grids, and with the addition of renewable resources the grid operation during these peak periods

will become even more difficult. Although peak shaving does not directly address integration of renewable resources, peak shaving will indirectly assist in integration by supporting the grid at critical time periods when instability and power shortages are most likely to occur. The chapter presents the generation of realistic electricity profiles using ESP-r and additional data sources, as well as the scoping peak shaving battery energy storage system (BESS) model developed in MatLab. The MatLab model is then used to provide the fundamental sizing parameters used in development of both the experimental BESS and the advanced battery model.

Chapter 4 presents a detailed discussion of the design, construction, and operation of an experimental BESS whose sizing parameters were based on the results presented in Chapter 3. The experimental BESS is composed of a battery bank, discharge system, charge system, and a measurement and control system. The system is capable of continuously variable discharge rates up to 5.2 kW and charge rates up to 2.7 kW. Individual cell measurement is included for battery safety and high accuracy pack measurements were used to enable the development of the battery model. The system is completely customizable using CRBasic with the CR1000 controller.

Chapter 5 presents a new implementation of an existing lithium-ion battery model. The existing battery model was developed for lithium cobalt batteries [24] and the new implementation of the model is for lithium iron phosphate (LFP) batteries. LFP batteries have a significantly lower voltage (~20%), less energy density (~25% less), and more power capability (~8 times) than lithium cobalt batteries [18]. As such, this represents new modeling work for lithium ion batteries. The model requires experimental data for calibration and through the use of the experimental BESS presented in Chapter 4 the calibration data was obtained. The model utilizes discharge curve scaling and an internal resistance value to adapt a reference discharge curve to meet various discharge rates. The model is both calibrated and validated using the experimental BESS and further simulation of peak shaving operation is conducted to update and confirm results obtained in Chapter 3.

Overall, the work presented in the following chapters advances the state of knowledge of building level energy storage systems for renewable integration with the electricity grid

and electricity peak shaving. An up to date review and analysis of renewable integration requirements is presented, as well as a thorough examination of the state of development of several leading edge battery technologies. Based on this review of the state-of-the-art in energy storage and renewable integration, specific and well-supported recommendations for appropriate battery technologies for various integration applications are made. Peak shaving is selected as the addressed service based on consideration of the need for distributed storage, and a new peak shaving model is developed. Peak shaving for five major Canadian regions were simulated and the results were then used to design/build a fully controllable and full-scale experimental BESS that was then used for experimental calibration and validation of a new battery model.

CHAPTER 2 SELECTION OF BATTERY TECHNOLOGY TO SUPPORT GRID-INTEGRATED RENEWABLE ELECTRICITY

This chapter has been published as:

J. Leadbetter and L. G. Swan. Selection of battery technology to support grid-integrated renewable electricity. J. Power Sources 216(0), pp. 376. 2012. Available: http://dx.doi.org/10.1016/j.jpowsour.2012.05.081

It is reprinted here under the terms of the license agreement with Elsevier B.V. The copyright license agreement in provided in APPENDIX A.

Jason Leadbetter is the principal researcher and author of the article. He conducted the research as part of his MASc. Thus, while he received supervision and guidance from his supervisor Dr. Swan, he carried out the work, wrote the published article, communicated with the editor of the journal, and carried out the necessary revisions before publication. Writing support in the form of editing assistance and content guidance was provided by Lukas Swan. Minor grammatical changes have been made to integrate the article within this thesis.

2.1 INTRODUCTION

It is well established that dependence on fossil fuel resources creates vulnerability to price fluctuations in international fuel markets and leads to anthropogenic greenhouse gasses causing human induced global warming. With a peak in global oil production likely occurring before 2020, the pressure to use alternative energy sources is greater than ever [25]. Governments around the world are developing aggressive renewable energy and electricity plans focused on increasing the installed capacity of wind, solar, and other intermittent renewable generation devices (e.g. in-stream tidal).Worldwide wind turbine generating capacity grew from 17,400 MW in the year 2000 to 197,039 MW in the year 2010 and continues to show exponential growth rates worldwide [5]. Solar energy is observing similar growth with cumulative global installed photovoltaic capacity doubling since the year 2007 to 39,800 MW at the end of the year 2010 [6, 7]. With such rapid growth of these technologies, the implications of high penetration levels of renewable generation must be carefully considered.

To consider the impact intermittent renewable generation has on the existing electricity grid Figure 5 gives a time series plot of measured values of electricity demand and several renewable generation types within Nova Scotia, Canada. Electricity demand is the total provincial load on the electricity grid[1]; tidal stream speed is approximated as the time derivative of tide height in the Bay of Fundy[2]; wind turbine power is the output of a single 0.8 MW rated wind turbine in the Cobequid Mountains[3]; solar radiation is the total incident upon a collector inclined 45 degrees and facing due south at Dalhousie University[4]; and cumulative renewable represents the combined output of the three renewable energy types. All values are normalized by maximum monthly value and are based on ten minute averages with the exception of one hour electricity demand.

Figure 5 shows electricity demand fluctuating with higher daytime and lower nighttime values. The three renewable resources are distinct with tidal being sinusoidal, wind being stochastic, and solar occurring only during daytime. It is evident from the cumulative renewable profile that using several renewable resources has a smoothing effect, although it does not mitigate peaks or valleys and does not align with the electricity demand.

[1]Nova Scotia Power Incorporated. Hourly Total Net Nova Scotia Load.http://oasis.nspower.ca/en/home/default/monthlyreports/hourly_ns.aspx
[2]Fisheries and Oceans Canada. Saint John Station #65 Tide and Water Level Archive. http://www.charts.gc.ca/twl-mne/index-eng.asp
[3]Colchester-Cumberland Wind Field Incorporated. Contact Lukas Swan (Lukas.Swan@Dal.Ca) for further information.
[4]Dalhousie University, Halifax.Contact Peter Allen (Peter.Allen@Dal.Ca) for further information.

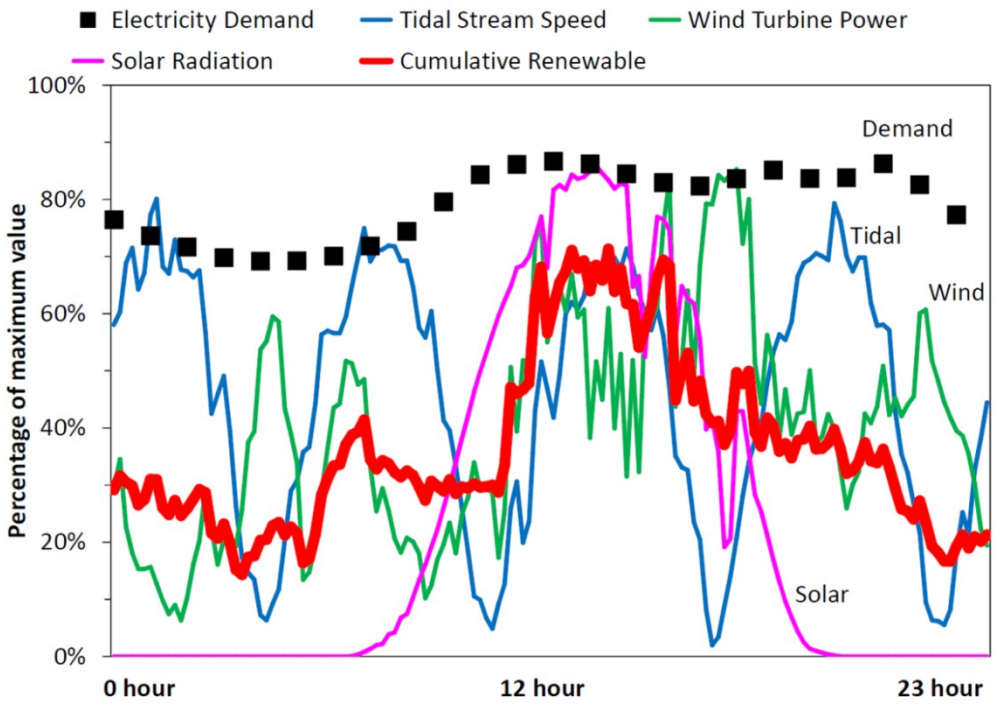

Figure 5: One day profile of electricity demand and renewable generation for the province of Nova Scotia (10 September 2011)

In addition to the obvious mismatch of renewable resources with electricity demand, there exist operational issues related to fossil fuels being used as backup for high penetration rate renewable generators Figure 6 shows the required dispatchable generation which is the difference between the electricity demand and cumulative renewable output. This represents the performance requirements of controlled output generators such as fossil fueled thermal units. As noted in Figure 6, the dispatchable generation must be capable of throttling back to minimum power output while also having sufficient capacity to meet nearly all of the electricity demand. Furthermore, renewable resources may be decreasing while electricity demand is increasing (or vice versa). This requires the dispatchable generation to have positive and negative ramp rate capabilities (i.e. change in power output per unit time) that are significantly greater than would be expected based on electricity demand alone. Conventional steam cycle generators suffer in both regards as they are limited to minimum power output of one-half rated capacity, and ramp rates of 1% per minute [26].

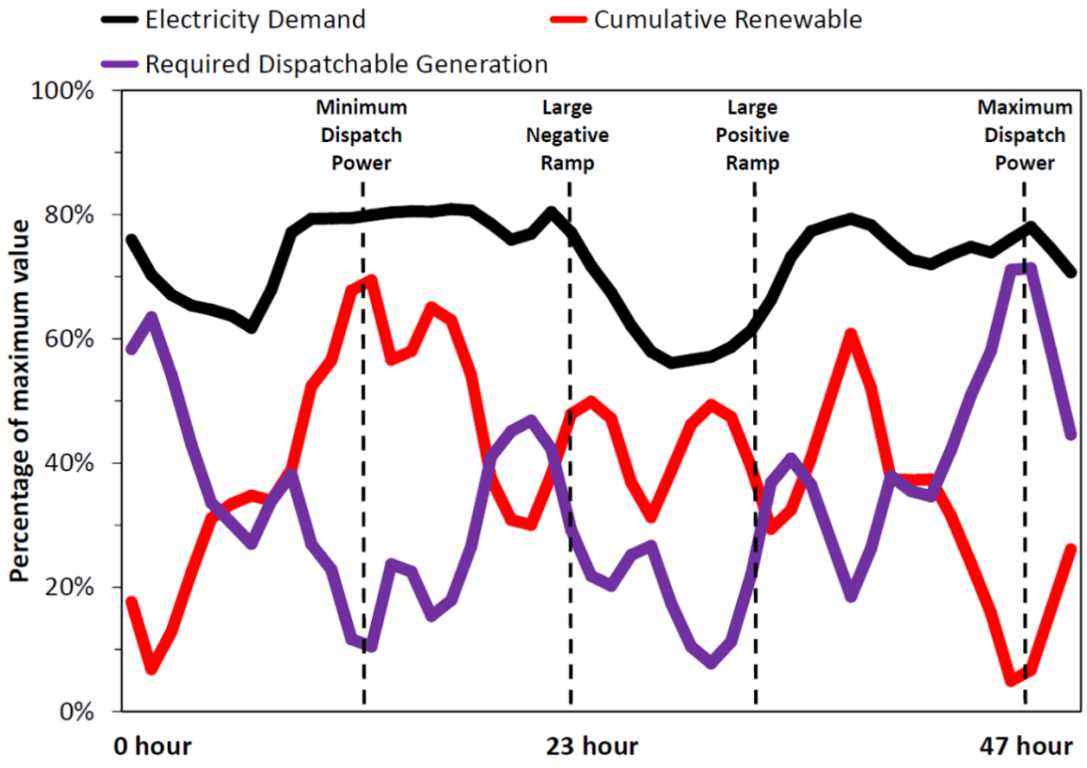

Figure 6: Two day profile of electricity demand, cumulative renewable generation, and the resultant required dispatchable generation for the province of Nova Scotia (16-17 September 2011)

In-stream tidal generation is predictable and reasonably consistent, a unique quality of this resource. In contrast, wind and solar renewable resources are such that they respond on timescales of seconds and minutes due to gusts and clouds. Figure 7 illustrates this characteristic by providing high rate minimum/maximum values recorded during each ten-minute timestep. Wind turbine power varies considerably throughout each ten-minute period, often ranging from 20% to 95% of the maximum monthly value. In this example the variation of solar radiation is minimal during the morning, but with the onset of afternoon clouds the minimums drop to less than 10%. These brief renewable resource variations may be partially mitigated through the use of geographically separated generators. However, this assumes sufficient transmission capacity is available within the transmission and distribution electricity grid.

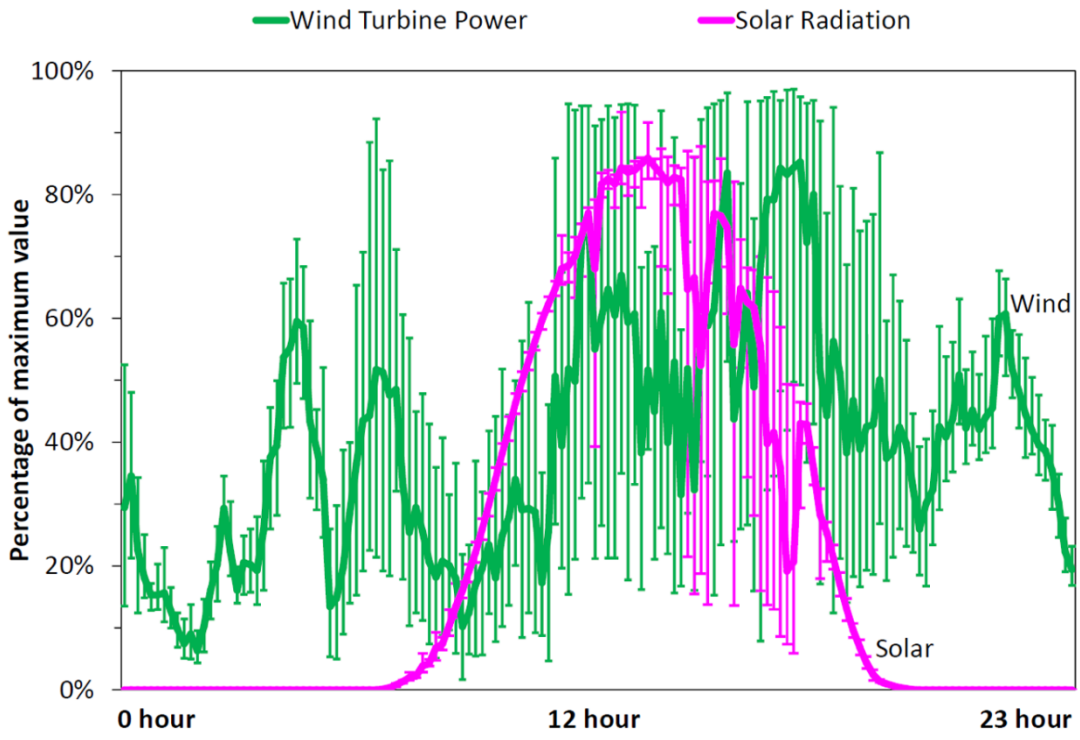

Figure 7: One day profile of ten-minute timestep renewable generation with one-second minimum/maximum values for the province of Nova Scotia (10 September 2011)

The preceding figures and discussion identify the range of variation in renewable resources corresponding to resource type, influence on conventional generators, and individual renewable generator response. These variations necessitate the use of energy storage if renewable resources are to meet a significant portion of electricity demand without curtailment or fossil fuel backup. There are a variety of options available for both small and large scale energy storage systems. Numerous literature reviews compare these various energy storage technologies using several assessment methods [19, 20, 27-32]. Many of these comparison/review articles recommend certain technologies for certain applications and an applicability map is created showing technologies plotted as duration versus power. An example is given in Figure 8.

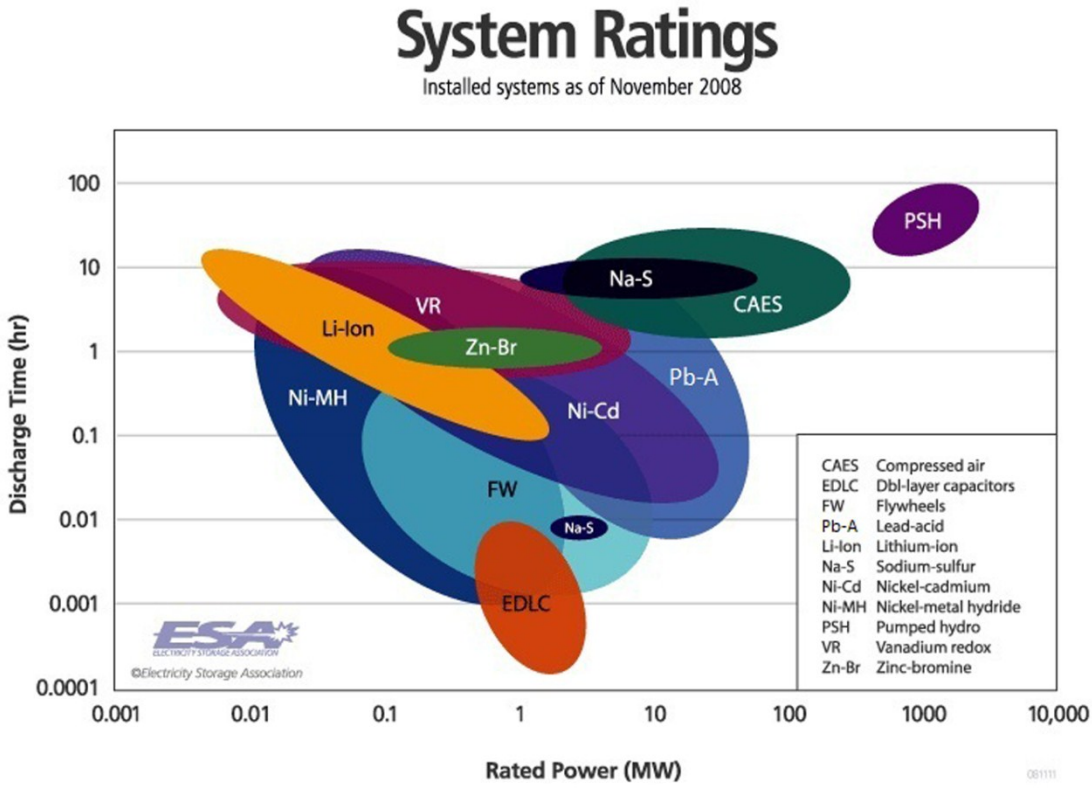

Figure 8: Duration vs. power of energy storage projects as of 2008 [33]

The ranges shown in Figure 8 include installed energy storage projects to the year 2008. The product of duration and power is energy storage capacity, and thus Figure 8 shows that PHS and CAES are used in large storage projects, FW and EDLC are used in small storage projects, and batteries (all remaining abbreviations) are used in medium storage projects with extensions into the small and large categories. The unique characteristics of each renewable resource results in different power output variation periods and influence the selection of an energy storage technology.

PHS and CAES are appropriate for long duration energy storage measured in hours or days [19, 30, 32, 34]. PHS is constrained by topography, demanding significant elevation difference and water reservoir volumes. CAES is constrained by geology as it typically stores air in voids created in subterranean salt domes. Both PHS and CAES require large capital investments that deter its application to smaller distributed projects [19, 30]. In contrast, supercapacitors and flywheels are applicable to short duration (seconds), high power density applications such a power quality control [15, 19, 30, 34]. Self-discharge

of capacitors and flywheels (e.g. frictional losses) render them unsuitable for longer-term energy storage [19, 20, 30].

Batteries encompass a broad range of duration and power with Pb-A, Na-S, Li-ion, VRB, and nickel based technologies defining the envelope [15, 19, 29-32, 34]. As a consequence of the high price of nickel the availability and use of this technology is diminishing. Pb-A, Li-ion, Na-S, and VRB batteries will be the focus of this article due to the broad duration and power ranges available in these technologies.

Section 2.2 of this article discusses the role that energy storage serves in electricity grid systems. Section 2.3 describes the selected battery technologies, notable installations with renewable energy, and the forefront of research specific to each chemistry. Finally, the unique characteristics of each battery chemistry are compared with electricity grid services, resulting in selection and justification of a particular technology for each service.

2.2 THE ROLE OF ENERGY STORAGE

Energy storage systems will play a significant role in the integration of high penetration renewable energy sources. Before addressing the specific roles, it is worthwhile to examine the traditional functions energy storage systems have played in the conventional electric grid. Energy storage systems are already used extensively in many countries for conventional grid support purposes in a variety of applications, with approximately 2.5%, 10%, and 15% of all electricity being cycled through energy storage in the USA, Europe, and Japan, respectively [15].

2.2.1 Energy Storage Duration Categories

Energy storage used for electricity grid services can be broadly grouped into three categories, *short, medium, and long*, based on the duration of its charge/discharge cycle. The principal distinction between the duration categories is the power and energy characteristics required of the storage. The short duration category lasts up to one minute and is concerned primarily with power quality. This category specifies power

characteristics of the storage. The medium duration category spans minutes to hours to compensate for the temporal mismatch between generation and demand. The medium category specifies both power and energy characteristics of storage because it must respond to changes in generation/demand for several minutes or more. The long duration category provides energy wheeling services over periods of hours and days, and as such specifies the energy characteristic of the storage. A summary of services provided by these duration categories is given in Table 1.

Table 1: Energy storage duration categories based upon [8, 10, 15, 17, 27, 29, 30, 35]

Duration Category	Conventional Services	Renewable Energy Services
Short (up to one minute)	- Angular Stability - Voltage Stability - Frequency Stability - Interruption Response	- Flicker reduction - Voltage Control - Reactive power control - Resource variation
Medium (minutes to hours)	- Spinning reserve - Contingency reserve - Ramp rate compensation - Peak shaving - Transmission and distribution (T&D) upgrade deferral	- Output smoothing/enhanced dispatchability - Demand shifting - Ramp rate compensation - Avoidance of energy production vs. dispatch mismatch penalties - Curtailment prevention
Long (hours to days)	- T&D upgrade deferral - Load-shifting - Energy Arbitrage	- Enhanced dispatchability - Curtailment prevention - Generation shifting/Renewable Energy Arbitrage

The services shown in Table 1 are separated as conventional functions and those to support the integration of renewable energy. The conventional services are primarily to support fluctuations in demand and the limited ramp-rate capabilities of centralized generators. In contrast, renewable energy services are to support generation fluctuations inherent to renewable resources and the integration of decentralized generators throughout radial structured electricity grids.

2.2.1.1 Conventional Services Provided by Energy Storage

Conventional services have traditionally been performed by spinning reserve and load-forecasting techniques [10]. The services provided by conventional support technologies allow demands to be met by adjusting power output from flexible generation sources. This support is uni-directional and can only adjust generator output to meet higher or lower demands. Conversely, storage technologies can absorb excess energy or export stored energy thereby providing bi-directional support services. Long term storage seeks to take advantage of low demand periods by charging the system when generation costs are the lowest and discharging during high price periods for economic gains and grid congestion reduction. It is interesting to note that short and medium term services are provided in conventional grids by traditional power quality control methods such as Flexible AC Transmission System (FACTS) devices and spinning reserve [27]; however, no such methods exist to directly take advantage of the long duration services listed in Table 1 other than energy storage devices.

2.2.1.2 Renewable Energy Services Provided by Energy Storage

Short term services provide power quality support. Flicker, voltage excursions, and reactive power disturbances from wind turbines or other intermittent sources are examples of such power quality issues. Power quality issues caused by renewable energy generation are best solved by improved power electronics at the location of the power generation rather than large central or smaller distributed energy storage facilities [8, 36]. It has also been suggested that using hybrid systems with FACTS devices backed by some amount of energy storage could be used to address multiple duration functions required for energy systems [27, 37].

Medium duration energy storage functions include ramp rate compensation, time shifting, and output smoothing/dispatachability. Ramp rate compensation is required as some renewable energy sources display very large swings in output. If the output of a renewable source declines over several minutes there must be enough flexible generation capacity to meet the corresponding demand that will no longer met by the renewable energy source [10]. An example of when sufficient flexible generation was not available during a rapid decline in wind production is found in [38], during which power

production in the ERCOT grid did not meet required levels and very high cost units had to be brought online to prevent massive blackouts and system disruption, all while low cost units sat unused.

Generation shifting and energy arbitrage refer to taking energy generated during high output periods of a renewable energy source to a high-demand or high cost period. This can be done over several hours or days to take advantage of the diurnal demand fluctuations seen in nearly all electricity grids.

During low grid demand and high renewable production the power generated from renewable and base load generators on the grid may be larger than the load. Base load generation is generally slow to respond and cannot produce lower than a prescribed safe operation level based on the generator type (coal, nuclear, oil, etc.). This minimum base load is one of the significant aspects of grid flexibility as referred to in [10] and ultimately leads to renewable energy generation curtailment. Curtailment of renewable generators is highly unfavorable as the wind, solar, and other renewable resources are essentially free, making the economics of such action unfavorable.

Output smoothing and dispatachability refer to the action of specifying and meeting an output level for a given future time period using predicted output values. The energy storage system enables this by providing a means to source or sink the difference between specified output levels and actual generation. This function serves several purposes. First, it allows a system operator to decide with greater confidence which conventional generators will remain as base or intermediate load. Second, it reduces requirement for spinning and contingency reserve as the non-dispatchable renewable resource now has prescribed dispatched levels that can be given hours in advance. Finally, it protects the grid from rapid swings in output levels from power generated from renewable resources.

Energy storage requirements for renewable energy integration can be thought of in several ways. In [10], renewable generation is treated as a “negative” demand on the electrical grid because the output is not dispatchable, and therefore behaves more like conventional demand rather than conventional generation. Using this methodology, the remaining demand after subtracting the renewable generation is that which the

conventional electricity generators must satisfy. This approach performs well when considering the medium and long term energy storage situation, and demonstrates how curtailment and excessive ramp rates are a serious concern when renewable energy is involved. Alternatively, intermittent renewable energy sources can be thought of as non-dispatchable generation that can be coupled with energy storage systems to create a semi-dispatchable, or at least reasonably predictable, output [37, 39-41].

For low penetration of wind and other renewable energy sources, grid operation changes are minimal, and integration costs are very low [42]. As a result, the complexity and cost of energy storage systems makes them unnecessary at low penetration levels [8, 10, 42]. In [8, 9], the costs of implementing wind into the electric grid on a delivered energy basis is listed from several case studies in the USA. The integration costs of wind energy range from 1 US$/MWh to approximately 9 US$/MWh for studies performed with penetration levels from1% up to 30%[5] and generally show higher integration costs with higher penetration levels. For comparison, average electricity prices in the United States are ~127 US$/MW and can be up to twice that in certain states [43] indicating integration costs between 1 % and 8% based on penetration level. As the penetration level of wind or other renewable energy resource increases, the conventional methods of dealing with short, medium, and long term generation variability from these resources begin to encounter difficulty and integration becomes more challenging and costly.

In [10] a flexibility factor is presented as the ability of a grid to ramp down conventional generation to accommodate wind or other variable generation sources. Additional intermittent resources can be added without the need for curtailment during low demand, high renewable generation periods in flexible grids. Energy storage is shown to be a method of increasing this grid flexibility by absorbing otherwise curtailed energy. Various other methods of increasing grid flexibility exist, many of which are lower cost than energy storage; however, as penetration levels increase these conventional methods cannot provide enough flexibility, at which point energy storage is required to further increase renewable energy penetration. The cost of integration of renewable energy

[5] Penetration is defined as the ratio of installed renewable power generation capacity to the total installed power generation capacity in the given electricity grid.

resources increases with penetration level and at a certain level energy storage systems become a viable, and even essential technology. Energy storage will play a vital role as renewable energy penetration levels increase and electricity grids are no longer able to support renewable energy integration using conventional means.

2.2.2 Defining the Energy and Power Relationship Required of the Storage

With the several types of energy storage systems and the range of requirements for the various services categories, it can be difficult to determine the suitability of a system for a given application. Discharge time of a system is one characteristic that can immediately identify possible options for a given application. By comparing the stored energy quantity and power requirements of the application with the characteristics of the battery technologies, one or more suitable types may be identified. Following this process, battery technologies can be compared on other merits such as cycle life, cost, and efficiency. This energy and power comparison is completed using a figure of merit defined as the ratio of energy to power, E/P. The values used in this calculation are based on the maximum continuous discharge rating required of the application (electricity grid service category).

Table 2 presents the E/P ratios required for each service duration category. The calculation accounts for the realities of batteries by defining a battery state-of-charge (SOC) operating window. Significant heat is generated during high rate discharge (short category) and can overwhelm the thermal mass of the battery and as such the SOC range is limited to 40%. Medium rate discharge (medium category) is limited to 75% due to heat rejection characteristics of the battery. Low rate discharge (long category) is limited to 80% to preserve battery cycle life and lifetime energy throughput that would be reduced via complete discharges (i.e. 100% SOC range).The required E/P ratio for a given duration is calculated according to:

$$E/P = \text{Duration(hours)}/\text{SOC Range(decimal)} \quad (1)$$

The inclusion of SOC range within the calculation enables an immediate comparison of the requirements with the characteristics of specific battery technologies. This

comparison and selection of batteries for specific categories is given in Section 4 based on the characteristics presented in Section 3. The E/P values for each duration are summarized in Table 2 by order of magnitude.

Table 2: E/P requirements of electricity service categories including a modifier for useful battery operating range

Grid Service Duration Category	Duration	SOC range (%)	E/P (kWh/kW)	E/P order of magnitude (kWh/kW)
Short (up to one minute)	1 second	40	0.0007	0.01
	60 seconds	40	0.04	
Medium (minutes to hours)	6 minutes	75	0.13	1
	60 minutes	75	1.3	
	3 hours	75	4	
Long (hours to days)	6 hours	80	8	10+
	2 days	80	64	

2.3 BATTERY TECHNOLOGIES AND CHARACTERISTICS

This section briefly describes the four considered battery technologies including their history, chemistry, existing systems integrated with renewable energy, and present research areas.

2.3.1 Lead-acid (Pb-A)

2.3.1.1 Overview

Pb-A batteries were first created in the 1860's and are one of the most mature, least expensive and widely used rechargeable battery technologies in the world today. Decades of research and development have been spent on all aspects of the Pb-A battery including plate design, active material composition, electrolyte composition, separator materials, and case design [44]. The defining characteristics of lead-acid batteries include relatively low cost, technological maturity, low energy density, and limited cycle life. The specific values for various characteristics of Pb-A batteries can be found in Table 3.

The basic composition of a lead-acid battery is a metallic lead negative electrode and a lead-oxide positive plate with sulfuric acid solution as the electrolyte. Many additives have been developed for the positive and negative plates which increase cycle life (in the case of antimony) or enhance other desirable properties of the battery such as reduced corrosion or decreased self-discharge [44, 45]. The open-circuit potential of the fully charged lead-acid cell is approximately 2.15 V however this value varies with temperature and decreases significantly as the battery is discharged [44].The following reaction occurs in a lead-acid battery [44].

$$Pb + PbO_2 + 2H_2SO_4 \rightarrow 2PbSO_4 + 2H_2O \text{ (discharge)} \quad (2)$$

There are two classifications of lead-acid batteries: flooded and valve regulated. There are also a variety of electrode designs including prismatic (flat plate), tubular, and spiral wound. Flooded type Pb-A batteries contain mobile liquid electrolyte with non-restrictive vents to atmosphere, requiring replacement of water due to gassing caused by electrolysis. Valve regulated types allow recombination of the hydrogen and oxygen that evolves during charge completion and overcharge reactions, eliminating the need for electrolyte maintenance. The electrolyte in valve regulated Pb-A batteries is typically immobilized using either advanced glass mat (AGM) or a gel. Pb-A batteries have relatively lower cycle life due to the participation of both active materials and the electrolyte in the reaction, corrosion of the positive plate during overcharge, and the passivation of the negative electrode due to sulfation [45]. As such, lead-acid batteries have seen limited use for heavy cycling applications (such as those seen in many grid support applications) and instead find application in float service or infrequent cycle applications such as uninterruptible power supplies and demand peak shaving. Spiral and tubular type batteries better compress the electrodes which has been shown to increase cycle life through improved cohesion of the positive active mass during heavy cycling [44].

2.3.1.2 Existing Installations

There exist numerous large Pb-A grid connected energy storage systems functioning in various roles around the world. The largest Pb-A system was located in Chino, California and was rated 10 MW, 40 MWh. The system was installed as a demonstration project and

performed a large number of services including peak shaving, load leveling, load following, spinning reserve, frequency control, voltage and reactive power control, and black-start operations. The system operated with 72% overall efficiency and used lead-acid cells that were warranted for a minimum of 2000 deep discharge cycles [46, 47]. The battery performance met expectations and demonstrated the potential of large scale Pb-A systems. Another notable Pb-A installation was the 17 MW, 14 MWh BEWAG test facility in Germany used for frequency regulation and spinning reserve applications. This installation provided nearly 7000 times its nominal storage capacity over a 9 year service life [48].The Puerto Rico Electric Power Authority installed a Pb-A battery sized at 20 MW, 14 MWh which provided spinning reserve, frequency control, and voltage regulation [46]. Unfortunately several of the cells in the PREPA battery bank failed prematurely due to inadequate charging resulting from poor measurement and control methods, indicating the importance of appropriate battery management methods [49].

2.3.1.3 Active Research

Despite the accepted classification of this technology as very mature, a wide array of research efforts continue today by addressing limitations in order to make it competitive with other technologies. Areas of research include use of secondary lead through hydrometallurgy production of plates [50], grid alloys [51], advanced models [52, 53], charge methods [54, 55], battery health monitoring [56-61] and carbon electrode materials for enhanced cycle life [62-66]. Lead-carbon batteries are presently a very active area of research as initial results from lab tests and a limited number of demonstration projects have shown dramatically increased cycle life over conventional lead-acid batteries [67]. Lead-carbon batteries have carbon in the negative electrode in the forms of carbon additive, carbon foam skeleton, or partial carbon electrodes. Initial estimates and tests suggest cycle life during high rate partial state of charge operation of lead-carbon batteries to be 4-5 times greater than a comparable valve-regulated battery (12,000 cycles at 10% depth cycles with lead-carbon vs. 2000 cycles with standard VRLA), potentially making this a promising and low cost technology option for this application [67-71].

Accurate determination of the SOC of Pb-A batteries is an area that continues to see active research. Knowledge of the SOC is crucial to battery lifetime as very deep discharges or excessive overcharges can severely and prematurely limit the cycle life of cells [44, 45, 72]. Only within the last 20 years has sufficient technology become readily available that can use various measurements from the battery to accurately determine the SOC of lead-acid cells. Methods range in simplicity from basic amp-hour counting with charge loss estimation to Kalman filters and neural networks and combinations thereof [56-61]. The most recent implementations of neural networks have been able to estimate the SOC within 2%, while a method using a Kalman filter has shown accuracy within 1% of the actual SOC [58, 61]. Many of these methods of SOC determination require significant processing, complex coding, and prior knowledge of the particular physical constants for a given Pb-A cell. This makes implementation of accurate SOC determination very much a custom procedure for each battery system.

2.3.2 Lithium-ion (Li-ion)

2.3.2.1 Overview

Li-ion batteries are a recent technology with roots based at Bell labs in the 1960's and the first commercialization by Sony in 1990 [19].The defining characteristics of Li-ion batteries are high cycle life, high energy density, high efficiency, and high cost (see Table 3), which have led to their use in small format consumer electronics.

The electrochemical action of a Li-ion battery is different than most types of cells. Charge transfer occurs through ion intercalation rather than chemical reaction of the electrodes. Because overcharge and side reactions are minimal the Li-ion battery can achieve over 90% energy efficiency and nearly 100% coloumbic efficiency [19]. The cathode of a Li-ion cell is commonly made of some form of lithiated metal (M in the following equation) oxide, and the anode is commonly graphitic carbon. The basic intercalation reaction for Li-ion batteries is as follows [73]:

$$yC + LiMO_2 \rightarrow Li_xC_y + Li_{1-x}MO_2 , \; x = \sim 0.5 , \; y = 6 \text{ (discharge)} \qquad (3)$$

The roots of Li-ion batteries are in small portable electronics devices, and as such typical storage capacity ranges from 100 to 5000 mAh. These small batteries are not practical for

bulk, utility scale energy storage, and several companies have since developed large prismatic type batteries [33]. These larger cells still retain the distinct performance advantages of the smaller cells but are capable of integration with multi-MW systems for grid applications.

The lack of overcharge and side reactions requires the use of complex control circuitry to prevent overcharge which immediately results in overheating and possible failure. Their efficiency enables high discharge and charge currents which increase the risks associated with overcharging [32]. Fortunately, accurate determination of the SOC is possible through various means including amp-hour counting, voltage limits, and others [74-77]. When combined in series each cell or cell grouping must have control circuitry to ensure balance between each cell. This requires reliable and somewhat expensive circuitry, pushing the cost of an already expensive battery even higher [30].

2.3.2.2 Existing Installations

The application of Li-ion batteries to grid scale storage is a recent development. A123 Systems has installed 36 MW, ~9 MWh of grid connected lithium battery systems in various locations serving needs including renewable integration and grid stability [78]. As recently as August 2011, Electrovaya agreed to install a 1.2 MWh lithium battery bank in Ontario for renewable energy integration purposes. Additionally, SAFT announced in August 2011 that it will be providing 3 MWh of lithium batteries for renewable integration in France [33]. Overall, the outlook for lithium batteries in grid applications is very positive as the price continues to decline and the performance is improved.

2.3.2.3 Active Research

Li-ion batteries are presently the most actively researched battery technology due to their wide range of potential uses and superior performance to other battery technologies. Present research objectives include reducing production costs, enhancing performance, increasing lifetime, and enhancing safety. These are being implemented by research in cathode and anode materials, electrolyte materials, and manufacturing processes [79, 80].Cathode research is the most common area of research for commercial batteries and is focusing on replacing the traditional $LiCoO_2$ cathode with materials as $LiFePO_4$,

$LiMn_2O_4$ (manganese spinel), $LiNi_{0.5}Mn_{1.5}O_4$ (spinel structure) and other materials for increased energy density, safety, and material availability (cost reduction) [73]. Each new cathode material brings a host of new challenges such as reduced cycle life, voltage differences, incompatibility with existing electrolytes, or other considerations [73, 81, 82]. Anode material innovation includes use of Li-Sn and Li-Si electrodes for increased specific energy. Unfortunately such anodes suffer from material expansion which is being partially mitigated through mechanical design [73, 83, 84]. Highly specialized electrodes such as the titanate anode aimed at high rate charge/discharge are in early stages [79, 85]. Electrolyte selection is a significant component of overall cell safety with the limited stabilityrange and high vapor pressure of commercial electrolytes being unfavorable. Research is ongoing to identify additives for thermal stability, redox shuttles (to protect from overcharge), shutdown separators (to prevent thermal runaway), and other lithium salts for use as electrolytes [73]. Ionic liquids may be used as electrolytes as they withstand higher overvoltage than lithium salts are often non-toxic [86, 87]. As with other chemistries, accurate determination of SOC remains an objective and recently developed methods can determine it to within 1% of the true value [74-77].

2.3.3 Sodium-sulfur (Na-S)

2.3.3.1 Overview

Na-S batteries are another relatively new battery technology. Development was seen in many countries starting in the late-1960'sthrough mid-1990's, at which point electric vehicle research programs abandoned it as it was becoming apparent the chemistry was not appropriate for this application[29]. In the 1980's NGK Insulators began work on developing Na-S for grid-scale applications and ultimately developed a grid-scale product that has seen exponential growth rates of implementation related to grid support and renewable energy applications [29, 30, 88]. Na-S batteries are regarded as one of the lowest cost options for grid-scale energy storage [89]. The defining characteristics of Na-S batteries are high cycle life, high energy density, high pulse power capability, and average to low cost as given in Table 3.

A Na-S battery is constructed with a liquid sodium negative electrode and a liquid sulfur positive electrode. The two electrodes are separated by a solid beta-alumina electrolyte through which only positive sodium ions can pass during charge/discharge. Figure 9 shows the conceptual schematic of a Na-S Battery [88]. The open-circuit voltage of a Na-S cell varies between 1.8 and 2.0 V depending on the SOC [29]. The basic chemical reaction is a combination of positive sodium ions with the molten sulfur according to the following chemical equation:

$$2Na + 2S \rightarrow Na_2S_4 \text{ (discharge)} \quad (4)$$

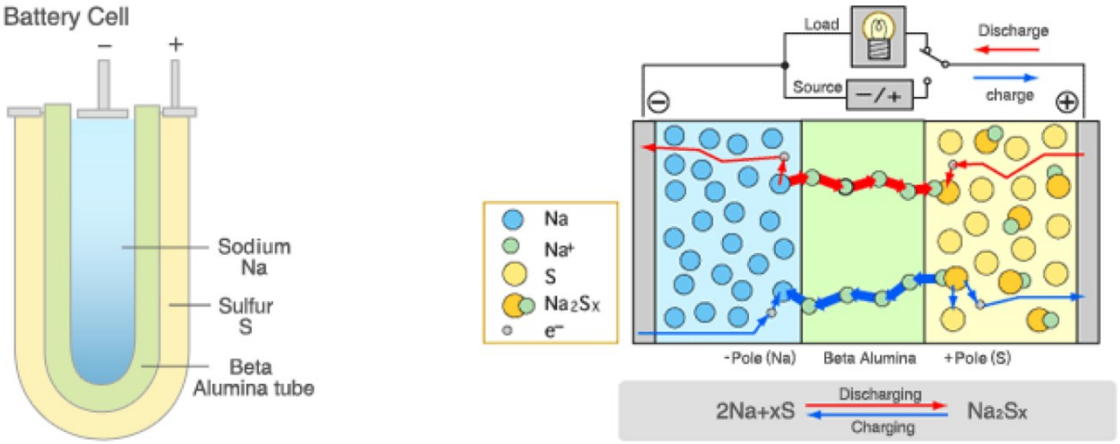

Figure 9: Sodium-sulfur battery schematic [88]

There are significant operational considerations with Na-S batteries including the high temperature operation for liquid sodium (300-350^{o}C) and the high reactivity of sodium with the atmosphere should containment fail [19, 29]. If the battery in non-operational, approximately 20% of total capacity is lost daily due to heat loss, requiring energy to maintain the high temperature liquid electrodes [19]; However, if the battery is operating, the inefficiencies provide sufficient heat for the electrode and therefore little or no input energy is required to heat the battery [29].

2.3.3.2 Existing Installations

Na-S battery installations have seen rapid growth in recent years from 10 MW installed capacity in the year 1998 to over 300 MW by 2010 [88, 90]. The world's largest battery energy storage system is rated 34 MW, 245 MWh and is installed in conjunction with a 51 MW wind farm for output stabilization [33]. A typical small scale (distributed energy

storage) installation consisting of 1.2 MW, 7.2 MWh is described by [91]. The detailed project report published by SANDIA National Laboratories (USA) established that installed total system cost is approximately 2500 US$/kW. This was based on 50 kW, 360 kWh modules each with a cost of approximately 350 US$/kWh.

2.3.3.3 Active Research

The significant research area for Na-S batteries has been development of a high quality, low manufacturing cost beta-alumina separator with long cycle life capabilities [92-95].To contend with the high temperature issues all-solid Na-S batteries are under investigation [96, 97]. These room temperature Na-S batteries presently display unfavorable cycling characteristics and are not expected to achieve the performance levels of existing high temperature Na-S batteries. Additionally, battery sealing methodologies are an active research area [98, 99].

2.3.4 Vanadium Redox Battery (VRB)

2.3.4.1 Overview

Development of the VRB began in the early 1980's at the University of New South Wales [19]. VRB cells use V^{2+}/V^{3+}ions in the negative half-cell electrolyte and V^{4+}/V^{5+} oxidation states of vanadium in the formsVO^{2+} and VO_2^{+}respectively [19]. The defining characteristics of the VRB include extremely large cycle life, independent energy and power construction, low to average energy density, moderate efficiency, moderate cost, and no self-discharge (see Table 3).

Vanadium Redox battery operation is different than that of other batteries because it is a flow battery. In a flow battery two liquid electrolytes are stored in separate tanks to create two separate half cells. A simple schematic of the VRB can be seen in Figure 10. The battery operates by circulating the half-cell electrolytes located in separate chambers through to a membrane in which H^{+} ions transfer, resulting in a redox reaction which creates electrical current.

The result is a battery with 1.4 to 1.6 V potential which does not suffer from self-discharge [19]. The separate electrolyte storage tanks and reaction membrane decouples

the energy and power characteristics of VRB. Increasing the tank size raises the storage capacity but doesn't change power capability. Increasing the membrane area raises the power capability with no change in storage capacity.

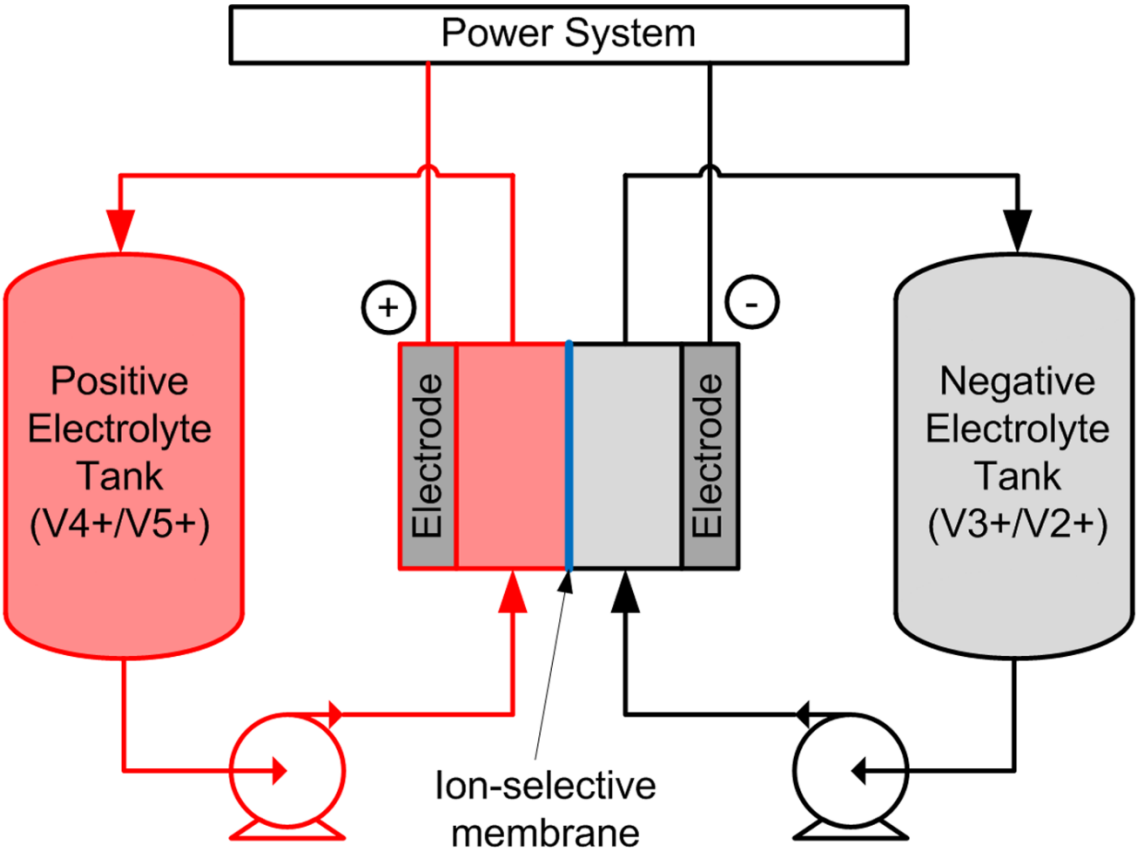

Figure 10: VRB schematic

A significant issue with the VRB is the limited operating temperature range (10 ^{o}C through 35^{o}C) [100]. This limitation warrants use within a climate controlled environment. Additions to the electrolyte are capable of expanding this range [101].

2.3.4.2 Existing Installations

VRB installations are few and small in scale. The largest proposed system to date was announced by Prudent Energy in October 2011, with a capacity of 8 MWh but has yet to be completed and delivered to the customer [102]. The largest existing VRB installation to date was a 4 MW, 6 MWh unit designed to stabilize the output of a 32 MW wind farm [103]. This installation performed roughly 270,000 shallow discharge cycles before it was decommissioned. Many smaller installations exist for a worldwide total of 20 MWh

installed capacity used primarily for load leveling, remote area power supply, renewable energy stabilization, uninterruptable power supply, and power quality regulation [30].

2.3.4.3 Active Research

In March 2011 a method was discovered to increase volumetric energy density by 70% while also increasing the working temperature range of the battery to -5 ^{o}C to 50 ^{o}C [101]. The VRB is still in its infancy with respect to commercial and developmental maturity, with nearly all aspects of this technology presently under development. The most active research area is design, manufacturing, and use of various separator/membrane materials, as this significant affects power performance and lifetime [104-109]. High ionic conductivity and good resistance to degradation are the key qualities researchers seek for membrane materials. Electrolyte mixtures containing various additives and at varied concentrations yield increased energy density, increased operating temperature range, and reduced production costs [109-111]. Electrode material, design, and manufacturing research focuses on reducing reaction inefficiencies through increased conductivity and surface area of the electrodes [109]. Even basic operational methods such as SOC monitoring, flow rate control and charge-discharge characteristics are still under development [109, 112-115]. Models of VRB are also under development to enable specific design to support particular applications [114, 116].

2.3.5 Comparison of Battery Technologies

To select a particular battery type for a given application a multitude of factors must be considered. The most significant factor is the E/P ratio based on the maximum continuous discharge rating of the battery. The ratio of E/P provides discharge time, but will be left in units of kWh/kW to distinguish E/P using continuous ratings from other non-maximum discharge ratings. Of course the storage could be discharged at a slower rate (increasing E/P) although this may not take advantage of the capabilities of the storage.

A selection of battery characteristics, including the E/P ratio (highlighted in bold), are given in Table 3. Pb-A and Li-ion chemistries have been sub-divided into power cells and energy cells, representing the commercially available range. This categorization is provided because it is possible to design both of these batteries for either high specific

power or high specific energy through modifications of dimensions of the active material or different anode/cathode materials. In other publications the large ranges are provided to capture these differences; however, this incorrectly implies that the maximum values are achievable for each characteristic in a single battery. In practical application, improving one characteristic (power, energy, or life) often comes at the expense of the other two. Power and energy cell categories were included to capture this tradeoff behavior of a particular cell design.

Table 3: Battery technology characteristics (based primarily upon [19, 30] **and/or other sources as noted)**

Battery Type	Pb-A		Li-ion		Na-S	VRB
	Power Cell	**Energy Cell**	**Power Cell**	**Energy Cell**		
Cycle Life (cycles @ % SOC variation)	50 to 200 @ 80% [44], 1000's for shallow cycles [45]	200 to 1800 @80% [32, 44]	3000 @ 80% [32]	3000+ @ 80% [32]	4500 @ 80%, 2500 @ 100% [88]	10,000 to 12,000+ @100% [100] >270,000 @ few %[103]
Specific Energy (Wh/kg)	30 to 50 [44]	30 to 50 [44]	75 to 200 [30, 32]	75 to 200 [32]	150 to 250	10 to 30[100]
Specific Power (W/kg)	300*	75*	2400[117]	75 to 300*	150 to 230 possible, commercial ~30 [88]	N/A
Energy Density (Wh/L)	50 to 80	50 to 80	200 to 500 [117]	200 to 500	150 to 250	16 to 33
Power Density (W/L)	300 to 400	10 to 100	4500 [117]	1500	N/A	N/A
E/P ratio (kWh/kW)	**0.13**	**0.5**	**0.025 to 0.075***	**0.27 to 0.6***	**6** [88]	**1.5 to 6+** [103]
Self-Discharge per day	<0.5% [32]	<0.5% [32, 44]	0.1-0.3%	0.1-0.3%	20%**	Negligible
Cycle Efficiency	63 to 90% [32, 118]	63 to 90% [32, 118]	79 to 98%* [32]	80% to 98%* [32]	75 to 90% [32, 118]	75 to 80%
Format	Cylindrical	Prismatic	Cylindrical	Prismatic	Tall cylindrical	Separate tanks
Active material phase	Solid	Solid	Solid	Solid	Liquid	Liquid
System Level Cost(US$/kWh)	200 to 600	200 to 600	600 to 1200 [32]	600 to 1200 [32]	350	150 to 1000
Maturity Level	Mature	Mature	Commercial	Commercializing	Commercializing	Developed
Notable characteristic	Modular	Modular	Sealed, modular	Sealed, modular	High temperature	Flowing liquids

* Based on the authors' laboratory results from testing several different power and energy cells.

** Although heat input requirement is ~20% of battery capacity, thermal losses are mostly or entirely counteracted by internal I^2R losses and therefore little to no actual parasitic discharge is observed.

2.4 BATTERY TECHNOLOGY SELECTION AND APPLICATIONS

By comparing the requirements presented in Table 2 (E/P of grid service categories) and the battery characteristics presented in Table 3 (E/P of battery chemistry) the appropriate battery technologies can be selected to suit the various duration categories. Note that the E/P of grid service categories ranges five orders of magnitude (0.0007 to 64) and the E/P of battery technologies range between two and three orders of magnitude (0.025 to 6), lying within that of the grid service values.

The comparison of battery and grid service category E/P values are presented in Table 4.There are suitable battery technologies to meet the three grid service duration categories. However, the minimum and maximum E/P values of the service categories are beyond the capabilities of batteries and thus alternative energy storage technologies such as capacitors (short) and pumped hydro (long) will be required. Only Li-ion power cells meet the short duration category. All battery technologies meet the medium category with Pb-A and Li-ion more suitable for minute-level distributed smaller scale storage and Na-S and VRB for hour-level centralized facilities. This owes both to the E/P characteristics as well as the high temperature and liquid electrolyte storage of the Na-S and VRB technologies, respectively. Regarding long duration category the Na-S and VRB are only suitable for applications less than one day, unless the electrolyte tanks of the VRB are very large.

Table 4: Recommended battery energy storage technologies to meet specific grid services

Grid Service Duration Category	Duration	Required E/P (kWh/kW)	Suitable Battery Technologies (Battery E/P in brackets)
Short	1 second	0.0007	N/A
	60 seconds	0.04	Li-Ion power cell (0.05)
Medium	Minutes	<1	Pb-A energy cell(0.5), Li-ion energy cell (0.4)
	Hours	>1	Na-S (6), VRB (1.5+)
Long	6 hours	8	Na-S (6), VRB (1.5+)
	2 days	64	N/A

The battery technologies listed in Table 4 were selected based on maximum continuous discharge capability. Doing so takes advantage of both the power and energy characteristics of the storage. In practice, certain battery systems can provide peaking power for a short period of time. As such a selected system may be able to perform some functions associated with a shorter duration grid service categories. Operating in a hybrid mode maximizes provided services and in some cases a storage system would only be economical if such modes were used [15]. However, these additional capabilities are limited to peak power of the battery. It should be noted that specific battery systems cannot perform services of a longer duration category than for which they were designed. Doing so would fully deplete the system rendering it unavailable.

Table 4 indicates that multiple battery technologies are suitable for the medium and long grid service durations. Figure 11 compares two competing battery types in a given duration by providing relative quantities. For example, considering the long term system characteristics of medium (minutes) duration, Pb-A costs less than Li-ion, but also has less cycle life.

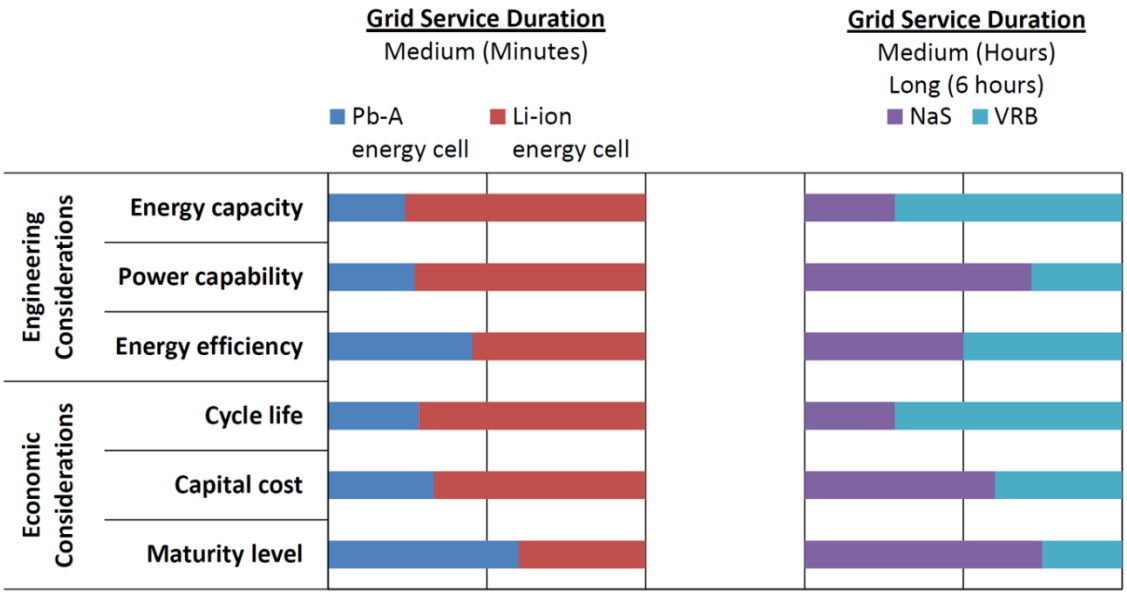

Figure 11: Relative comparison of suitable battery technology characteristics for a given grid service duration

2.4.1 Lead-acid Battery Applications

Pb-A storage systems operate well on the minute-timescale medium duration grid service category. The low cost and high maturity level of this technology offset the relatively low energy and power characteristics (see Figure 11), making Pb-A competitive for several applications. However, if frequently deep cycled they will require maintenance and eventually battery replacement. The limited cycle life of Pb-A batteries suggests applications which are called on infrequently (once per day).Note that the E/P ratio of a grid utility service is independent of its frequency of use. Regarding replacement, Pb-A batteries are highly recyclable, accounting for 70% of the lead used in USA manufacture [119] and therefore have scrap value. The low energy density of the Pb-A battery makes it undesirable for mobile or space limited applications (e.g. cellar of a wind turbine tower). Ideal applications include uninterruptable power supply and short duration grid support to prevent failure or instability that could result in large financial losses [19, 29].The Electricity Storage Association (ESA) states Pb-A batteries are “fully capable and reasonable” for power applications and “feasible but not quite practical or economical” for energy applications [33]. SANDIA national laboratory along with EPRI has identified several applications and several combination of individual applications for

Pb-A batteries in [15, 120], all of which pertain to short/medium duration storage and infrequent deep discharge cycles.

2.4.2 Lithium-ion Battery Applications

Li-ion batteries possess high power capability, good cycle life, high energy density, and high efficiency; however, they are relatively expensive. The E/P ratio indicates ideal application in short and medium duration grid services. Li-ion power cell designs are the only suitable technology for second-timescale services. Employing other battery technologies for these purposes would result in dramatic oversizing of the storage capacity. Due to high energy density, portable grid storage battery banks have been suggested for temporary or semi-permanent application for T&D deferral or other non-permanent applications [85]. The ESA finds Li-ion batteries to fall under the same application category as Pb-A batteries with "fully capable and reasonable" rating for power applications (short duration storage) and "feasible but not quite practical or economical" for energy applications (long duration storage) [33]. However, Referring to Figure 11, it becomes clear Li-ion outperform Pb-A batteries in all engineering consideration categories, but not maturity or cost. This cost advantage is less distinct than Table 3 would indicate as the Li-ion cycle life is greater than that of Pb-A, and consequently this allows for more energy throughput (i.e. service). Furthermore, the cost of Li-ion is primarily related to storage capacity (i.e. active materials) and less so due to power (i.e. electrical design). As such its use in short duration services is advantageous. Because of these cost and life characteristics, the choice of lead-acid or lithium ion remains application specific.

2.4.3 Sodium-sulfur Battery Applications

The E/P ratio for commercially available Na-S cells suggests its application to hour-timescale medium and long duration grid services. Na-S batteries are the only technology to receive "fully capable and reasonable" ratings from the ESA in both power and energy applications, suggesting this technology will become valuable in grid-storage applications [33]. Due to the high cycle life, energy and power densities, reasonable cost, and benign

environmental effects of the battery, Na-S batteries are poised for several energy storage applications [19, 30, 33]. Unfamiliarity and production capacity (single vendor [33]) will be the limiting factors in deployment of this technology for grid-storage applications. It is evident from Table 4 and Figure 11 that Na-S has advantages over VRB in the storage duration lasting several hours. Beyond this however, the scalability of VRB gives it competitive advantage.

2.4.4 Vanadium-redox Battery Applications

VRB's has relatively low energy density, and small incremental cost for increasing the storage capacity. The E/P ratio suggests ideal application in medium to long duration storage systems. As it requires sufficient space and maintenance (e.g. pumps) this technology is ideally suited to centralized large-scale long duration storage. Although several VRB demonstration projects are operating, this technology has still not achieved commercial level. The ESA rates VRB (and other flow batteries) as "reasonable" for power applications and "fully capable and reasonable" for energy applications suggesting it could very well fulfill a hybrid role where long duration storage is the primary concern, and power quality improvement is a secondary concern [33].

2.4.5 Distributed versus Central Energy Storage

Ideal placement of energy storage is system specific and models are required to assess the particular benefits of a given placement. Many programs have been developed for simulation of power systems with renewable energy and energy storage systems, of which an excellent review of such programs can be found in [121]. Excessive transmission of electricity results in increased losses, and therefore storage should generally be located as close to the generation and/or electricity demand as possible. Considering the distributed nature of renewable energy developments and the urbanization of populations, both distributed and centralized storage have value.

Distributed storage has the advantage of placement directly alongside distributed generators to support rural integration, especially within medium-voltage distribution electricity grids. Pb-A and Li-ion batteries are most suitable for this application due to

their compact, safe, sealed, non-liquid, zero maintenance, and modular format. This small capacity market will likely not see the use of Na-S or VRB as they either operate with high temperatures, possess liquid connections, or show poor scaling to small storage capacities. In this application the majority of the services will be short and medium duration as they are associated with the medium-voltage grid difficulties.

Central storage has the advantage of economies of scale and dedicated personnel, lending itself to the high-temperature Na-S battery and VRB requiring liquid transfer. With increased scale application to medium and long duration services can be achieved. Management of such systems will appear to the system operator like a highly flexible traditional generation source with the added ability to sink power when required. In both the distributed and centralized storage categories communication and control is a critical aspect which will be met with smart-grid technologies.

2.5 CONCLUSION

The electricity grid services required for renewable integration have been identified and discussed with regards to energy storage systems. Energy storage systems provides an means of increasing grid flexibility and enabling integration of intermittent non-dispatchable generation sources by temporally decoupling this generation from demand. There exists a wide range of storage durations for various integration services and a single technology is unlikely to fulfill all of these roles. Using E/P values of the grid services, several battery technologies were identified and selected on the basis of their own E/P values, after which additional cycle life, capital cost, energy efficiency, and maturity level are considered. It was found that the variety of grid services do indeed demand different battery technologies. Based on this framework the applicable battery technologies for short, medium, and long durations were determined and presented in Table 4. A relative comparison of competing technologies for a particular grid service range is given in Figure 11.

CHAPTER 3 BATTERY STORAGE SYSTEM FOR RESIDENTIAL ELECTRICITY PEAK DEMAND SHAVING

This chapter was published as:

J. Leadbetter and L. G. Swan, "Assessment of battery energy storage characteristics to perform residential peak demand shaving," in Proceedings of eSim, 1-4 May 2012, Halifax, pp. 366-379.

Jason Leadbetter is the principal researcher and author of the article. He conducted the research as part of his MASc. Thus, while he received supervision and guidance from his supervisor Dr. Swan, he carried out the work, wrote the published article, communicated with the scientific committee of the conference, and carried out the necessary revisions before publication. Writing support in the form of editing assistance and content guidance was provided by Lukas Swan. Some minor grammatical and content changes have been made to integrate the article within this thesis.

3.1 INTRODUCTION

The storage of electricity for the purpose of peak demand shaving is receiving great interest, with numerous pilot projects being conducted in several countries [19]. Such demand management is important to electricity utilities as additional non-dispatchable generators, such as wind turbines, are installed [1]. Examples of electricity demand peaks and wind power generation are shown in Figure 12 for the Canadian province of Ontario, which experiences one daily demand peak in winter and two in summer. It is apparent from Figure 12 that wind power generation experiences large and rapid output variations that are unrelated to changes in electricity demand. As a consequence of these demand and renewable generation changes, fast-response generators must be available, often consisting of fossil-fuelled generating technologies operating at part load (e.g. natural gas turbines).

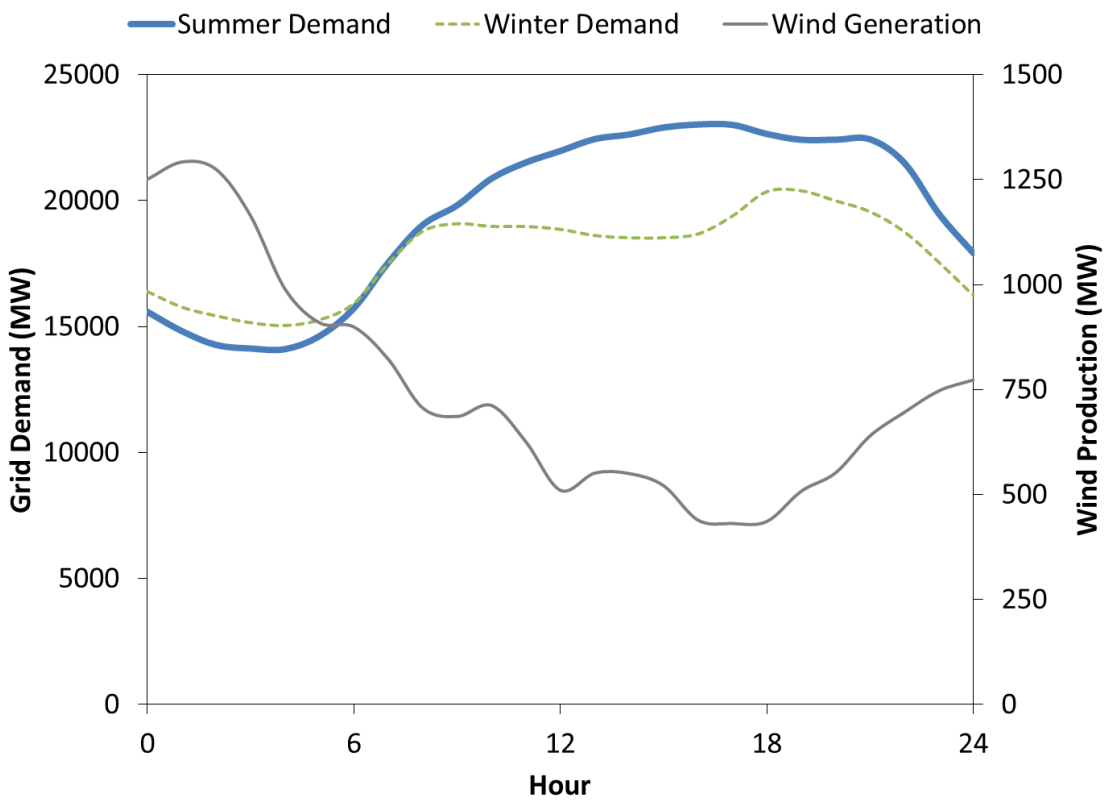

Figure 12: Ontario grid demand for a summer and winter day overlaid with total wind generation for the summer day based upon [122]

As an alternative, energy storage has been implemented on large centralized scales using technologies such as pumped hydro, compressed air, and megawatt-hour class battery energy storage systems [19, 29]. Such storage is an effective tool to fulfil grid support functions related to centralized generator limitations and transmission infrastructure constraints [10, 29, 31, 123]. As such, central storage technologies are used in many parts of the world, storing up to 2.5% (USA), 10% (Europe), and 15% (Japan) of all electricity produced [15]. Despite the usefulness of central energy storage, there are issues that it cannot address. These are primarily related to the distribution grid and include: growing end-use demand, transmission substation limits, and voltage drop. In addition, renewable electricity generators may be connected within weak distribution grids due to prime renewable resource availability. Wind electricity generation is particularly challenging to integrate at high penetration levels as it is difficult to predict, highly intermittent, and can cause grid disturbances (e.g. flicker) [8].

To address these distribution grid level constraints, utilities have introduced time-of-use tiered tariffs and smart-grid programs to modify the end-user demand experienced by the grid, as well as uni-directional thermal energy storage units [23, 124, 125]. Such distributed thermal energy storage, located within buildings or communities, poses one solution to such issues by providing a means to store electricity during off-peak and/or high renewable electricity generation times, and utilize this stored energy when peak electricity demand occurs. However, it is generally limited to heating end-uses such as space heating and hot water. The next generation of distributed energy storage will absorb and release electricity so that it is suitable for all end-uses, including space cooling, appliances, and lighting, as well as allowing for bi-directional electricity transfer with the utility for added grid support functionality.

Battery energy storage systems (BESS), consisting of batteries and an inverter/charger, are an option for this next-generation distributed energy storage and are particularly well suited to buildings and communities due to their safe, silent, scalable, zero/low-maintenance, and efficient operation that does not depend upon topography, geology, or moving parts. This article describes a new BESS scoping model based on building performance simulation with the objective of providing peak electricity demand shaving. It focuses on the residential sector because of its highly distributed nature and year-round operation.

The objective of this work is to determine storage characteristics of capacity, power, and cycle life, and to examine the effects of using such a residential scale, grid-interconnected BESS. The storage system consists of a rechargeable battery, a bi-directional grid-integrated inverter/charger, and a controller as seen in Figure 13. The inverter/charger cycles the battery to reduce the house demand peaks as seen by the electricity grid. The following sections discuss the simulation method, results of the electricity demand and BESS simulations, and give recommendations suitable to the residential sector of Canada.

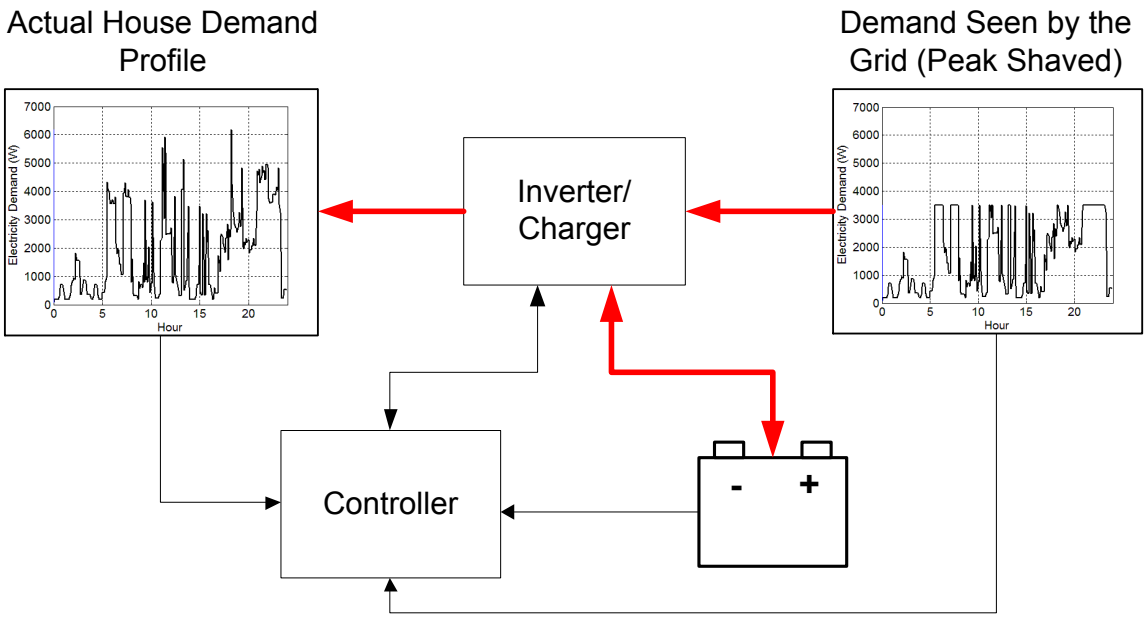

Figure 13: Peak shaving BESS diagram (thick red lines indicate electricity flow and thin black lines indicate communication)

3.2 METHOD

To assess the sizing and performance of a BESS for peak demand shaving requires information on the electricity demand of the residence as well as a model of the battery and inverter/charger. First, a set of houses representing a variety of those found in the residential stock is selected. Second, an annual energy simulation of these houses is conducted on a five-minute interval so as to capture the peaks in electricity demand from the end-uses. Third, a battery energy storage model is developed and applied to the electricity demand profiles to determine the energy storage and power characteristics required of the BESS to reduce the peak demand of the house as seen by the grid to specific value.

3.2.1 Residential Electricity Profiles

The use of building performance simulation uniquely identifies each energy end-use within a residence: space heating (SH), space cooling (SC), domestic hot water (DHW), and appliances and lighting (AL). Electricity may be used to meet all of the end-uses. Nearly all SC and AL is provided by electricity; however, SH and DHW may be met with other energy sources such as natural gas, heating oil, and wood.

The residential electricity profiles used in this work were provided by the Canadian Hybrid Residential End-Use Energy and GHG Emissions Model (CHREM) which estimates the energy consumption and GHG emissions of nearly 17,000 unique and individual houses that statistically represent the Canadian housing stock [126, 127]. First, the CHREM database is reviewed to identify and select typical houses from each of the five major Canadian regions. The major regions are Atlantic (AT, provinces NF, PE, NS, NB), Quebec (QC), Ontario (ON), Prairies (PR, provinces MB, SK, AB), and British Columbia (BC). The CHREM housing database contains fields describing characteristics that significantly influence electricity consumption of the four major energy end-uses, with the following fields used to select houses: heating energy source, DHW energy source, air conditioner (i.e. SC) presence, city, heated floor area, annual AL energy consumption, annual DHW volume consumption, construction year, window area, exterior wall thermal resistance, and air leakage characteristics. A histogram of each selection parameter for each of the five major Canadian regions was created and used to identify the typical values. Houses were selected from the possible 16,952 houses in the CHREM database by progressively filtering each field towards the typical value until only 1 or 2 houses remained for each region. The selection was done to provide a real data record of a typical house found in each major region of the Canadian housing stock. A basic flow chart of CHREM can be found in Figure 14.

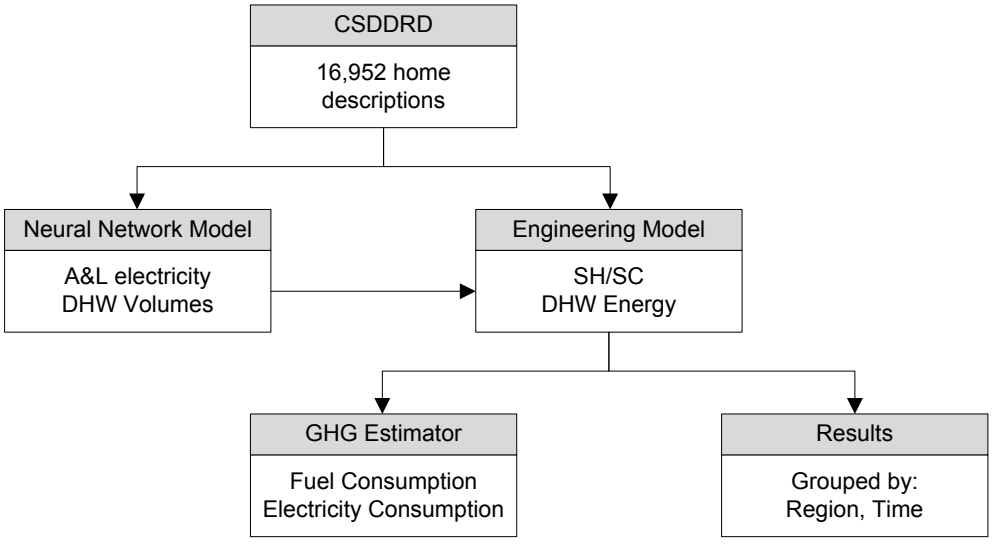

Figure 14: CHREM diagram

The simulation of electric load profiles was performed using the building simulator ESP-r [128, 129]. The prototypical AL profiles of ESP-r were replaced with 5 minute time-step electricity demand profiles for the Canadian housing stock that were developed using a bottom-up approach considering each appliance and lighting requirement individually [130]. This 5 minute time step was selected based on [130, 131] who showed that it adequately captures demand peaks, with little to no averaging effects. The results of this simulation provide a complete year of 5 minute time-step electricity demand information suitable for use with a BESS model.

3.2.2 BESS Operation and Simulation

The BESS is operated to charge and discharge with the intention of temporally decoupling a portion of the peak house demand from the electricity grid. The energy storage model used in the present work can evaluate a variety of battery systems; however, lithium-ion battery parameters were used for this study as lithium-ion batteries are very suitable for such an application based on their favourable power and energy characteristics, cycle life, and continuously declining costs [19].

The following variables will be used in the subsequent discussion and Figure 15:

t – time of day

Δt – time-step length

η – One-way system efficiency

P_H – House electricity demand (power)

P_G – Grid demand (power)

$P_{G,Limit}$ – Grid demand limit (power)

P_{Inv} – Inverter output power

$P_{Inv,Max}$ – Inverter maximum power output

E_B –Stored energy remaining in the battery

To conduct a peak shaving simulation a maximum electricity grid demand limit is first defined for the house (e.g. $P_{G,Limit}$ = 5 kW). If the house demand is above this limit (e.g. P_H = 6 kW), the BESS activates and the inverter discharges the batteries to meet any house demand beyond the grid demand limit (e.g. $P_{Inv} = P_H - P_{G,Limit}$ = 1 kW), thereby maintaining the grid demand at the specified maximum grid demand limit (e.g. $P_G = P_H - P_{Inv}$ = 5 kW). The inverter must be sized to meet the required power demand during the highest peak of the year to prevent a system failure. The BESS operates the battery between 15% and 85% state of charge (SOC) to extend cycle life and ensure the system remains within safe operating conditions. Operation at SOC outside this range decreases cycle life and has the potential to cause malfunction [132]. The system recharges fully (to 85% SOC) during a 5 hour nightly period when house demand is at a minimum and additional demands are easily supported by utilities. This period is evidenced by the favourable time-of-use rates (e.g. time t = 00:00 to 05:00) offered by utilities in many jurisdictions throughout Canada [23, 124].

The BESS scoping model was developed in MatLab and does not estimate operating voltage, thermal considerations, or any other advanced operating parameters; instead the simulation only considers the efficiency of the BESS, defined as the ratio of output electricity to input electricity. An input to output efficiency of 80% was assumed in the model as this agrees with reported system efficiency values for lithium-ion BESS inclusive of the inverter/charger [19]. This assumption translates into 89% one-way efficiency (η). Calculation of remaining energy storage during each time step is conducted by adding/subtracting the energy used for a given time step from the previous time step value. Figure 15 shows a process flow diagram of the BESS operation method.

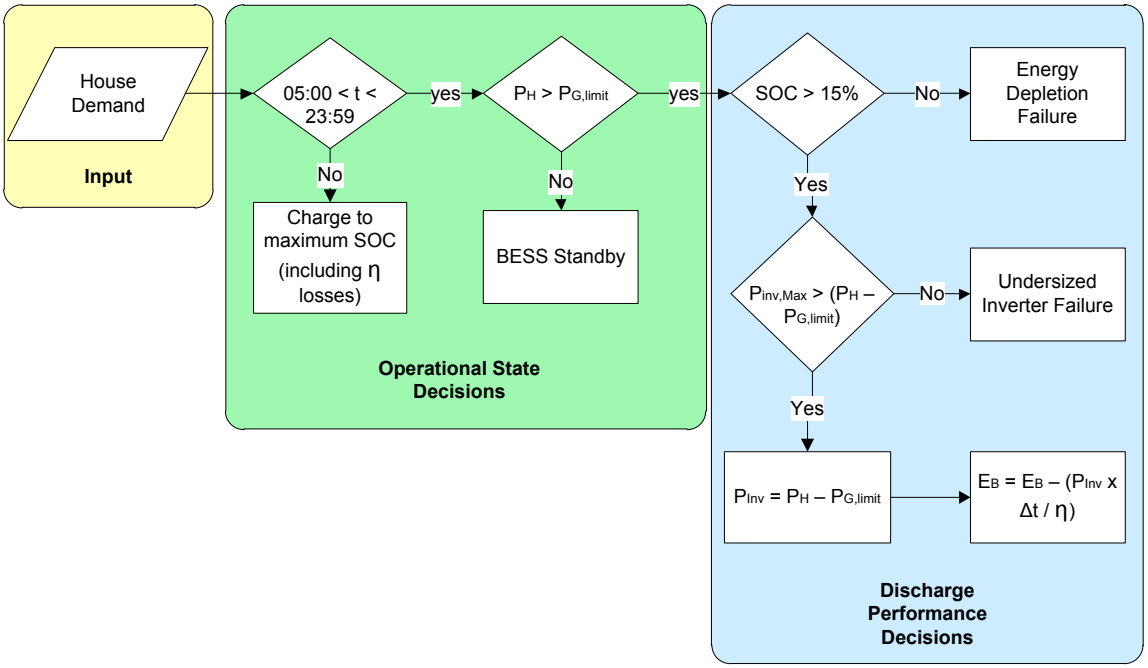

Figure 15: Simulated BESS operation process flow diagram

As shown in Figure 15 the model places the BESS in one of three states: charging, standby, or discharging. While discharging the BESS can either successfully transfer energy (with associated losses), or enters a failure state due to energy depletion or insufficient inverter power.

Selection of the grid demand limit has a significant impact on the required energy storage and power capacities of the BESS. As such, the grid demand limit is based on a percentile selection method using the house demand. Percentile selection method uses a statistical analysis to obtain the value of house demand below which 98.0%, 98.5% or 99.0% of the electricity draws occur. As an example, Figure 16 shows the grid demand limit selection for the Atlantic region house using a 98.5% (1.5% highest) selection level on a load curve diagram.

This percentile method is suggested for peak shaving, as the top 1 to 2% of power draws are the most expensive and challenging periods of operation of an electricity grid [1, 15]. By selecting a system that addresses these brief periods of high power requirement, the system size (power, energy, and cost) can be minimized. For the highest 1.5% peak level the system will discharge for 131.4 hours per year (1.5% of 8760 hours) during the

highest demand periods. This operation characteristic is independent of region or demand profile, and is the direct result of the method of peak shaving used.

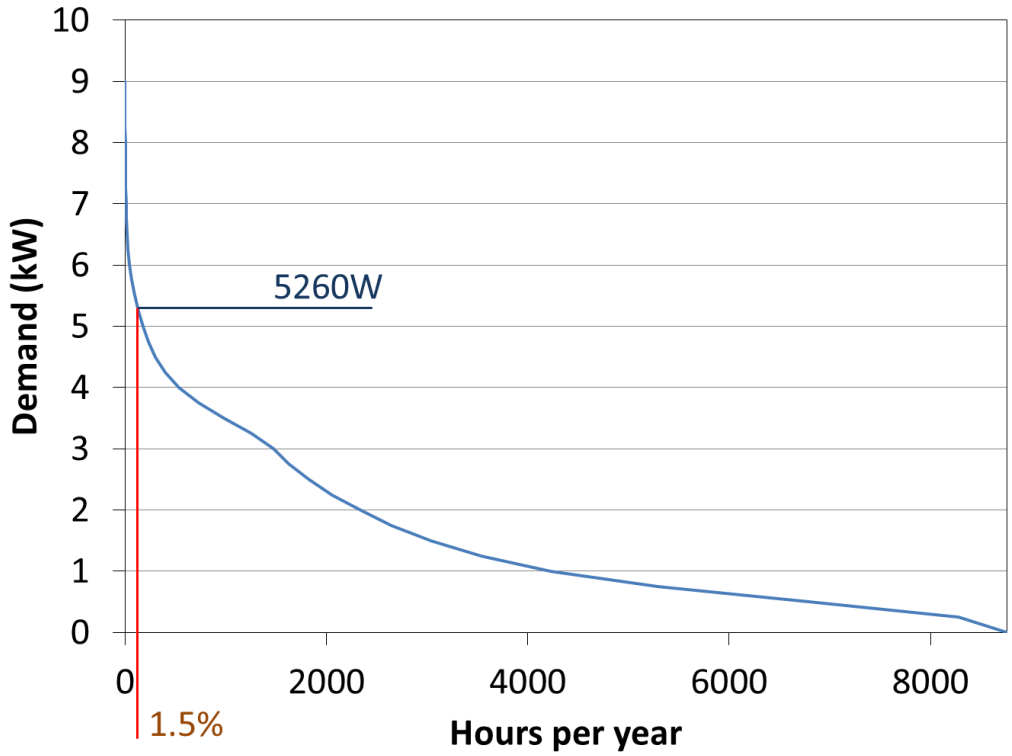

Figure 16: Grid demand limit selection (98.5%) for the Atlantic region

Once the grid demand limit has been determined using the above method, the BESS is simulated and failure events are assessed for each inverter size and energy-storage capacity combination. A failure event occurs when the BESS is incapable of supplying sufficient electricity to maintain the demand as seen by the grid within the limit.

3.3 Results and Discussion

The results of house selection and building performance simulation of electricity profiles are presented first. Using the electricity profiles the BESS simulation is conducted and results analysed to select appropriate system characteristics for houses of each region. Battery life is then estimated based on resultant cycling characteristics of the BESS during simulation.

3.3.1 Selection of Typical Houses

Examination of the CHREM database was conducted on the basis of 11 selection parameters as given in Table 5. A single house was selected from each of the five major regions of Canada which corresponded to typical parameter values based on histogram analysis. The results of the housing selection process are given in Table 5.

Table 5: House selection results

	Regions				
Selection Parameter	**Atlantic (AT)**	**Quebec (QC)**	**Ontario (ON)**	**Prairies (PR)**	**British Columbia (BC)**
City	Halifax	Montreal	Toronto	Edmonton	Vancouver
Heating energy source	Fuel Oil	Electricity	Natural Gas	Natural Gas	Natural Gas
DHW energy source	Electricity	Electricity	Natural Gas	Natural Gas	Natural Gas
Air conditioning	None	None	Electricity	None	None
Heated Area (m^2)	197	179	247	192	198
AL (GJ/year)	29.6	17.7	19.8	23.3	62.4
DHW (litres/day)	220	229	140	179	160
Construction year	1980	1987	1991	1980	1981
Window area (m^2)	24	22.6	17.3	24.3	23.2
Exterior wall thermal resistance (RSI)	3.0	2.1	2.1	2.1	2.1
Air leakage (ACH_{50})	7.9	4.8	4.5	6.2	9.9

Several important characteristics can be noted from this table of house parameters. First and foremost, the variations of each parameter in different regions across Canada suggest a single optimal system does not exist and instead regionally specific sizing is required. Second, most homes in Atlantic and Quebec regions do not use natural gas as a fuel for space heating or DHW. This is significant, as space heating and DHW both constitute significant portions of residential energy consumption. Other regions which lack these electrical end-uses will have significantly less electricity consumption. Third, although many houses in BC do fall under the "medium" AL energy intensity category defined in

[130] a large number of houses in the BC region (much more than any other region) fall under the high demand intensity category. For comparison and contrast purposes a high demand intensity house was selected for this region.

3.3.2 Electricity Profile Characteristics

To be concise, detailed explanation of results will be given for the Atlantic region and any significant differences in general behaviour between regions will be listed in tables. Figure 17 shows the annual average daily electricity profile for the house overlaid with a specific electricity load profile for January 1st of the same house. The single day electricity profile shows strong peaking due to individual appliance use. The annual average profile shows that the duration of major peaks consistently occurs in the morning and evening. The averaged profile is similar to the summer months total grid demand figure presented in Figure 12, and shows that the contribution of residential loads to peak grid demand is very significant.

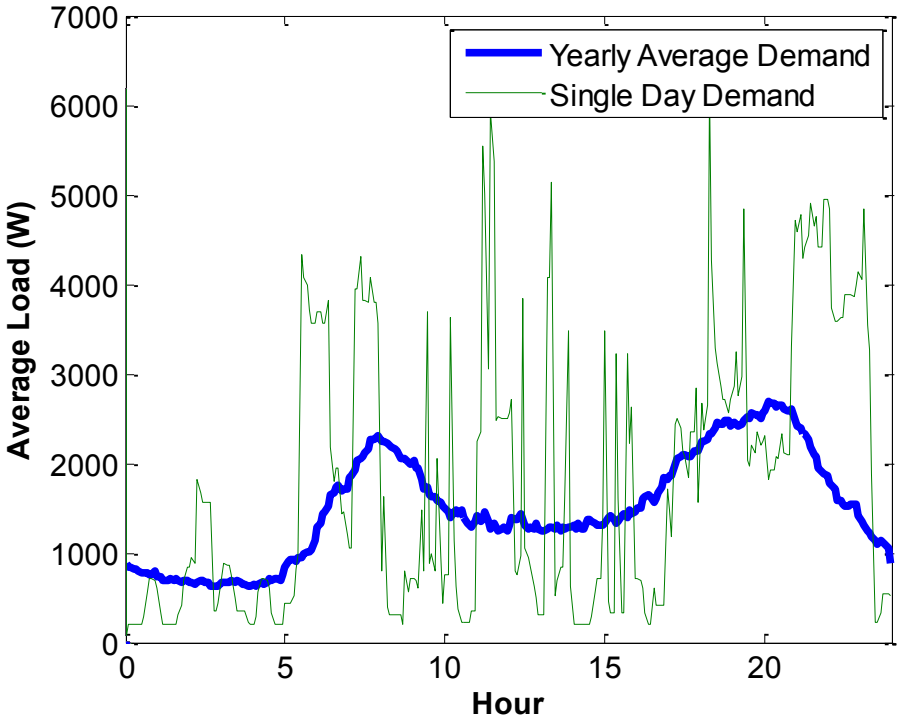

Figure 17: Daily demand profiles (annual average in thick blue, Jan 1 in thin green)

The CHREM was used to model the electricity demand of each end-use for the houses. A statistical analysis of the results is given in Table 6. The annual electricity consumption varies from region to region by as much as a factor of three. Additionally, the maximum demand (peak) compared to average demand also varies significantly from region to region, indicating custom system sizing for each region is likely required. The percentile rows in Table 6 represent the electric load in watts below which the listed percentages of the 5 minute load periods occur.

Table 6: Statistical analysis of regional electricity profiles

Region	AT	QC	ON	PR	BC
Annual electricity consumption (MWh)	13.2	32.8	8.4	5.8	17.3
Average house demand (W)	1506	3746	958	661	1976
Maximum house demand (W)	9040	15230	7188	5120	12002
Standard deviation of house demand (W)	1318	2980	858	571	1568
Maximum demand as percent of annual average demand	600%	465%	750%	775%	605%
98.0 percentile (W)	5020	10510	3540	2480	6300
98.5 percentile (W)	5260	10910	3790	2600	6630
99.0 percentile (W)	5550	11350	4130	2780	7040

The mean and max values of electricity consumption can also be represented visually as seen in Figure 18.

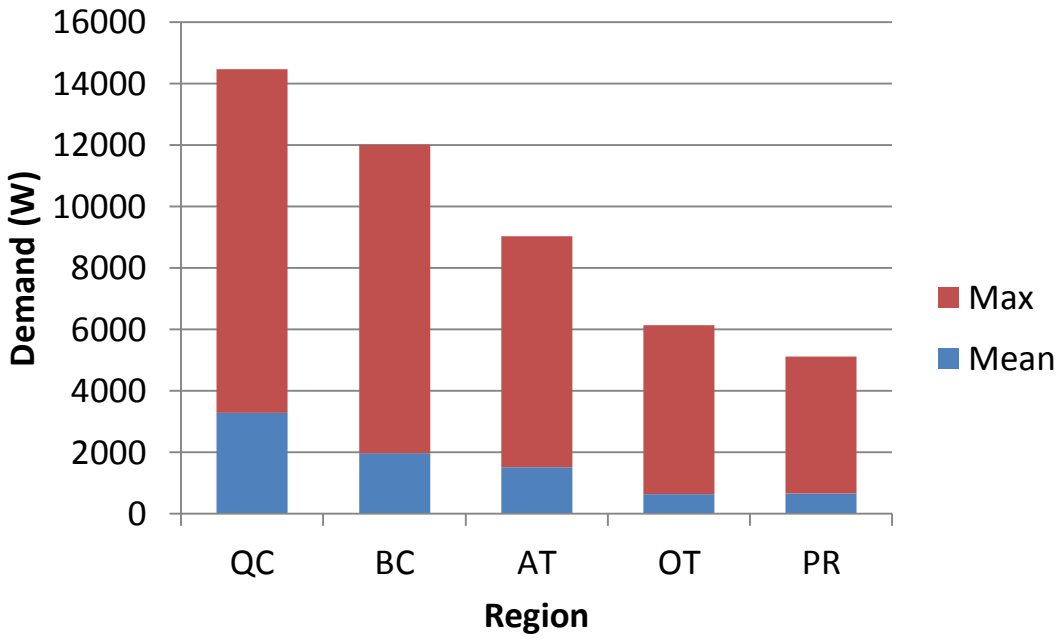

Figure 18: Mean/Max demand values for the 5 typical houses

3.3.3 BESS Simulation Results

BESS sizing is performed by selectively varying parameters and counting failure events for each simulated system. Two distinct types of failure events can occur. The first failure is an energy depletion failure that occurs when the BESS has no stored energy remaining, after which the system can no longer output power to offset house demand. The second type of failure is an undersized inverter failure, which occurs when there is insufficient power output ability of the inverter to reduce the house demand to the defined grid demand limit.

To assess the appropriate system several thousand iterations were simulated for each region and failure events were counted for each BESS system. The following BESS properties were varied: energy storage capacity, inverter size (power capability), and grid demand limit. The number of failure events should be limited to zero as a single failure event would indicate the system is undersized for the given application. More specifically, energy storage capacity related failures (energy depletion) represent a much

more significant concern than an undersized inverter failure. In the event of an energy depletion event, all subsequent system demands cannot be met and the house load is not peak shaved. In the case of an undersized inverter failure only the load above the inverter size cannot be met, which represents only a small portion of the load being met, and is therefore not a critical failure. When an energy depletion failure event occurs it is likely the time when the utility expects the system to perform and should be avoided by slight over-design of the storage capacity. Over-design of the inverter size is not required as the impacts of a power failure event less significant than and energy failure. The sizing of the inverter could possibly be designed using a 10 or 20 failure criteria as these failures are not significant; however, as previously stated, energy capacity should be sized to perform with zero failures.

The energy storage requirement is assessed in Figure 19 by simulating a system with a very large power output ability (eliminates undersized inverter failures). This is displayed as a 2D iso-failure plot for the Atlantic region in which system sizes that fall on the various lines fail the indicated number of times per year (one failure is a 5 minute timestep failure). The results are slightly discretized due to simulation of systems at discrete intervals (see Figure 19 1 iso-failure line for an example of this discretization). If an infinite number of system were simulated the lines would appear completely smooth, similar to the 5000 iso-failure system in Figure 19. Any systems whose size falls in the regions to the upper-right of the failure lines does not experience any failure events, while systems to the lower-left of the failure lines experience the noted number of failure events.

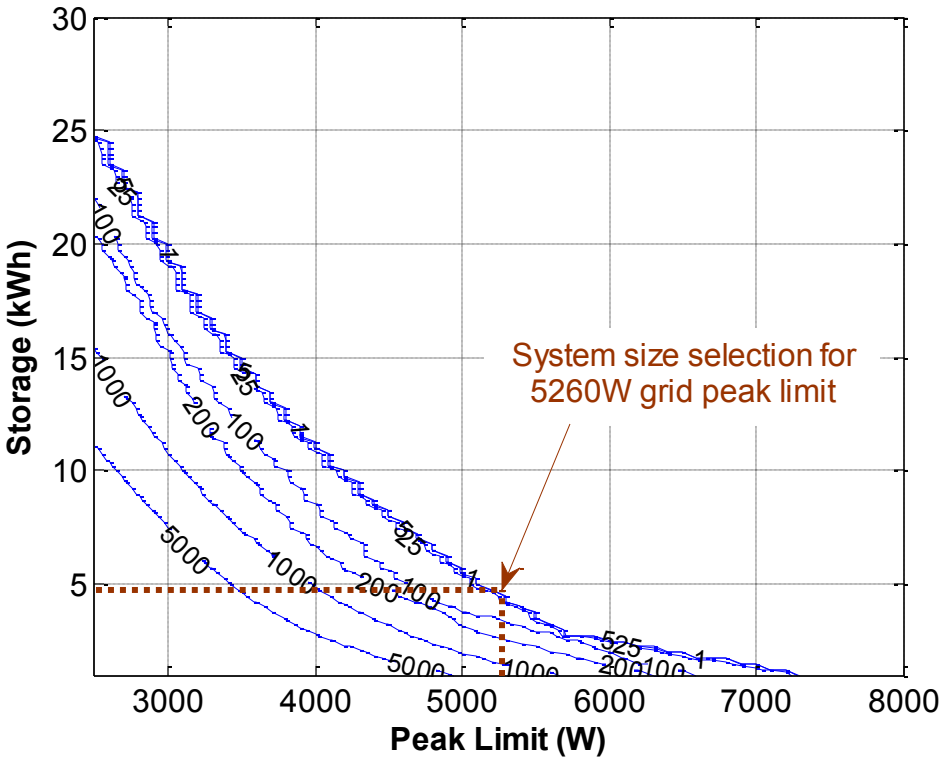

Figure 19: 2D iso-failure plot of BESS capacity

The result of the shape of this plot indicates diminishing returns with respect to increasing energy storage. A 4 kWh BESS can reduce the maximum peak by 40% (to 5500 W) while a pack twice the size (8 kWh) only reduces the peak by 51% (to 4430 W). This corresponds to doubling the battery size to gain only 25% greater peak shaving capability.

Figure 20 plots iso-failure lines of inverter size versus grid demand limit with a very large BESS energy storage capacity (eliminates energy depletion failures). This linear behaviour is expected as inverter power corresponds directly to the amount of demand that can be offset.

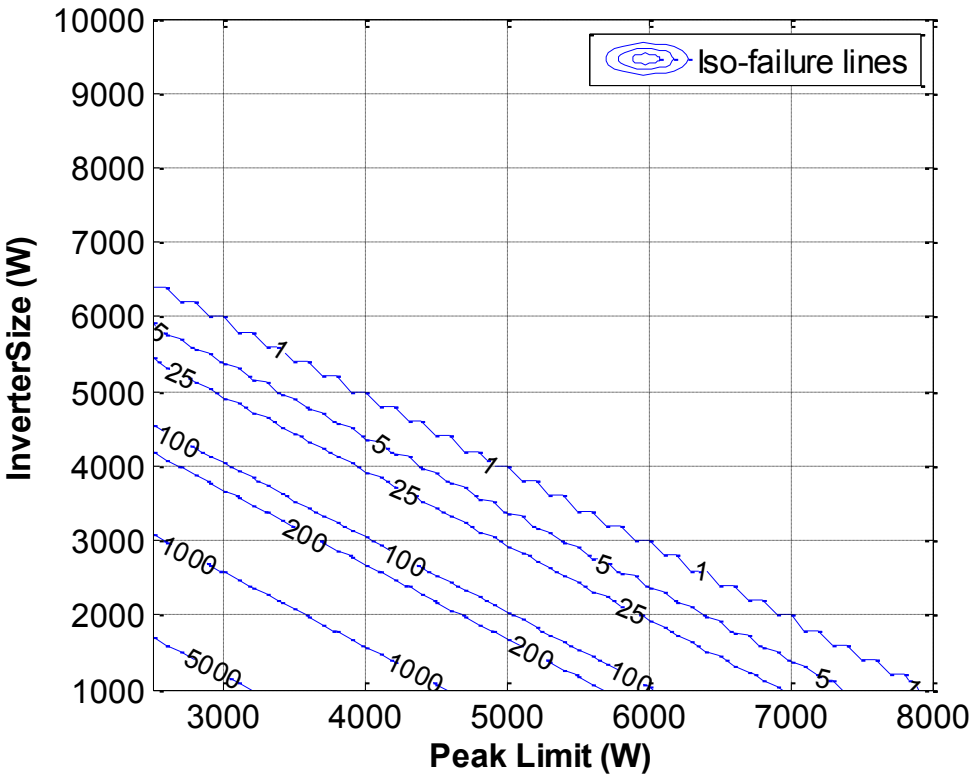

Figure 20: 2D iso-failure plot of BESS power

3.3.4 BESS Sizing

The diminishing returns of the energy versus grid demand limit plot suggests the selection should be based on reducing the peak as much as possible before reaching the region of steep incline in battery capacity requirement. A minimum peak shaving percentile level constraint of 98.5% (1.5% of system load periods, see Figure 16 for an example of this) was specified as this level of peak shaving will adequately meet many of the peak shaving operations required by the electricity grid. An example of system size selection using the Atlantic region house can be seen in Figure 19; The same method can be applied to Figure 20 to assess inverter size.

Selection was completed by plotting storage capacity versus inverter size for the specified grid demand limit determined by the 98.5 percentile load value and selecting the smallest possible system size. An example of this plot for the Atlantic region is shown in Figure 21.

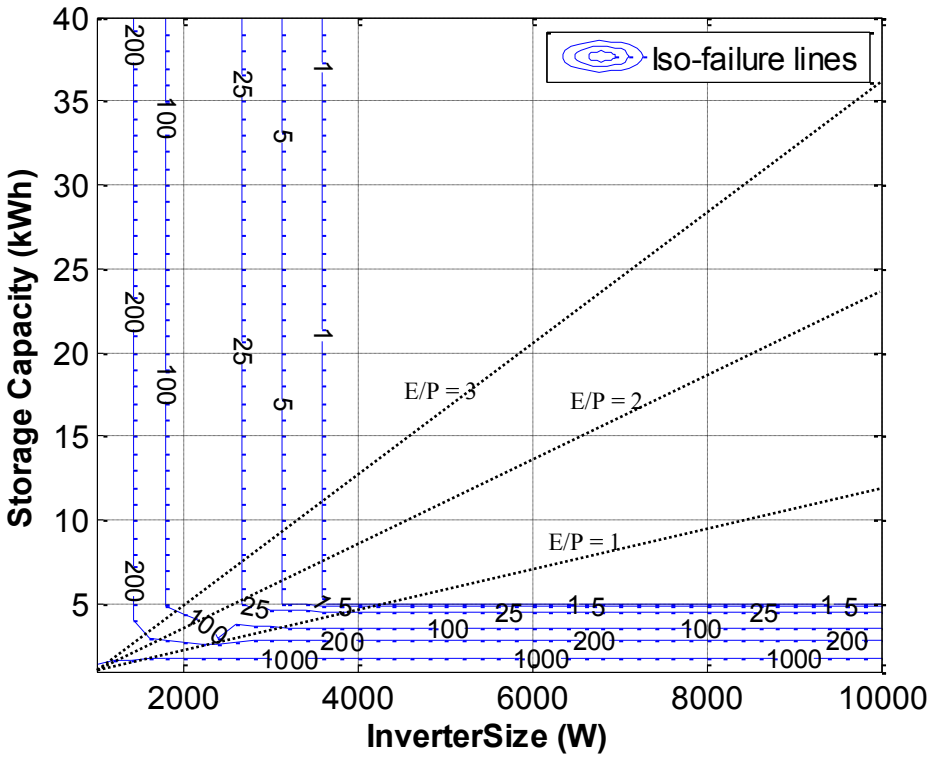

Figure 21: 2D BESS iso-failure plot with 5260 W peak limit (constant E/P lines plotted for battery selection assistance)

Constant E/P lines are also plotted on this graph to provide a reference for battery technology selection. In this case the minimum system size represents an E/P ratio between 1 and 2. This would suggest peak shaving is a medium duration service and lead-acid or lithium-ion batteries are appropriate for use in this application. Based on additional factors presented later in this document, lithium batteries were ultimately selected for this application.

Using this system selection procedure, BESS sizes and grid demand limit set points for each region were selected and are shown in Table 7, along with the reduction in maximum peak load that would be achieved using 1.5% percentile peak limit selection. Results in Table 7 are rounded up to the nearest 0.5 kWh and 100 W to avoid under-sizing and eliminate excessive precision. Percent reduction in peak demand is the percent of the existing maximum peak that is reduced, in Atlantic Canada this would be 1 – (5260W / 9070 W) = 42%. A complete collection of sizing iso-failure plots for all regions assessed can be found in APPENDIX B.

Table 7: BESS sizing and estimated peak reductions

Region	AT	QC	ON	PR	BC
BESS energy storage capacity (kWh)	5	22	8	5	5
Inverter power(W)	3600	4400	3200	2600	5200
Grid demand limit (W)	5260	9570	3790	2600	6630
Percent reduction in peak demand	42%	28%	47%	49%	45%

The resulting system sizes appear to follow expectations when compared to annual average house demand and maximum house demand with the exception of the BC storage requirement. Despite having an average demand nearly three times larger than the Prairies the resulting energy storage requirement is the same in BC as it is for the Prairies. Energy consumption of the QC region is very high and both DHW and space heating are provided via electricity, so it is expected that the storage requirement is significantly higher than other regions. The Quebec house is the only one with electric heating, and despite having similar AL electricity consumption, DHW consumption, and housing parameters as the Atlantic region house, the energy storage required is four times that of the Atlantic house and the peak reduction is significantly less than any other region. This indicates electric space heating is the largest influence on BESS storage requirements (as would be expected based on observation of gross heating energy requirements) and can severely inhibit the ability of a BESS to provide adequate peak shaving due to the long duration of peaks experienced by electric heating. Inverter sizes line up with expectations based on maximum house demand for each region.

Both storage capacity and inverter sizes presented in Table 7 are feasible for installation at a typical home. Lithium-ion batteries readily achieve performance values of 200 Wh/L [18]. Therefore, a 5 kWh lithium-ion battery pack will occupy approximately 30 L volume (0.03 m^3) and can easily and safely fit in a small cabinet along with a 3000 to 5000 watt inverter for installation in a mechanical room or basement location.

For the interested reader, a three dimensional iso-failure plot was created by grouping system variations (3 parameters) which limit failures to a specific value. This plot is essentially a combination of both 2D iso-failure plots to create a three-dimensional failure surface. An iso-failure surface plot (1 failure) for the Atlantic house is given in Figure 22.

System sizes that are on the surface experience a single five minute failure event per year. Systems sized above the surface and out of the page experience no failures. Systems sized below the surface and into the page fail on more than one five minute occasion per year.

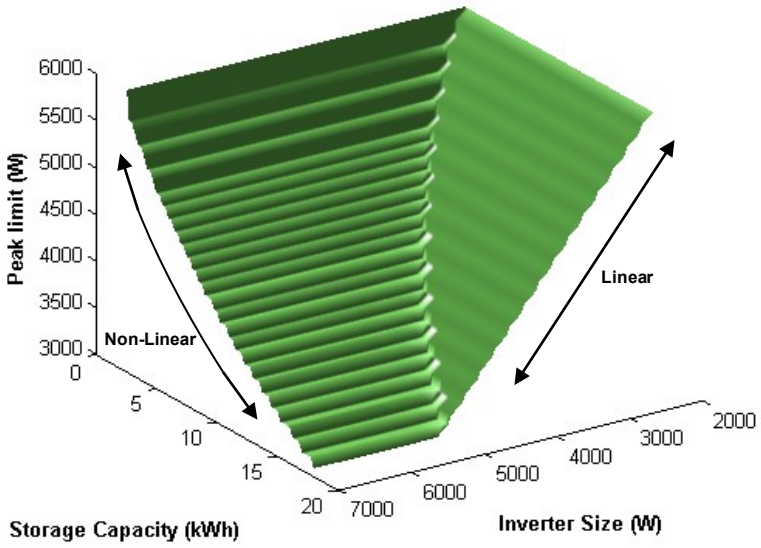

Figure 22: 3D BESS iso-failure surface plot of capacity with 1 failure event

This surface reveals several interesting results that describe optimal system configurations. In the plot two "walls" of failure intersect to form a non-linear corner geometry. The "wall" on the left is the energy failure wall where complete discharge failures occur if a smaller energy capacity is selected. The "wall" on the right is where undersized power failures occur if a smaller inverter size is used. The energy failure wall displays a non-linear profile and the power failure wall displays a linear profile.

3.3.5 BESS Lifetime

The system will eventually fail due to battery capacity fading, and the batteries will need to be replaced if continued operation is desired. The lifetime of a BESS is dependent on many factors including battery chemistry, state-of-charge, number of cycles, temperature of operation, time, and many others. Modern day lithium-ion batteries have been shown to last more than 3000 full discharge cycles [18, 19]. To assess the lifetime of the BESS

for the peak shaving application, Figure 23 shows a histogram of the lowest state of charge at the end of each day for an entire year for the Atlantic region.

The operation of the system between 85% and 15% SOC is evident from this plot. On 200 days of the year, the system either does not discharge at all, or only discharges between 0 and 2.5% of its capacity. This means that the system only experiences discharge 165 days of a given year, resulting in 165 shallow cycles per year. The cycles are generally limited to less than 20% of capacity and therefore the actual cycle life of the batteries would be much greater than the 3000+ deep cycle life of lithium-ion batteries. This would imply the system could continue operating for 20-30+ years; however, Lithium-Ion batteries also experience calendar aging due to parasitic reactions that gradually consume active materials and reduce capacity [133]. As a consequence the system will only last as long as the calendar life of the batteries themselves.

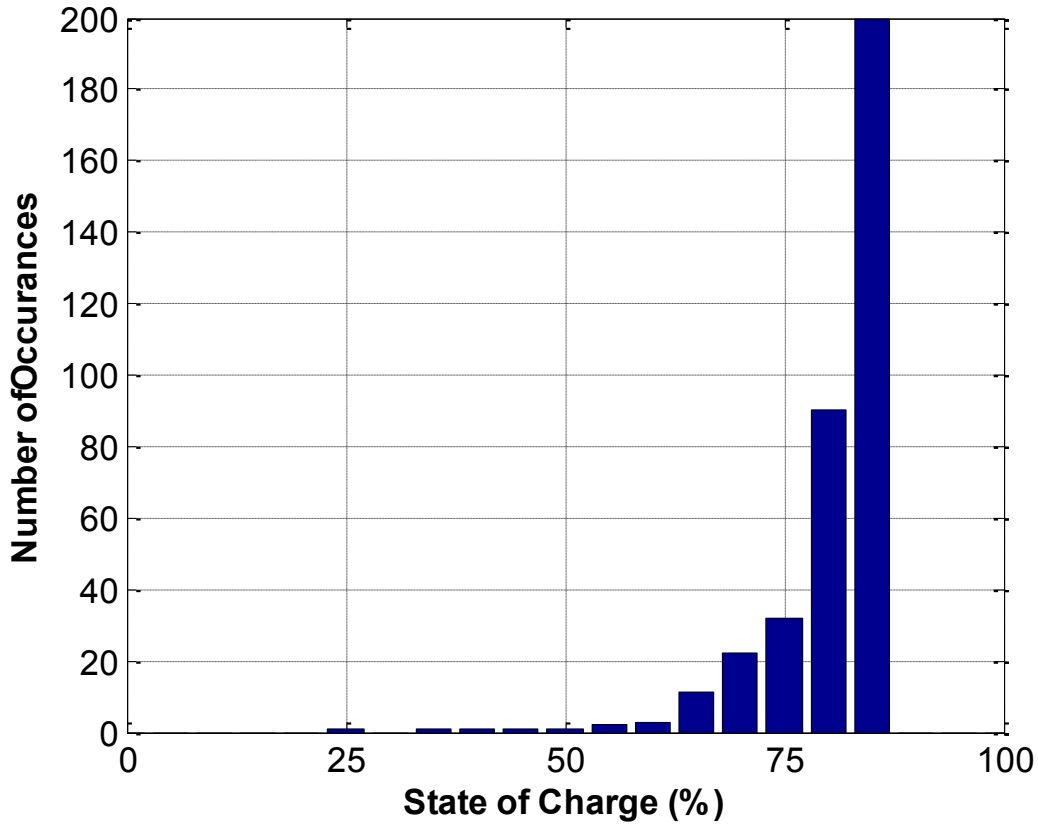

Figure 23: Histogram of lowest battery state of charge experienced each day of a year

Tests on commercially available lithium-iron phosphate indicate that even during storage at 25 ℃, approximately 3% of capacity is lost in the first year of operation. Under constant complex cycling (24 hours/day for 365 days) 7-8% of capacity can be lost per year [133]. The batteries used in this energy storage system are likely to behave similarly to the "stored" capacity loss as they are minimally cycled and infrequently experience complete discharge. Assuming 4% capacity loss in the first year and 2% per year for the remaining years the system will operate for eight years before the generally accepted 80% capacity failure criterion is observed. This is a very conservative estimate, and other commercially available large format lithium battery types have estimated operational lives of 10-20 years for shallow infrequent cycling operation at 25 ℃ [134].

With reduced capacity caused by years of operation it is advisable that the peak limit be adjusted or the inverter maximum output capacity be limited to ensure energy failure type

events do not occur. Energy failure events cause complete system shutdown during the peak demand times of the year and should be avoided.

One additional point of interest raised by the knowledge of discharge occurrences for various depths is the possibility of operating the BESS between the full 0% and 100% states of charge, or at least expanding the range beyond 15-85%. As deep discharges are so infrequent, this will have little impact on overall battery life and would allow reduction of storage requirements by 15% for 10-90% SOC operation and reduction of storage requirement to 42% for 0-100% SOC operation. Alternatively, the sizing could be performed as presented and the allowable SOC range increased over time to accommodate the gradual capacity reduction. Another possible modification would be to have a floating grid demand limit which would allow more frequent utilization and additional peak shaving during both high and low demand times of year.

3.4 Conclusion & Recommendations

Using the CHREM, residential electricity profiles were generated for 5 regions across Canada. The houses were selected based on typical values for various parameters within each region. Once simulated, the profiles underwent a statistical analysis to determine electricity requirements for each region. A BESS model was developed for peak shaving applications, into which the electricity demand profiles for each region were input. Through parametric study the failure levels of each system were identified and an envelope of BESS sizing based on maximum grid demand limits was determined. Peak demand reductions of between 42% and 49% are achievable in all Canadian regions except Quebec (peak reduction of 28%). These reductions are achieved with a BESS energy capacity of 5 kWh in the Atlantic, Prairies, and BC regions, and an 8 kWh capacity in Ontario. The typical Quebec house requires a significantly larger energy storage capacity of 22 kWh which results from the use of electric heating in this region. Such a large system size in the Quebec house indicates the use of a peak shaving system may be unfavourable in this region, or more generally in houses with electric heating. Inverter sizes are fairly similar, ranging from 3.2 kW to 5.2 kW.

The systems failure method is the eventual calendar aging of the lithium-ion batteries and is expected to occur after 10-20 years as the batteries experience light cycling and infrequent deep discharge.

This scoping model is suitable for preliminary assessment of BESS storage and power requirements of individual residential peak shaving systems. It would also be worthwhile to study of the benefits of aggregation of demands in a community type energy storage system. The present work could be combined with work presented in [135] to quantify the effects and possible benefits of community based systems. It is likely that some degree of communal benefit would be achieved with respect to energy storage and power capacity requirement on a per house basis.

CHAPTER 4 EXPERIMENTAL BATTERY CYCLING APPARATUS

The peak shaving model presented in the preceding chapter provides a starting point for the design and accurate simulation of a residential scale BESS. Using the results obtained from the peak shaving BESS system scoping model the requirements for an experimental BESS can be specified. Then, using this experimental system, a more advanced battery model can be developed, calibrated, and validated with measured system performance data under complex peak shaving loading profiles. The details of construction and operation of the developed experimental BESS is the topic of this chapter. Results from the previous chapter indicate energy storage capacities of 5-8 kWh and inverter sizes of 3.2 – 5.2 kW satisfy the peak shaving requirements of the typical home in all but one region (QC) in Canada. These sizing values provide the basic design parameters for the experimental BESS.

4.1 BATTERY BANK

Selection of the battery type used in a BESS is the single most important factor with respect to overall success and longevity of the system. Without the correct underlying characteristics of a specific battery technology, even a BESS with excellent control and management methods will not achieve the performance and cycle life levels of a BESS with a more appropriate battery technology. Chapter 2 presents appropriate battery technologies for various applications based on E/P ratio (discharge duration) and Chapter 3 suggests lithium batteries are appropriate for the applications discussed. Lithium iron phosphate (LFP) batteries are one type of commercial lithium-ion power cells and display high cycle life, excellent power output capabilities, decreasing costs, and relative safety over other lithium battery technologies. As such, LFP batteries were selected as the technology to be used (and modeled) in the experimental BESS.

Based on results presented in Chapter 3 (5 – 8 kWh / 3.2 – 5.2 kW) a battery bank capacity of approximately 6 kWh was selected as this level of storage exceeds the Atlantic, Prairies, and BC home storage requirements by 20%. This excess capacity was included to prevent under-sizing resulting from any inaccuracies present in the scoping

model. In practice 20% excess capacity should also be included to account for long-term capacity fade, enabling the system to perform the required operations until the widely accepted 80% of original capacity end-of-life criteria is reached. Battery pack voltage should be maximized to reduce current requirements compared with typical 12 or 24 V systems, thereby reducing cabling and connection losses and costs. The availability of 72 V equipment in the Renewable Energy Storage Laboratory (RESL) where the work was to be conducted was the principal reason for selecting this voltage level.

LFP batteries have a nominal operating voltage of 3.3 V. To simplify wiring and reduce the number of connections a system of series connected cells was designed. In this configuration, 22 cells are required to achieve a nominal 72 V (3.3 x 22 = 72.6 V). A storage capacity of 6 kWh at 72.6 V nominal requires 82.6 Ah total (6000 Wh/72.6 V = 82.6 Ah). Because of the series connection, individual cell capacities must each be 82.6 Ah. The next available LFP cell size after 80 Ah is 100 Ah. LFP cells rated 100 Ah are available at RESL. The cells were donated to Dalhousie University by ZENN Motor Company in the summer of 2011. They were originally intended for use in a prototype compact electric vehicle, and experienced limited cycling during their time at ZENN (less than 50 cycles). They were received at Dalhousie in excellent physical condition, and between 50-75% state-of-charge. A single battery cell is shown in Figure 24.

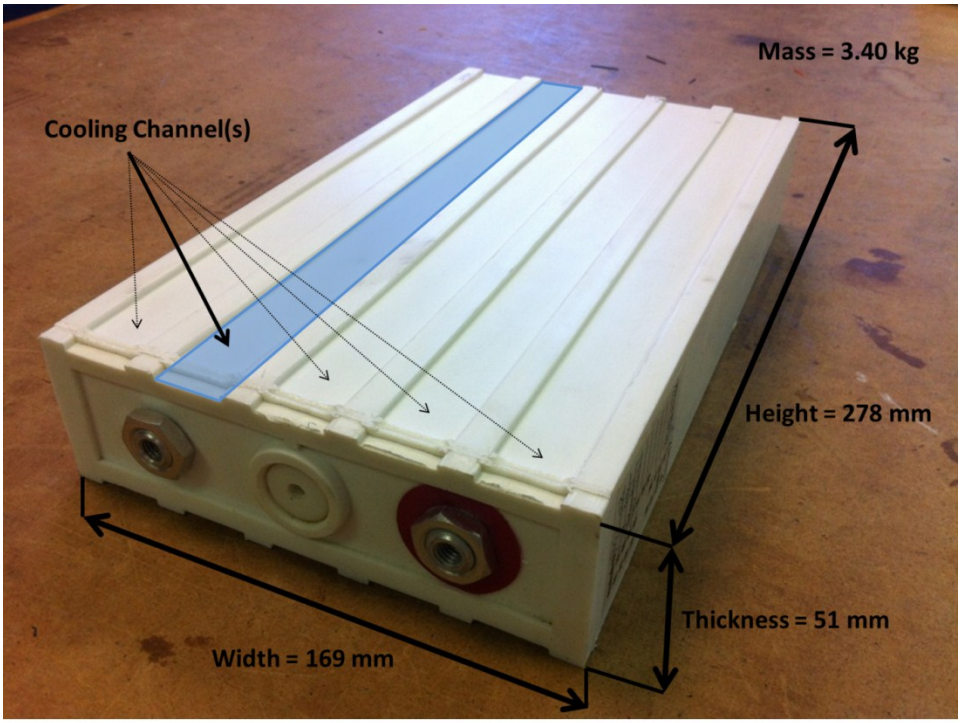

Figure 24: Lithium iron phosphate cell with nominal ratings of 3.3 V and 100 Ah

At the rated 100 Ah capacity, the storage capacity of 22 cells would represent a total energy storage capacity of 7.26 kWh (1.26 kWh larger than required). Capacities listed from the manufacturer are often for 20 hour rate discharge tests, and for a 1 or 2 hour discharge the capacity should be expected to 10-20% less depending on battery chemistry. To establish the actual capacity several cells were cycled using a power supply and several power resistors. Cycling tests revealed the actual capacity of the cells tested was approximately 88 Ah at a 4 hour rate. A bank of 22 cells rated 72.6 V with 88 Ah capacity corresponds to 6.39 kWh of storage capacity; reasonably close to the desired 6 kWh.

The assembly of 22 cells into a complete battery bank requires consideration of a number of mechanical and electrical factors. First and foremost the battery bank must be safe under all modes of operation, including emergency situations such as fire resulting from short circuits or severe overcharge. Emergency situations require that the battery bank either be completely enclosed in a fireproof container, or have enough mobility to be removed from the building. A protective fire-proof case would be the only solution in a

home installation as the user would not be responsible for monitoring or addressing emergency situations. In a laboratory scenario a mobile battery bank provides a means to remove the battery bank in the case of an emergency, while also allowing flexibility in lab setup. This safety method (mobility) was selected to allow for simple of operation and modification of the experimental test setup. A large metal cart with a 500 kg rated load capacity and large castor wheels (see Figure 26) was used as the means of support and mobility of the battery bank.

Case or terminal damage resulting from falls can result in loss of containment of the internal contents of the batteries and therefore must be avoided through proper design of a stable support structure. By clamping many batteries together and increasing the width of the base through the use of wide end-plates, a stable support structure was created for the experimental BESS. Two banks were assembled rather than a single large bank to accommodate the use of a mobile cart. The wiring layout of the battery pack can be seen in Figure 25.

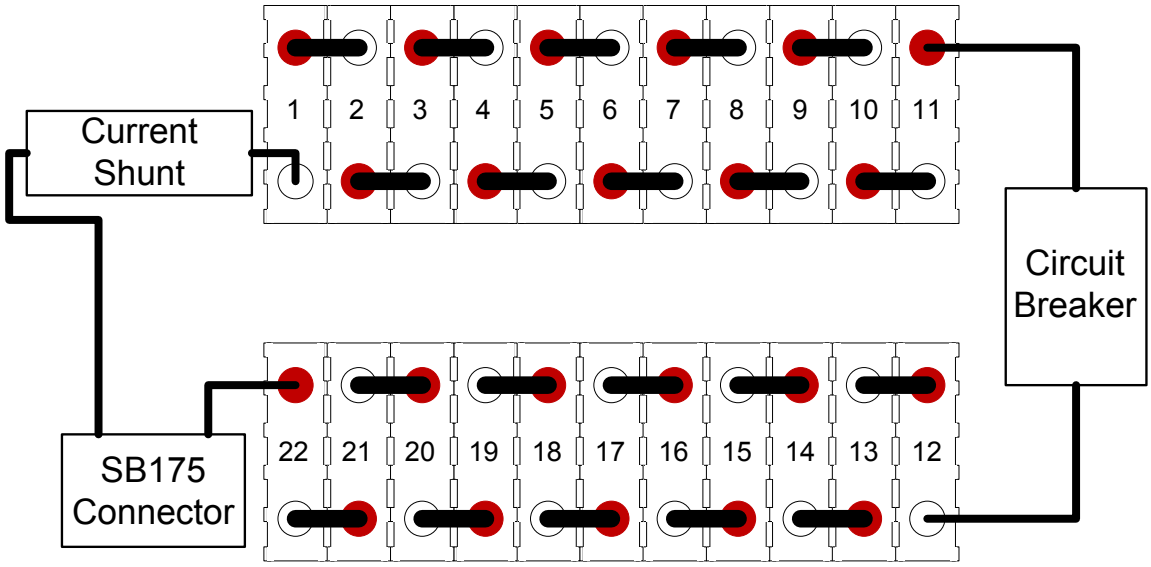

Figure 25: Battery pack wiring

The two battery banks resting on top of the mobile battery cart (along with other system devices) can be seen in Figure 26. The clamping pressure used to secure the batteries was kept as low as possible to prevent excess compression of the electrodes and separator material. In [136], Peabody et. al. showed that increasing stack pressure results in

separator layer degradation through closure of separator layer pores. Pore closure impedes ion migration and consequently increases internal resistance and accelerates capacity fade. The carbon anode in lithium batteries expands nearly 10% when cycled from fully discharged to fully charged, which already introduces stress in the separator layer; therefore, the clamping pressure must be maintained at the lowest possible level to prevent additional separator layer degradation.

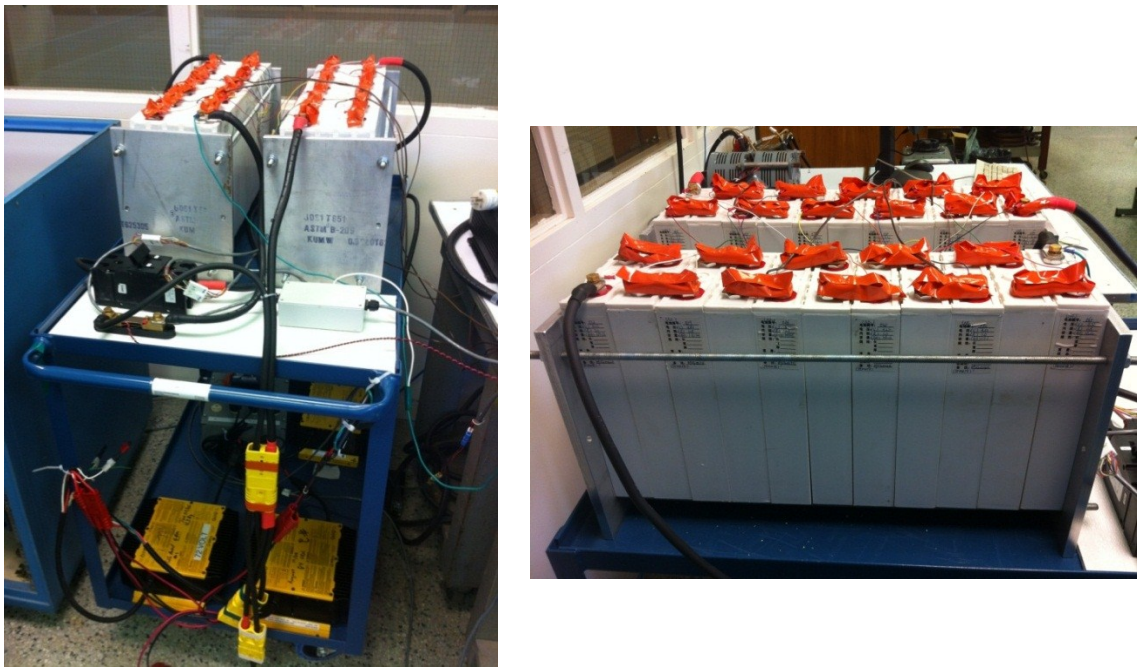

Figure 26: Battery banks & mobile battery cart (with breaker, voltage divider, current shunt, chargers, AC box, and cabling also showing)

The support structure also elevates the cells (as can be seen in Figure 26). This elevation is included to enable natural convective cooling to occur between the cells. Lithium-ion batteries operated at temperatures significantly higher than room temperature (40+ degrees) display significantly reduced cycle life and storage life [44]. Additionally, heating of cells within the pack causes increased self-discharge rate [137, 138], with uneven heating within the pack eventually leading to cell imbalance. The cells have ridges along the vertical surfaces between cells that create thin channels as can be seen in Figure 24. If the cells are sufficiently elevated, natural convective currents can develop in these channels and draw air in from beneath the cells to enhance overall cooling of the cells, and help extend the cycle life of the BESS and reduce cell balancing requirements.

The final consideration in battery bank design is the electrical interconnection and electrical protection of the cells. To reduce resistive losses and simplify pack assembly 1/16” by 1” copper bar was bent into shape using a custom made dyie and press, and 8 mm holes were drilled on either end for battery terminal connection. An arc was pressed into the bar to minimize lateral forces on battery terminals created by differences in cell size and terminal placement from cell to cell. The resulting connection piece can be seen in Figure 27.

Figure 27: Cell connection bar

To protect against short circuit and provide an emergency shutoff method, a circuit breaker was included between cells 11 and 12 of the battery pack. By including the breaker in the middle of the battery bank, the maximum possible voltage between safety devices in the battery bank is reduced by a factor of two, which lowers the maximum possible voltage to approximately 37 V.

4.2 Power Equipment (Charge and Discharge)

The charge and discharge equipment required for the experimental BESS needs to provide power output levels of 5.2 kW discharge and enough charge capacity to fully charge the battery bank from 0% to 100% in 5 hours or less (as specified in Chapter 3). Based on these requirements a 5.2 kW discharge system and a 2.7 kW charge system were designed and built.

4.2.1 Discharge System

The discharge system in this experimental BESS is designed to fulfill the roll of the house electricity demands by offering continuously variable and programmable discharge operation. In order to achieve continuously variable discharge a 72 V DC/DC motor controller was selected as the power output device. Although this device does not convert the electricity to AC as would be the case in a house, adjustments can be made in coding for the efficiency difference between this DC/DC device and a similar quality DC/AC (inverter) device should consideration of these differences in efficiency be required. The main function of this discharge apparatus is to develop and validate a battery model, therefore measuring DC/AC efficiency is not crucial to the success of this system.

The 72 V motor controllers used in the system was a GE 72V IC3645SR7A353T4 DC motor controller. The controller is designed for use with separately excited DC electric motors and offers numerous controllability and safety features, as well as power capability in excess of 5.2 kW. This controller was chosen because it met the power and continuous variability requirements of the discharge system, and also was also available at RESL (loaned by DHS Engineering Inc.). In this application the motor controller was coupled to large power resistors for ease of control code development and overall simplicity of the discharge system. The power resistors were wire-wound radiant/convective heat transfer type power resistors, each with a resistance of approximately 1.6 ohm and power rating of 1 kW. The bank of resistors was made of 6 parallel connected resistors for a total theoretical resistance of 0.233 ohms and a power capability of 6 kW. The actual resistance including wiring and connections was approximately 0.247 ohms. The resistance of the power resistors was selected to match the maximum voltage level of 36 V of the armature output of the DC/DC motor controller. With 36 V maximum output at the armature and 0.247 Ohms resistance, 5.2 kW discharge capacity is achieved.

The motor controller efficiency in the experimental setup was found to be approximately 80%, which was lower than anticipated. The 80% observed efficiency corresponds to over 1 kW of required heat dissipation during maximum operating conditions. The motor controller installation guide specifies bolting the controller to a large metal heat sink on

the chassis of the vehicle to increase heat transfer capability; unfortunately no such chassis was available in this system. In the place of a large heat sink chassis, an aluminum heat sink and fans were secured to the heat transfer area of the motor controller and the entire device was mounted vertically as seen in Figure 28.

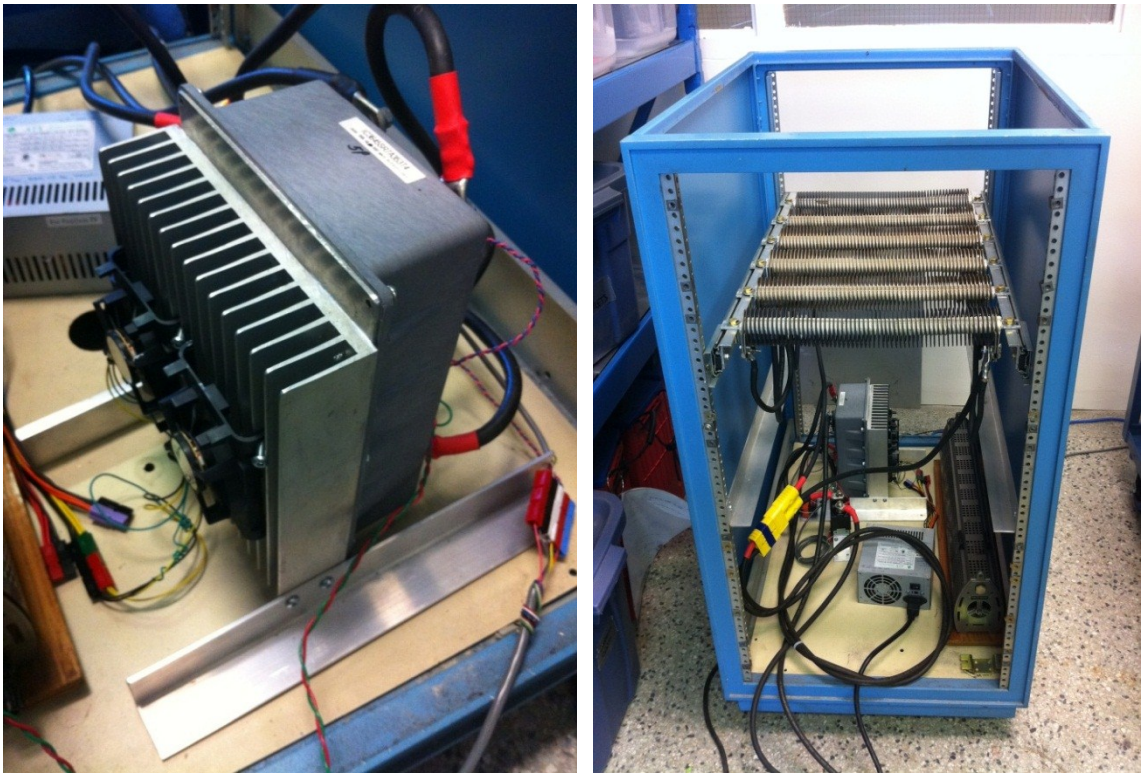

Figure 28: Motor controller heat sink & mounting and discharge assembly

A simple heat transfer analysis of this scenario was conducted to ensure cooling was adequate. The total surface area of the heat sink corresponds to 2.65 m^2. The attached fans create a forced convection scenario, which can easily achieve convective heat transfer coefficients of 100 W/m^2K [139]. Based on these values, the thermal resistance is decreased sufficiently to achieve a temperature drop of only 4 ℃ across the convective layer according to:

$$\Delta T_{convective} = \frac{1000\text{W}}{2.65\text{m}^2 \times 100\ \frac{\text{W}}{\text{m}^2\text{K}}} = 3.8\ ℃ \approx 4\ ℃ \qquad (5)$$

Heat transfer compound was included between the heat sink/controller interface as per specifications in the controller manual. It was assumed that by following manufacturer specified setup methods the temperature drop across the thermal interface layer and

internal controller heat sink are kept to a minimum. With only 4 ℃ temperature drop across the convective layer and use of the specified mounting setup to minimize internal temperature gradients, the controller will easily maintain an output level of 5.2 kW in an ambient temperature of 25 ℃. With 0.028 $\frac{m^3}{sec}$ of airflow provided by the attached fans, the 1 kW required heat dissipation is achievable with only a 3 ℃ temperature rise in the air stream according to:

$$\Delta T = \frac{1000\text{W}}{0.0283\frac{\text{m}^3}{\text{sec}} \times 1.2\frac{\text{kg}}{\text{m}^3} \times 1000\frac{\text{kJ}}{\text{kg} \times \text{K}}} = 2.94℃ \quad (6)$$

More detailed treatment of the heat transfer was not conducted due to the very low temperature rises found using this simple method and experimental results showing the controller can run continuously at 5.2 kW.

The motor controller requires several on/off control signals (key, start, forward) as well as a throttle signal to control the output level of the device. The motor controller has a built in high DC contact coil driver for a contactor that is installed in line with the positive terminal of the motor controller. This high current contactor is used to shut down the motor controller if a dangerous condition, such as short-circuit, reverse polarity, or overheating, is present and was used as the main protection device for the discharge system. Additional protection was incorporated into the discharge system by including manual connectors. The connectors are Anderson Power Products SB175, high strength casing, 10 kg disconnect, 175 A continuous current, connectors capable of several hundred hot disconnect cycles at 75A.

4.2.2 Charge System

The most widely used charging method for LFP batteries (and batteries in general) is a two stage method which first charges at a constant current until a set voltage level is achieved, and then charges at a constant voltage with continually decreasing current. This method is known as constant-current, constant voltage (CC/CV) charging and minimizes charge time, while also protecting the cells from damaging high voltage states. An

example, the voltage and current profile for a CC/CV charge provided by the LFP battery manufacturer is shown in Figure 29.

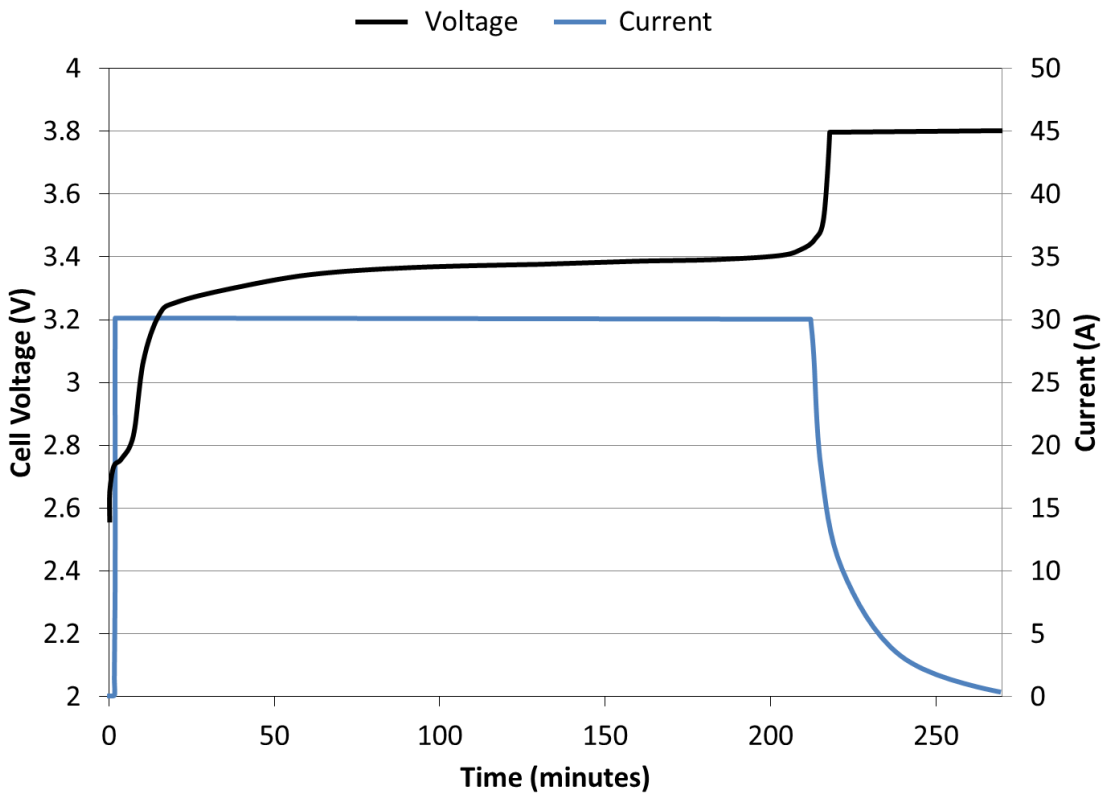

Figure 29: CC/CV charge profile

For lithium batteries, the majority of the capacity is charged in the CC stage, and the constant voltage stage charges the battery to the full 100% over several hours. As the CC stage current is increased the time spent in the CC stage decreases; however, the time spent in the CV stage increases with the final result being decrease in total charge time. There are limitations on maximum charge current imposed by thermal considerations of the battery, with higher temperature charging creating reduced cycle life and potential safety issues. For this BESS, the power capacity of the battery charger was selected such that a C/3 rate was achievable, as this was indicated in the specification sheet to charge the cells in 5 hours. Increasing charge rate would decrease charge time but increasing current would also increase charging cell temperatures and reduce cycle life. With a full 5 hours available for charging in this application there is no need to increase the charging rate.

Selection of battery chargers was based on achieving at least a C/3 rate which corresponds to 30 A for the 88 Ah LFP pack. Three DeltaQ battery chargers with 12A, 11A, and 9A capability were available in the RESL lab (donated in kind by DHS engineering) for a total current capability of approximately 33 A. With this charge capability a full charge is possible in just under 5 hours. The chargers are high-efficiency, power-factor corrected units that are very representative of the charge system that would be used in an in-home installation of the peak shaving system described in Chapter 3. The controllability of the chargers is not continuously variable and instead one of the chargers was configured to step down in several amp increments based on control signals received from the control and measurement system. This controllable charger requires 2 relays to change the resistance in a control circuit from 5 kΩ (decreases current) to 12.5 kΩ (holds current steady) to 20 kΩ (increases current). As a result of the stepped behavior of this charger, the actual current profile of the experimental BESS during the CV stage of charge is more discretized than the characteristic smooth decay that might be expected. An example of this is shown in Figure 30.

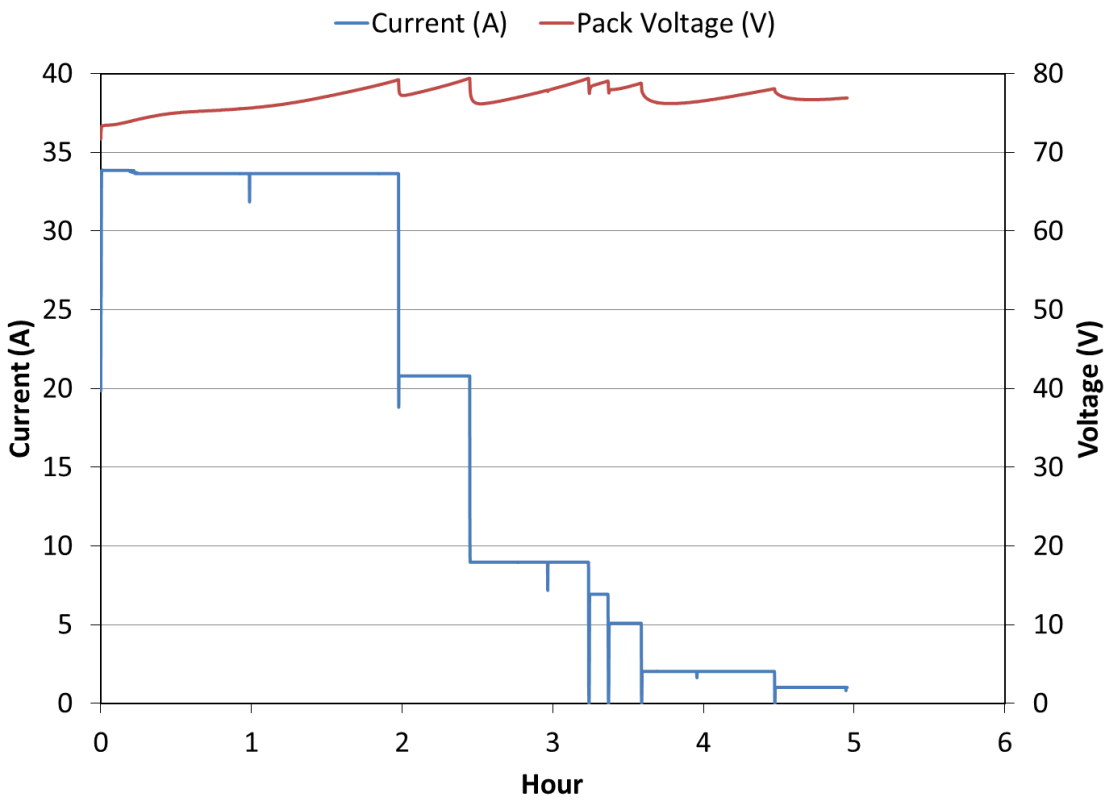

Figure 30: Stepped charge voltage/current profile

The plot in Figure 30 shows a constant current stepped charge profile and the resulting voltage response to such a charge method. It should be noted that the pack voltage peaks continue to decline as the end of the charge cycle approaches. This is the result of slight cell imbalances that cause one cell to trigger the high voltage cutoff before the other cells reach the same voltage level. As current decreases this difference becomes more pronounced because the apparent internal resistance of the highest cell rises much more rapidly than that of other cells. The use of this stepped charge method slightly increases overall charge time but efficiency remains similar to the idealized CC/CV method.

The battery charging system in the experimental BESS is a combination of the three battery chargers already discussed as well as AC fuses, AC contactors, and AC measurement equipment. These three functions (fusing, contactors, measurement) are performed by the custom designed AC control box shown in Figure 31.

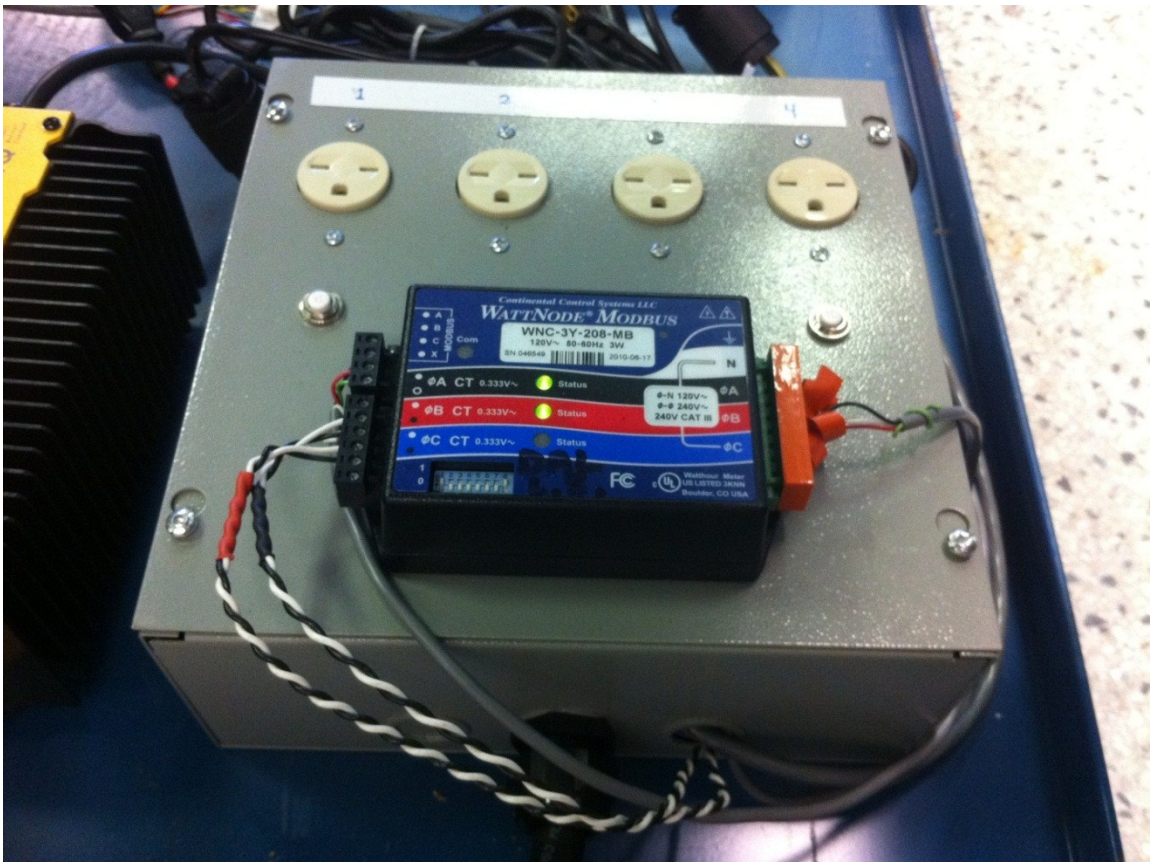

Figure 31: AC control box for charging equipment

Measurement of the AC voltage and current is accomplished through the use of a WattNode ModBus WNC-3Y-MB that communicates serially with the main measurement and control system. The circuits available in the RESL lab include a single-phase 208 V 50 A circuit (obtained from 2 phases and ground of a 3 phase wye 208 V circuit). This is the only laboratory circuit capable of supplying 2.7 kW of power required for the three chargers. For individual device protection a 15 A, 250 VAC fuse was included in the AC control box for each of the charger plugs. Additionally, a 15 A, 250 VAC contactor was installed in line with the fuse to enable on/off switching of individual chargers. Manual disconnection for simplicity and emergencies was also included through the use of NEMA 6-15 outlets for each charger.

4.3 MEASUREMENT & CONTROL SYSTEM

To control and measure all aspects of the charge/discharge system and battery bank, a reliable, accurate, and compatible control and measurement system was designed and constructed. Measurements must be conducted with frequency on the order of seconds to respond to all changes quickly to prevent dangerous operating conditions from arising. Table 8 lists the measurement and control features that the suitable system should provide.

Table 8: Measurement & control system requirements

Sub-System	Measurement/Control	Accuracy objective	Comments
BESS	22 cell voltages	1%	
	Cell temperature readings	±1 ℃	Min. 4 measurements
	DC current (150A shunt)	1%	60Hz noise cancellation recommended
	3 digital out for MUX control	N/A	For voltage divider MUX control
Discharge System	2 low coil current contact drivers for on/off control	N/A	5 V, 75 mA coil
	1 variable analogue out	1%	0-3.5V range required
Charge system	Serial CANbus communications for Wattnode connection	N/A	
	6 low coil current contact drivers for charger control	N/A	5 V, 75 mA coil

In addition to the requirements listed in Table 8 the measurement and control system must be able to operate during extended power outages and communicate all operational data to a computer for later analysis. Based on these requirements a Campbell scientific CR1000 was selected as the main control and measurement device, supported with the Campbell Scientific SDM-AO4 and the Campbell Scientific SDM-IO16 and a custom designed 24 input channel voltage divider with three CD74HCT4051 multiplex chips.

The requirement for individual cell measurement arises from the nature of series connected lithium batteries. To understand this requirement it is worthwhile to explain why some other batteries do not require individual cell measurements. In some battery chemistries (eg. lead-acid) a fully charged battery can still accept some amount of current through a bypass reaction. This allows series connected cells to be balanced by applying overcharge to some cells while the remaining cells reach 100% state of charge. Unfortunately lithium-ion batteries do not have a bypass reaction and once fully charged all current goes directly to heating of the battery, which inevitably results in overheating and failure. Because over-charge cannot be applied, some cells will slowly become unbalanced as cycles are performed due to differences in self-discharge rate resulting from slight variations in manufacturing and uneven pack heating. As a result, the entire pack is limited by the weakest batteries in the pack. For safety reasons the charge/discharge voltage cutoffs trigger based on the highest/lowest cell in the pack, which unfortunately means the weakest (lowest capacity) cell will cause the shutdown of discharge and charge before all other cells are completely discharged or charged respectively. To properly trigger charge and discharge limits all cell voltages must be measured, with the weakest dictating the operation of the BESS.

The 22 cell voltage measurements required both a multiplexer and voltage divider circuit to successfully and safely measure all cell voltages. This circuit is shown in Figure 32.

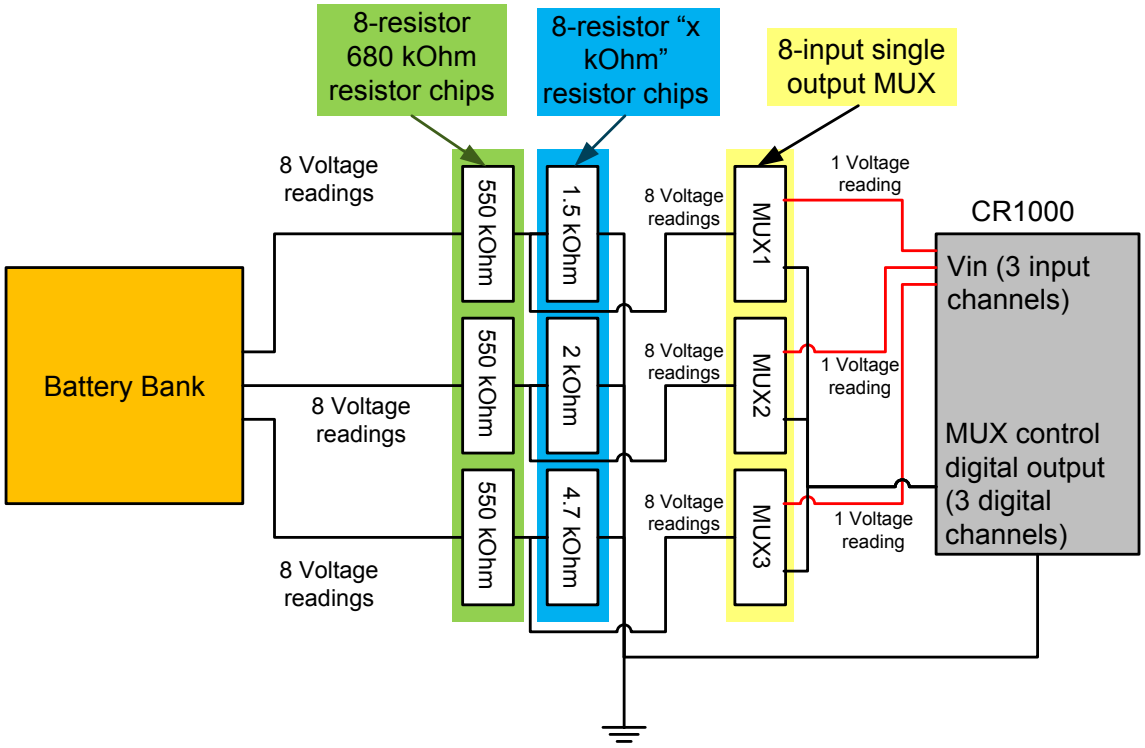

Figure 32: Cell voltages measurement circuit

The number of channels required to measure all 22 cell voltages exceeded the number of analogue to digital measurement channels on the CR1000, so to accommodate the large number of analogue input channels, three 8-channel multiplex chips were used to combine the 22 channels into 3 channels. Multiplexer control was accomplished through the use of three digital logic output ports on the CR1000. Cell measurement was conducted by cycling through the 8 multiplexer channels of each MUX and reading the output voltage of each MUX to one of three analogue input channels on the CR1000. The measurements conducted were of each intermediate pack voltage, and cell voltages were calculated by subtracting adjacent intermediate voltages. Additionally, the 5 V maximum input limit on the analogue input channels on the CR1000 made a voltage divider necessary to lower the measurements which ranged from 3 volts to 80+ volts down to a 0-5 V range. The voltage divider was calibrated in place using a Fluke 87 multimeter capable of 0.05% of reading + 1 significant figure accuracy. All measurements of cell voltages also underwent 16.66 ms integration to eliminate 60 Hz noise. The measurement error of the CR1000 is ±0.06% of the reading which corresponds to 0.048 V when measuring the highest voltage in the pack during charge (80.5V). Given the voltage

divider calibration was performed with the Fluke 87, error of 0.04 V + .01 V = .05 V is also introduced. Cell voltages are calculated according to:

$$V_{cell} = V_n - V_{n-1} \tag{7}$$

Based on this formula the root sum square error in the highest cell measurement (80.5 V) corresponds to:

$$V_{error,cell} = \sqrt{2 \times 0.05V^2 + 2 \times 0.048V^2} = \pm 0.098\,V \approx 0.1\,V \tag{8}$$

Cells in the middle of the pack would experience a $\pm 0.05\,V$error boundary and the cell measurement at the bottom of the pack (lowest voltage) experiences 0.0005 V error. The 0.1V error in measurement corresponds to 2.7% total error on the highest voltage cell in the pack assuming cell voltage is 3.65 V (80.5 V / 22 cells).

Suggested uncertainty level in measurement of the cell voltage was 1%, and in the present system, cell measurement uncertainty of 2.7% is present. Unfortunately due to the voltage levels in the BESS and the cell measurement method used, uncertainty levels below 1% were not achievable. The lower third of the cells are measured with less than 1% uncertainty; however the upper two-thirds are above this uncertainty level. Fortunately for the modeling efforts described in this paper the total pack voltage is the value of interest, and assuming a maximum voltage of 80.5 V, the total uncertainty is only 0.057 V, or 0.07%. Individual cell voltages are only used to trigger charge and discharge start/stop actions once the appropriate cut-off voltages are reached by one of the cells in the 22 cell pack. Therefore, the cell voltage measurement uncertainty will only result in pre-mature or late discontinuation of charge or discharge, and will not affect the accuracy of the voltages to be used in creating the BESS model that is discussed in Chapter 5. To prevent this uncertainty from creating unsafe voltage levels the cutoff voltages for charge and discharge were reduced and increased by 0.1 V respectively. This will have a marginal impact on the working capacity of the pack but will not affect modeled discharge curves in any other way than slightly truncating each end of the discharge curve.

The number of digital output ports required also exceeded the number of available ports on the CR1000. These digital output ports were used to directly control the multiplexers

and also act as coil drivers for contactors that were used to control the discharge system and charge system. To increase the number of available digital output ports the SDM-IO16 module was connected with the CR1000 which added 16 digital ports. The additional digital output ports are used to control the DC motor controller, AC box, and the chargers.

The discharge apparatus required an analogue voltage output between 0 and 3.5 V to control power output levels. To accommodate this requirement the SDM-AO4 module was included in the measurement and control system. The SDM-AO4 is capable of outputting 0-5 V in steps of 5 mV. With an output resolution of 5 mV, continuously variable discharge control is possible when used with the GE 72 V motor controller. The GE 72 V motor controller analogue input throttle control behaves in a nearly quadratic manner. A single quadratic function still leaves some degree of error in output control, and as such two quadratic functions are used to describe the ratio of input throttle (in mV), to output power (in W). When less than 160 W are desired, the function: Power = 0.297x - 149.58 describes the input throttle (mV) to the output power (W). When the power demand is greater than 160 W the relationship between the input throttle (mV) to the output power (W) is Power = $0.00152x^2$ - 1.46x - 87.39.

A circuit diagram illustrating the experimental BESS is presented in Figure 33.

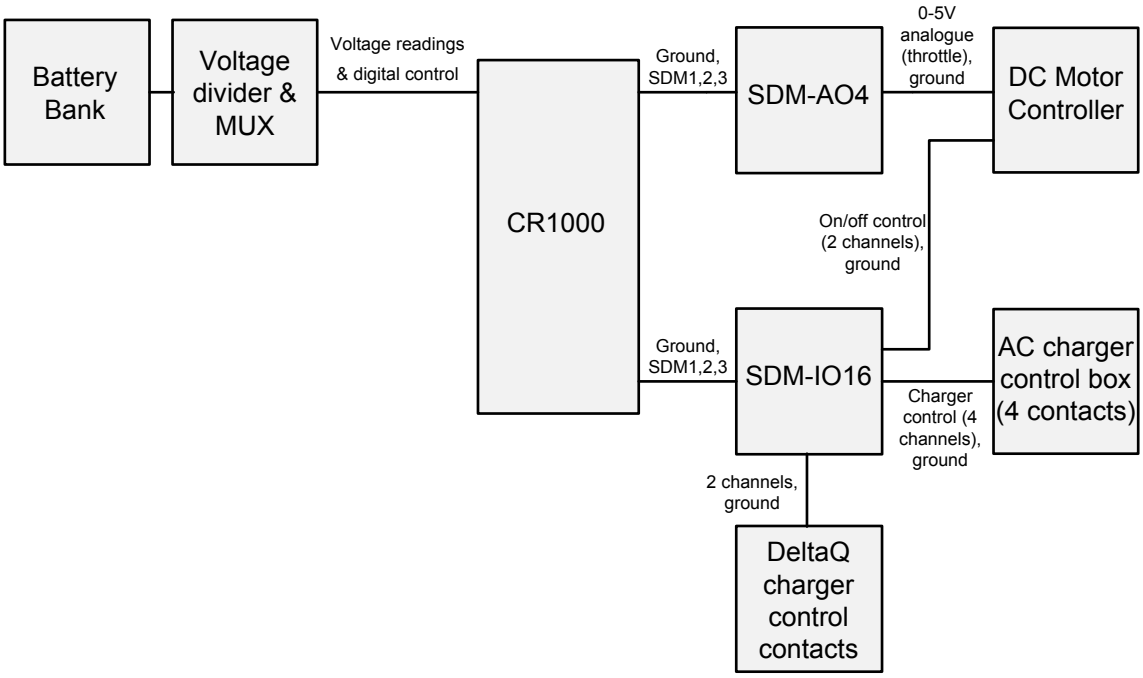

Figure 33: Control and measurement system wiring diagram

4.3.1 Code Strategy

During each one second scan interval of the CR1000 the following operations occur in the order listed:

1. Cell voltages, current, power, temperature, and energy are all measured or calculated

2. Safety and charge/discharge discontinuation parameter out of range conditions are checked (is $T_{max} > 40$ ℃, is $V_{cell,max} > 3.65$, is $V_{cell,min} < 2.65$)

3. Is discharge = yes? If so set throttle to appropriate value and begin throttle tuning

4. Is charge = yes? If so charge according to the previously described charging method.

5. Record data to data tables

6. Repeat scan at beginning of next one second interval

The throttle tuning described in step 3 of the code execution procedure refers to slowly increasing or decreasing the throttle value until the desired power or current level is achieved. During discharge, the input to output function changes as the battery voltage

declines. This throttle tuning is included to adjust the original throttle set point slowly until the desired output is achieved. This is performed by averaging the power or current (whichever one is the control) over several seconds and increasing or decreasing the throttle value slowly every 4-5 seconds until this averaged value is within 1% of the desired output level. Convergence to within 1% occurs within the first 30 seconds of the discharge period, and is maintained throughout the discharge period by continued throttle tuning.

CRBasic Code for BESS constant current and constant voltage discharge operation and CC/CV charge control can be found in APPENDIX C. Code for battery model validation (peak shaving operation) can be found in APPENDIX D. Additionally, the MatLab code for the peak shaving simulation and the LFP model can be found in APPENDIX E and APPENDIX F respectively. Detailed code operation is described in comments throughout each code.

4.3.2 Example cycling results

The main purpose of the experimental BESS is to provide a method to obtain experimental measurements from the battery pack to develop and validate a system model. The system model can then be used in conjunction with the previously developed peak shaving model to enhance the overall peak shaving model accuracy. An example cycle showing voltage and temperature profiles during constant current discharge and stepped charging (discussed earlier in this chapter) can be found in Figure 34.

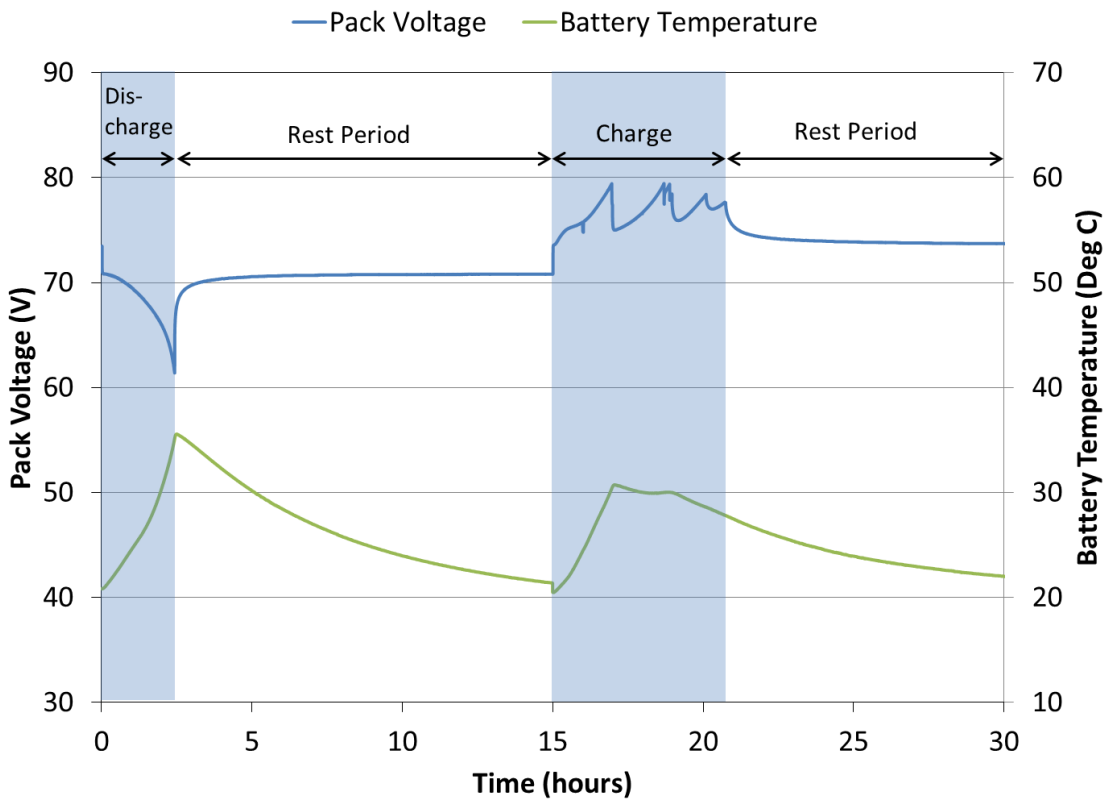

Figure 34: Voltage and temperature cycling profiles (35A discharge)

Profiles similar to this will be used in the following chapter to calibrate and validate a LiFePO4 battery model.

CHAPTER 5 LITHIUM ION BATTERY MODEL DEVELOPMENT AND CALIBRATION FOR PEAK SHAVING SYSTEM SIMULATION

This chapter has undergone scientific review and is accepted and will be presented at the 11th International Conference on Sustainable Energy Technologies (SET-2012) in Vancouver on September 2-5, 2012.

Jason Leadbetter is the principal researcher and author of the article. He conducted the research as part of his MASc. Thus, while he received supervision and guidance from his supervisor Dr. Swan, he carried out the work, wrote the published article, communicated with the scientific committee of the conference, and carried out the necessary revisions before publication. Writing support in the form of editing assistance and content guidance was provided by Lukas Swan. Some minor grammatical changes have been made to integrate the article within this thesis.

5.1 INTRODUCTION

Previous work presented a peak shaving energy storage system model that simulated house demand profiles when coupled with a simple battery energy storage system (BESS) model [141]. The profiles and models were then used to determine sizing and performance characteristics of BESS's for residential peak shaving applications in various regions of Canada. The battery model considered only stored quantities (no voltage or current characteristics) and constant efficiencies. This chapter presents an advanced battery model based on [24] as well as the experimental calibration and validation for the new battery model for use in the application described in [141]. Additionally, the results for the peak shaving model will be updated using the new battery model.

5.1.1 Battery Modeling

A detailed battery model is essential for accurate simulation of a peak shaving energy storage system. There exists a variety of battery modeling methods ranging from finite difference chemical simulation for high accuracy, high resolution (computationally

expensive) to simple equivalent circuit methods. For a comprehensive review of the various methods of lithium battery simulation the reader is referred to [142]. High resolution chemical and finite methods are computationally intensive and require a plethora of electrochemical parameters, many of which are not easily obtainable in the literature or using experimentation. The peak shaving model used in this work operates on 5 minute timesteps, and simulations occur over an entire year. Due to the large number of timesteps required, relatively coarse resolution, and availability of data, the high-resolution chemical simulations were deemed inappropriate for the application described in this paper.

5.1.2 Gao Model

The model presented in [24] was originally developed for lithium-ion batteries with cobalt based cathodes and has been shown to agree well with experimental manufacturer data of constant current discharge/charge curves. The basic premise of the model is to measure a single reference discharge curve at a rate close to the average expected operating range, and scale this curve using various factors to match discharge profiles at different rates. Based on assessment of energy/power and safety/modularity requirements from [141] and a review of the literature [18-20, 32] lithium-ion batteries with iron-phosphate based cathodes were selected for the peak shaving application presented in this work. As such, the Gao model was applied and required updating and calibration for a new cathode chemistry.

5.1.3 Peak Shaving Model

The peak shaving control methodology used is the same as is presented in Chapter 3. The energy storage system consists of a rechargeable battery, a bi-directional electricity grid-integrated inverter/charger, and a controller. The inverter/charger cycles the battery to reduce the house demand peaks as seen by the electricity grid. Once the new battery model is established, this chapter will examine a range of BESS for residences located in different Canadian regions and determine the most appropriate capacity, power, and cycle life to achieve the peak shaving objective.

5.1.4 Grid Electricity Storage

The storage of electricity for the purposes of peak demand shaving has been an area of great interest in the past several years, with numerous pilot projects being conducted in several countries [18, 19, 46]. Demand management is becoming important to electricity utilities as additional non-dispatchable generators, such as wind turbine generators, are brought online [1]. Daily peaking events can be costly and difficult to manage for utilities and one method to address these events at the distributed level is the use of small scale residential BESS. The peak shaving method presented in [141] and this article addresses peak loads directly, while indirectly supporting renewable energy integration by reducing maximum demands and thereby reducing grid congestion.

5.2 METHOD

Assessment of energy storage system performance requires information on the electricity demand of the residence as well as the battery system models.

First, a database of the Canadian residential sector (presented in [143]) was reviewed to identify and select typical houses from each of the five major Canadian regions. The major regions are Atlantic (provinces NF, PE, NS, NB), Quebec, Ontario, Prairies (provinces MB, SK, AB), and British Columbia. Second, an annual energy simulation of these houses was conducted on a five-minute interval so as to appropriately capture the peaks in electricity demand from the four major end-uses. Third, a peak shaving model coupled with a basic battery model applied to the electricity demand profiles to determine the energy storage and power characteristics required of the energy storage to reduce peak demand of the house as seen by the grid. This work was conducted and presented in [141]. The major results of Chapter 3 will be re-examined at various points in this chapter to provide context and support for the new research. The major focus of this chapter will be on developing and using an advanced battery model with the existing peak shaving model. The battery model presented in this chapter is experimentally validated, allowing a much higher degree of confidence in the results gained from the overall peak shaving model to which it is coupled.

5.2.1 House selection and simulation

A complete and detailed description of the housing selection and simulation process can be found in [141]. One typical house from each region (Atlantic, Quebec, Ontario, Prairies, British Columbia) was selected from the residential stock database. Houses were selected from the possible 16,952 houses in the database by progressively filtering each parameter towards the average value until only 1 or 2 houses remained for each region. The selection was done to provide a real data record of a typical house found in each major region of the Canadian housing stock.

The simulation of electric load profiles was performed using Canadian Hybrid Residential End-use Energy and GHG Emission Model (CHREM) [126, 127, 143] which employs the building simulator ESP-r [128] for the various selected houses using five minute time steps in combination with end-user non-HVAC electricity profiles developed in [130]. This time step was selected based on [130, 131] who showed that it adequately captures demand peaks, with little to no averaging effects.

5.2.2 Experimental BESS Setup

Figure 35 shows the experimental test setup used in developing the battery model of this paper. The test setup consists of four major components: battery bank (center top), control/measurement system (right), discharge equipment (left), and charge equipment (center bottom). In this setup the charging and discharging equipment is separate for testing purposes; however, in application combining these two devices would be more practical and reduce system cost.

Figure 35: BESS test setup

The charge and discharge equipment offers continuously variable power input/output to the battery bank at rates between 2.4 kW (charging) and 5 kW (discharging). The chargers are high-efficiency, power factor corrected DeltaQ units and the discharge side utilizes a GE 72 V DC motor controller coupled with two large resistor banks. The control and measurement device is a CR1000 from Campbell Scientific which is capable of measuring voltage to within 0.06% error and controlling and monitoring all associated charge/discharge equipment at a one second sampling rate.

The battery bank consists of 22 lithium-ion (iron-phosphate cathode) cells rated 3.3 V and 100 Ah per cell. The cells are connected in series to form a nominal 72 V battery bank. Such a battery bank was shown in [141] to be adequately sized for peak shaving operations of the majority of typical homes found in Canada.

5.2.3 Battery Model

The Gao model [24] is based on a lumped capacitance equivalent circuit approach and requires several constant current discharge profiles and pulsed current tests to obtain parameters for the model. Figure 36 shows the lumped capacitance equivalent circuit assumed in the Gao Model.

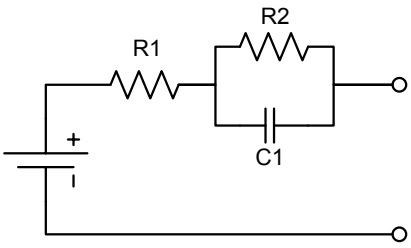

Figure 36: Lumped capacitance equivalent circuit

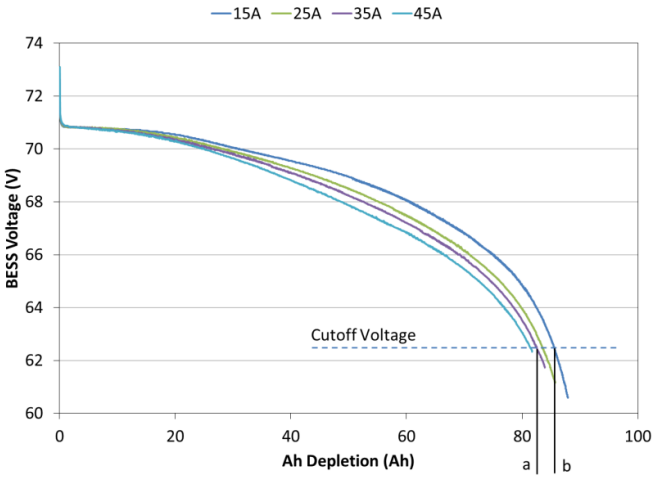

Figure 37: Vertically shifted discharge curves for model calibration

While some models attempt to derive complex relationships for the internal resistance component in the equivalent circuit as a function of current and depth of discharge (DOD), the Gao model instead scales a single reference constant current discharge curve to match discharge curves of different current levels. This is accomplished by introducing a scaling factor (α) for capacity change with respect to the reference curve. To calculate α the curve in question is first shifted up or down the voltage axis to the point where the voltage profiles match when DOD ~ 0 (i.e. the left side of the curves align) as shown in Figure 37. The two DOD's are taken as "a" and "b" at a specified cut-off and α is calculated according to equation 5 (see Figure 37 for location of a and b values).

$$\alpha = a/b \tag{9}$$

The values for α do not represent the actual change in capacity between varying current levels for a given cut-off voltage, as the actual change in capacity is more significant than the α values would indicate. Simply stated, α is the ratio of capacities between the shifted curve and the reference curve once the curve in question has been shifted up or down.

Once determined, α is included in the model as a scaling factor on the DOD calculation according to:

$$DOD_k = DOD_{k-1} + \frac{i \times t}{Cap_{ref} \times \alpha} \tag{10}$$

Where k is the index of the timestep, i is current, t is the timestep duration, and Cap_{ref} is the capacity (in Ah) of the battery pack at the reference curve rate.

Voltage is calculated according to:

$$V = V_{ref}(DOD) - i \times R_{int} \quad (11)$$

Where V_{ref} is a 5th order polynomial fit of the reference discharge curve and R_{int} is the internal resistance. The value of R_{int} is calculated by determining the resistance required to shift the curve in question up or down to the reference curve, as in Figure 37).

Consideration of temperature is achieved through introduction of a factor β; however in the present work battery temperature remains between 15 ℃ and 35 ℃ as these systems are installed in temperature regulated home environments. As shown in [24] the change in voltage and capacity is within 1-2% in this temperature range, which is well within acceptable error levels for such a model. As such, β was not considered in this implementation of the Gao model.

The effect of the capacitance (terms R2 and C1 in Figure 36) on voltage was not considered in the present work as all timesteps occur on a five minute duration (yearlong simulations prevent shorter timesteps from being computationally practical) and the transient characteristics of the battery occur on the order of 0.1-20 seconds. The loss in accuracy is small because these changes occur over short periods and display near first-order behavior. The final (pseudo steady-state) value is achieved in less than 5 seconds (1.6% of the timestep duration).

Once calibrated, the model provides voltage based on DOD and electric current. The model takes power requirement as an input, the voltage and current are calculated for a single timestep and the current is then integrated to determine the DOD and the next timestep. The DOD, voltage, and current are returned to the peak shaving model. The power requirement specified by the main program is increased in the battery model by a factor of 1.08 to include inverter losses assuming 95% inverter efficiency. These losses would place additional load on the battery pack itself and therefore must be included to maintain the accuracy of the simulation. Similarly, charging efficiency of 95% was

considered when calculating energy input required from the grid to charge the BESS. Measured calibration parameters that were used in the final model are presented in the results section of this paper.

5.2.4 Peak Shaving Simulation

The Peak shaving model remains nearly the same as in Chapter 3. The only difference is the inclusion of the updated battery model. The updated battery model takes the place of the simple energy calculation equation located in the bottom right hand corner of Figure 15.

Operation begins by determining the operational state: charge, standby, or discharge. The BESS operates the battery between 15% and 85% DOD to extend cycle life and ensure the system remains within safe operating conditions. Operation at DOD outside this range decreases cycle life and has the potential to cause malfunction [132]. The system recharges fully (to 12% DOD) between hours 00:00 and 04:59 if it is not fully charged. The system charges during the night as additional loads are easily supported by utilities during this off-peak period offered by utilities in many jurisdictions throughout Canada [23, 124]. During the hours of 05:00 to 23:59, if the power demand of the house is less than the specified grid power limit, the system does not charge or discharge (i.e. standby). If the house demands power in excess of the specified grid limit a series of logic operations are performed to determine the output required to keep the grid demand below the specified grid demand limit. Failure occurs if there is insufficient energy stored in the BESS or the inverter does not have enough power output capacity to meet the required demand.

During each timestep the peak shaving simulation sends the value of required power and present DOD to the BESS model; the battery model then returns the pack voltage, current, and new DOD to the main peak shaving program.

5.2.5 Peak Limit Selection

The grid demand limit is based on a percentile selection method using the house demand, that is fully described in Chapter 3.

5.3 RESULTS & DISCUSSION

The results of the battery model calibration and validation are provided in this section. Additionally, a summary of the results of the house electricity simulation profiles are included. Using the produced electricity profiles, the developed battery model, and the peak shaving model, peak shaving is simulated and results analyzed to select appropriate system sizes for houses of each region.

5.3.1 House Selection and Simulation

The full results of the house selection process can be found in Chapter 3. A summary/statistical analysis of results of the housing electricity load profile simulation is given in Table 9.

Table 9: Statistical analysis of regional electricity profiles

Region	AT	QC	ON	PR	BC
Annual electricity consumption (MWh)	13.2	32.8	8.4	5.8	17.3
Average house demand (W)	1506	3746	958	661	1976
Maximum house demand (W)	9040	15230	7188	5120	12002
Standard deviation of house demand (W)	1318	2980	858	571	1568
Maximum demand as percent of annual average demand	600%	465%	750%	775%	605%
98.5 percentile (W)	5260	10910	3790	2600	6630

5.3.2 Battery Model Calibration Parameters

The 35 A discharge curve was chosen as the reference curve for the Gao model. This selection was based on an operating range of 0-5200 W during discharge. Values of 35 A at 72 V corresponds to approximately 2500 W, very near the mean of the operating range, and using the reference curve near the average demand is specified to yield the highest

accuracy results in [24]. Figure 38 shows the resulting discharge curve and polynomial fit of the reference (35 A) discharge curve.

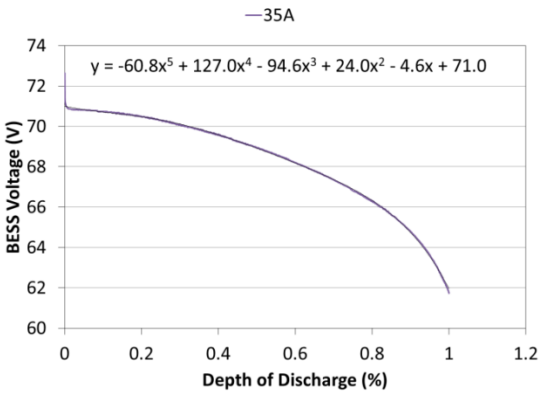

Figure 38: Reference constant current discharge curve (35 A)

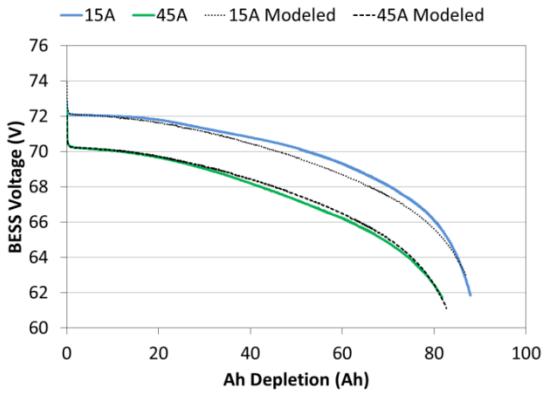

Figure 39: Modeled vs. experimental constant current discharge curves

Based on the steps outlined in the methods section the α values for various currents were calculated and are listed in Table 10.

Table 10: Measured alpha values

Current (A)	15	25	35	45	55
α	1.035	1.012	1.000	0.985	0.967

Internal resistance for the entire 72 V pack were found to be between 0.059 and 0.062 ohms at the start of discharge for all current rates tested. Internal resistance is a function of current and DOD; however, the current ranges in question show similar internal resistance at start of charge conditions.

To verify the functionality of the calibrated Gao model constant current discharges were simulated and plotted against the experimental results in Figure 39. The modeled results appear to agree well with experimental discharge curves.

Some discrepancy is seen in the discharge curves in Figure 39. For lower currents than the reference curve the model overestimates the voltage drop term during most of the discharge; however, the maximum error between the modeled and experimental voltage profiles is 1 V or approximately 1.5%. For higher currents than the reference curve less error is present. The error for the 35 A curve (not shown) is exactly zero at all stages, as it

is the reference curve. For lower currents than the reference curve the model tends to slightly underestimate the voltage drop. Actual internal resistance varies with both DOD and current and therefore these slight errors are to be expected in a model that adjusts a single curve to suit various rates of discharge.

5.3.3 Comparison of Modeled versus Experimental Peak Shaving

To test the accuracy and validate the battery model for this peak shaving application, modeled results and experimental results for an identical demand profile were captured and compared. The same apparatus that was used to calibrate the battery model was also used to run the experimental peak shaving profile to compare to the modeled results. Figure 40 shows the voltage profiles of both the experimental and modeled peak shaving operations for a given day of peak shaving of the Atlantic region house. Only periods of active discharge are shown as the model does not attempt to estimate resting voltage. Resting voltage has almost no impact on 5 minute averaged voltages or currents and therefore ignoring these will create no additional error.

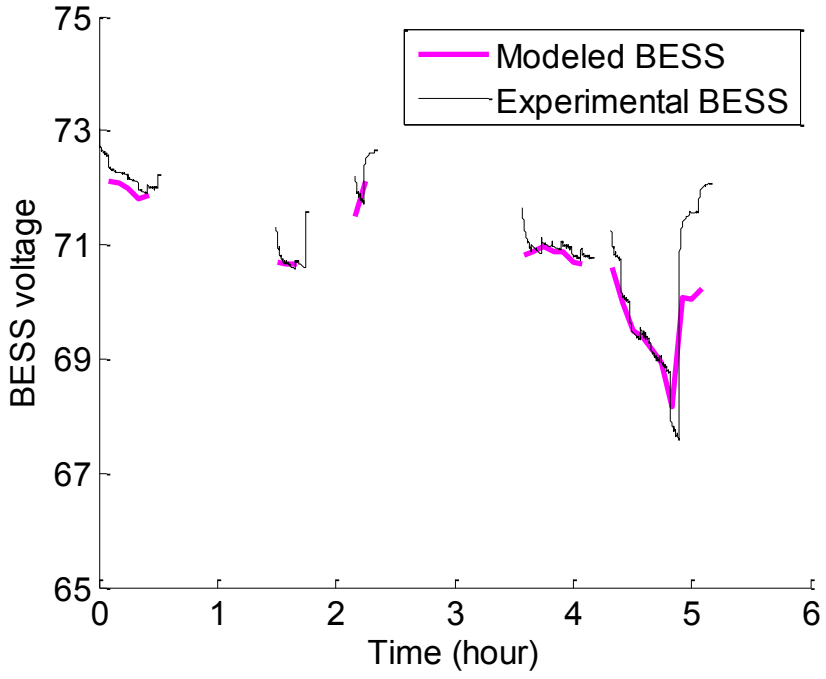

Figure 40: Modeled versus experimental voltage profile for one day of peak shaving operation

The results agree well with little visible error except for a slight difference after hour 5. This is the result of low power demand during this period, resulting in current requirement far from the reference curve value, where error is most likely to occur. Error at low currents is not as significant for energy considerations because the energy associated with these low current periods is small compared to energy required during high current periods. As a result, voltage error at these low current periods has less impact on overall energy error than voltage error at higher current periods.

To quantify the error, energy consumed during this peak shaving operation is found by integrating the power profile of either result. Experimentally, 2794 Wh were consumed during the peak shaving operations shown in Figure 40. The model result indicates 2762 Wh were consumed, a total error between experimental and modeled results of only 1.2%, well within acceptable limits for this application.

5.3.4 BESS Sizing Results

BESS sizing is performed by selectively varying parameters and counting failure events for each simulated system. Two distinct types of failure events can occur. The first failure is an energy depletion failure that occurs when the BESS has no stored energy remaining, after which the system can no longer output power to offset house demand. The second type of failure is an undersized inverter failure, which occurs when there is insufficient power output ability of the inverter to reduce the house demand to the defined grid demand limit.

To assess the appropriate system several thousand iterations were simulated in MatLab for each region and failure events were counted for each BESS system. The following BESS properties were varied: energy storage capacity, inverter size (power capability), and grid demand limit. The number of failure events must be limited to zero as even a single failure event would indicate the system is undersized for the given application. The reader should note that when a failure event occurs is likely the time when the utility expects the system to perform, and as such represents worst case and should be avoided by over-design.

The energy storage requirement is assessed in Figure 41 by simulating a system with a very large power output ability (eliminates undersized inverter failures). This is displayed as a 2D iso-failure plot for the Atlantic region in which system sizes that fall on the various lines fail the indicated number of times per year (one failure is a 5 minute timestep failure, 10 failures would indicate 50 minutes of failure to meet required loads). Any system sizes to the above-right of the failure lines experience no failures while systems to the below-left experience an increasing number of failures.

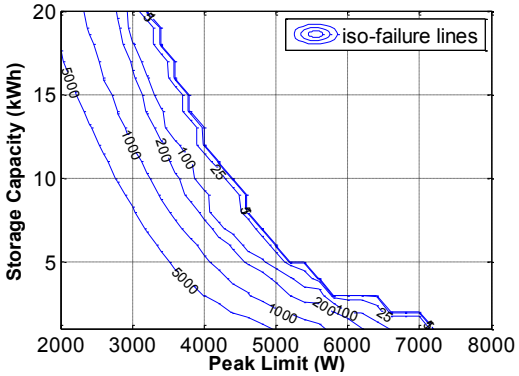

Figure 41: 2D iso-failure plot of energy storage (AT region, storage capacity vs. grid demand limit) lines indicate system sizes that experience the indicated number failures per year

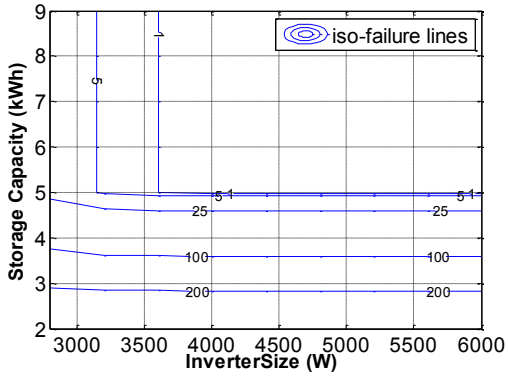

Figure 42: 2D iso-failure plot (AT region, 5260 W peak limit, storage capacity vs. inverter power) lines indicate system sizes that experience the indicated number failures per year

The shape of the plot in Figure 41 indicates diminishing returns with respect to increasing energy storage. A 3 kWh BESS can reduce the maximum peak by 36% (to 5800 W) while a pack three times the size (9 kWh) only reduces the peak by 49% (to 4550 W). This corresponds to tripling the battery size to gain only 36% greater peak shaving.

The diminishing returns of the energy versus grid demand limit plot suggests the selection should be based on reducing the peak as much as possible before reaching the region of steep incline in battery capacity requirement. A peak shaving percentile level constraint of 98.5% (1.5% of system load periods) was specified as this level of peak shaving will adequately meet many of the peak shaving operations required by the electricity grid.

Selection was completed by plotting storage capacity versus inverter size for the specified grid demand limit determined by the 98.5 percentile load value and selecting the smallest possible system size. An example of this plot for the Atlantic region is shown in Figure 42.

The resulting BESS sizes and grid demand limit set points for each region are shown in Table 11 along with the estimated reduction in peak load.

Table 11: BESS sizing and estimated peak reductions

Region	AT	QC	ON	PR	BC
BESS energy storage capacity (kWh)	5	28	8	5	5
Inverter power(W)	3800	4300	3400	2500	5400
Grid demand limit (W)	5260	10910	3790	2600	6630
Percent reduction in house demand	42%	28%	47%	49%	45%

The resulting system sizes appear to follow expectations when compared to annual average house demand and maximum house demand. Energy consumption of the QC region is very high as both DHW and space heating are provided via electricity, so it is expected that the storage requirement is significantly higher than other regions. Inverter sizes line up with expectations based on maximum house demand for each region. Overall, the results are similar to those generated with the scoping model presented in [141] but now more confidence can be placed in the performance values generated from the simulation as the model has been experimentally calibrated and validated for use in this exact application.

Lifetime of the batteries was estimated to be 10-20 years in [141] and based on the updated model cycling profiles and data from [134] the lifetime assessment remains the same.

5.4 Conclusion

Using the CHREM, typical residential electricity profiles were generated for 5 regions across Canada. The houses were selected based on typical values for various parameters within each region. Once simulated, the profiles underwent a statistical analysis to

determine electricity requirements for each region. A BESS model was developed for peak shaving applications into which the electricity demand profiles for each region were input. The battery model was experimentally calibrated and validated. Through parametric study the failure levels of each system were identified and an envelope of BESS sizing based on maximum grid demand limits was determined. Peak demand reductions of between 42% and 49% are achievable in all regions except Quebec (peak reduction of 28%). These reductions are achieved with a BESS energy capacity of 5 kWh in the Atlantic, Prairies, and BC regions. In Ontario only a slightly larger system (8 kWh) is required. The typical Quebec house requires a significantly larger energy storage capacity (28 kWh) which results from the use of electric heating in this region. Such a large system size in the Quebec house indicates the use of a peak shaving system may be unfavorable in this region, or more generally in houses with electric heating. Inverter sizes are all fairly similar, ranging from 3.4 kW to 5.4 kW.

CHAPTER 6 CONCLUSIONS

6.1 CONCLUSIONS

Due to continually increasing levels of renewable energy on the electricity grid, renewable integration is an issue that will require significant attention over the coming years. A critical and in-depth analysis of the state-of-the-art of renewable integration using energy storage systems was conducted, with the results published in both this thesis and Journal of Power Sources to assist engineers, utilities, and policy makers. Various grid support services to address increased ramp rates and less base-load generation will be required to successfully integrate renewable energy, many of which will require energy storage systems. By including energy storage systems in the grid the overall flexibility to absorb higher degrees of variance and distributed generators can be increased, enabling increased penetration of intermittent renewable resources. Many energy storage technologies exist and it is likely that a combination of these technologies will fulfill the energy storage requirements of the future grids, as a single technology is not appropriate for all of the services that are required. Battery technologies fulfill a wide range of the grid-support service requirements and will very likely find a place in grid support applications. The appropriate battery technology required can be selected based on the energy to power ratio as well as economic factors as presented in Chapter 2. For short duration applications (seconds to minutes) lithium-ion batteries are appropriate. In medium duration applications (minutes to hours) lead-acid, sodium sulfur, and lithium batteries are appropriate. In long term storage applications (hour to days) vanadium-redox and sodium-sulfur appear to be the most appropriate of the available battery technologies.

This work has identified distributed energy storage systems conducting peak shaving operation as one method of grid support and renewable integration support. Typical houses were identified in several major regions in Canada and the electricity demand profiles were simulated for these houses. The resulting profiles were used to simulate the peak shaving system and assess BESS sizing parameters for each region. Peak shaving was conducted by limiting the house demand to a set value that was selected using the yearly load curves of each simulated house. Results indicated that BESS systems sized

between 5 to 8 kWh and 3.4 to 5.4 kW satisfied the peak shaving requirements for houses in all regions except Quebec and reduced peak loads by 40-50%. BESS life using LFP batteries was also estimated between 10 and 20 years for this application. Overall impacts of peak shaving systems on the electricity grid were not assessed in this work. Consideration of such large scale implications would require additional simulation considerations of community, city, and province wide energy consumption, and such further considerations were outside the scope of this work, but could be added in future work.

Based on these results a 6.2 kWh LFP experimental BESS and cycling apparatus was constructed. The BESS was used to cycle the battery bank in order to obtain model calibration parameters for an advanced dynamic battery model. The LFP battery model developed in this work represents new development in lithium-ion battery models for LFP batteries. The model was developed by adapting a lithium cobalt battery model using the calibration parameters obtained through the experimental BESS. The BESS was also cycled to validate the battery model. Validation was performed by comparing the simulated peak shaving BESS results with the experimentally cycled BESS results under the same peak shaving regime. Updated results indicate that the original (scoping) peak shaving battery model described in Chapter 3 was reasonably accurate and results changed only slightly by including the more advanced battery model. Despite very little change in the results of peak shaving system sizing results, more confidence can be placed in the results because an experimentally calibrated battery model was used to obtain the results.

6.2 Future Work

Valuable results have been obtained as a result of the research efforts already conducted; however, continuation of the work and ideas arising from this work are recommended. This area of research is quickly becoming important to electric utility companies, renewable energy developers, and many others. Fully understanding the many issues associated with renewable integration and energy storage is critical.

6.2.1 Renewable integration using energy storage

The method of grid support studied throughout this thesis is peak shaving on a residential scale. Although this method is beneficial to grid operations, more direct methods of grid integration are possible and have been discussed in this thesis. Methods addressing optimal smoothing/dispatch and grid integration of wind farms are presented in [37, 39-41, 144]. In the dispatch/smoothing optimization problem the goal is to generate a steady, predictable output from a wind farm and predict this output 1 to 3 hours in advance. Energy arbitrage using renewable generation sources is addressed in [145, 146]. Developing these models and adapting the smoothing/dispatchability and arbitrage concepts to various Canadian electricity markets would be very worthwhile and may help Canadian utilities realize the value energy storage systems can provide as renewable energy penetration levels increase.

The underlying difficulty with energy storage systems is their dependence on a specific regions grid and price structures as well as the renewable resources present. Creating transparency as to the value of energy storage systems is crucial to allowing utilities to make informed decisions regarding possible implementation of energy storage systems. Papers such as [15, 147] provide an excellent overview and starting point, but the value of services in these papers was considered for average electricity markets under certain operating methods. Different locations with different system parameters can have substantially different results.

6.2.2 Peak Shaving Model

With respect to the developed peak shaving model, further development is possible in the area of peak shaving operation, economic considerations and community-scale implementation. Although the system does successfully reduce peaks by 40-50% the system does appear to be somewhat underutilized during lower demand times of the year. An adaptive peak limit could be implemented that shaves peaks daily based on recent peaking events and/or weather conditions to more regularly utilize the energy storage system. It may also be possible to have the system consider the wind production or solar production of a hypothetical nearby generation facility and adjust charge and discharge

schedules accordingly. The system sizes developed were to satisfy the peak shaving requirements of the house however it is not unforeseeable that a peak shaving system sized for this application could also provide additional services to the grid, operating in a hybrid support mode to maximum system value. The simulation could be expanded to community scale storage systems. Work presented in [135] could be combined with the models presented in this thesis to accurately simulate community demands and assess the influence of larger systems on sizing and performance of larger systems.

6.2.3 Battery Modeling

One shortfall of the present model is the slight divergence of the model compared to measured data at current far from the reference current during 25-75% states of charge. This error is the result of internal resistance that varies with both current and depth of discharge. One method to deal with this error would be to simply include an additional scaling factor that affects the voltage rather than the depth of discharge. Calculation of this factor could be completed using the constant current discharge curves that are already used to calibrate the model, which means no additional data collection would be required.

6.2.4 Experimental Apparatus

The developed experimental BESS is operational, and is fully capable of cycling 72 V battery banks. There are many future applications of the experimental BESS towards battery model development including: long term cycling tests, renewable integration cycling to assess battery models (short term) and battery life (long term).

Although the experimental BESS is very useful in its present state, there are three specific additions to the system that would enhance its cycling abilities. First, increasing the charging capacity to 5 kW would allow the system to discharge and charge at the same rate. This addition would allow studying of pack performance under a wider range of operating requirements. Second, the present cell measurement method introduces as much as 0.1 V error (2.7%) for the cells located closest to the positive terminal of the pack (cells with the highest voltage with respect to pack ground). This could be corrected

by installing a multichannel voltmeter capable of isolating itself from the ground and communicating digitally (optically-isolated serial communication) with the CR1000. Increasing cell measurement accuracy would allow detailed study of performance of individual batteries within a series connected lithium battery pack. The third and final addition would be a cell balancing device. For the present work, short term cycling was conducted to obtain calibration parameters and validation data. For longer term operation of the BESS a balancing setup would almost certainly be required to account for some cells being weaker or stronger than others (self-discharge rates, variances in internal heating between cells). Cell balancing devices are available commercially.

References

[1] P. Denholm and M. Hand. Grid flexibility and storage required to achieve very high penetration of variable renewable electricity. *Energy Policy 39(3),* pp. 1817-1830. 2011.

[2] Nova Scotia Power Inc. Hourly total net nova scotia load. *2011(December 12),* 2011. http://oasis.nspower.ca/en/home/default/monthlyreports/hourly_ns.aspx.

[3] Statistics Canada, "Electric power generation, transmission, and distribution 2007," Tech. Rep. 57-202-X, 2009.

[4] B. Kirby, "Frequency regulation basics and trends," Oakridge National Labratory, Tech. Rep. ORNL/TM 2004/291, 2004.

[5] Global Wind Energy Association. GWEC website. *2011(08/31),* 2011. http://www.gwec.net.

[6] A. Thilak. Analysis of polysilicon, wafers, PV cells and solar PV modules to 2015. *2011(02/01),* 2011. http://www.renewableenergyworld.com/rea/blog/post/2011/02/solar-photovoltaic-pv-supply-chain-global-market-size-and-company-analysis-of-polysilicon-wafers-pv-cells-and-solar-pv-modules-to-2015.

[7] British Petroleum. BP statistical review of world energy. BP. London, UK. 2011Available: www.bp.com/statisticalreview.

[8] P. S. Georgilakis. Technical challenges associated with the integration of wind power into power systems. *Renewable and Sustainable Energy Reviews 12(3),* pp. 852-863. 2008. Available: http://dx.doi.org/10.1016/j.rser.2006.10.007.

[9] J. DeCesaro and K. Porter. Wind energy and power system operations: A review of wind integration studies to date. NREL. 2009[Online].

[10] P. Denholm, E. Ela, B. Kirby and M. Milligan. The role of energy storage with renewable electricity generation. NREL. 2010Available: http://www.nrel.gov/docs/fy10osti/47187.pdf.

[11] W. A. Qureshi, N. C. Nair and M. M. Farid. Impact of energy storage in buildings on electricity demand side management. *Energy Conversion and Management 52(5),* pp. 2110-2120. 2011.

[12] L. Exarchakos, M. Leach and G. Exarchakos. Modelling electricity storage systems management under the influence of demand-side management programmes. *Int. J. Energy Res. 33(1),* pp. 62-76. 2009. Available: http://dx.doi.org/10.1002/er.1473.

[13] V. V. Ranade and J. Beal. Distributed control for small customer energy demand management. Presented at Self-Adaptive and Self-Organizing Systems (SASO), 2010 4th IEEE International Conference on. 2010, .

[14] Y. Strengers. Comfort expectations: The impact of demand-management strategies in australia. *Build. Res. Inf. 36(4),* pp. 381-391. 2008.

[15] EPRI-DOE. Handbook of energy storage for transmission and distribution applications. EPRI. Palo Alto, CA. 2003Available: http://www.sandia.gov/ess/publications/ESHB%201001834%20reduced%20size.pdf.

[16] G. Coppez, S. Chowdhury and S. P. Chowdhury. Review of battery storage optimisation in distributed generation. Presented at Power Electronics, Drives and Energy Systems (PEDES) & 2010 Power India, 2010 Joint International Conference on. 2010, .

[17] A. Mohd, E. Ortjohann, A. Schmelter, N. Hamsic and D. Morton. Challenges in integrating distributed energy storage systems into future smart grid. Presented at 2008 IEEE International Symposium on Industrial Electronics, ISIE 2008, June 30, 2008 - July 2. 2008, Available: http://dx.doi.org/10.1109/ISIE.2008.4676896.

[18] J. Leadbetter and L. G. Swan. Selection of battery technology to support grid-integrated renewable electricity. *J. Power Sources 216(0),* pp. 376. 2012. Available: http://dx.doi.org/10.1016/j.jpowsour.2012.05.081.

[19] H. Chen, T. N. Cong, W. Yang, C. Tan, Y. Li and Y. Ding. Progress in electrical energy storage system: A critical review. *Progress in Natural Science 19(3),* pp. 291-312. 2009.

[20] H. Ibrahim, A. Ilinca and J. Perron. Energy storage systems—Characteristics and comparisons. *Renewable and Sustainable Energy Reviews 12(5),* pp. 1221-1250. 2008.

[21] Ontario Power Authority. FIT program. *2012(07/18),* 2012. http://fit.powerauthority.on.ca/fit-program.

[22] Nova Scotia Department of Energy. Renewable electricity plan. NSDOE. 2010Available: http://www.gov.ns.ca/energy/resources/EM/renewable/renewable-electricity-plan.pdf.

[23] Nova Scotia Power Inc. Domestic service time-of-day service. *2012(6/25),* 2012. http://www.nspower.ca/en/home/aboutnspi/ratesandregulations/electricityrates/domesticservicetimeofdaytarriffoptional.aspx.

[24] L. Gao, S. Liu and R. A. Dougal. Dynamic lithium-ion battery model for system simulation. 2002, Available: http://dx.doi.org/10.1109/TCAPT.2002.803653.

[25] S. Sorrell, J. Speirs, R. Bentley, A. Brandt and R. Miller. Global oil depletion: A review of the evidence. *Energy Policy 38(9),* pp. 5290-5295. 2010.

[26] Hatch. Nova scotia wind integration study for nova scotia department of energy. Hatch. Oakville, Canada. 2008.

[27] K. C. Divya and J. Ostergaard. Battery energy storage technology for power systems - an overview. *Electr. Power Syst. Res. 79(4),* pp. 511-20. 2009. Available: http://dx.doi.org/10.1016/j.epsr.2008.09.017.

[28] N. C. Nair and N. Garimella. Battery energy storage systems: Assessment for small-scale renewable energy integration. *Energy Build. 42(11),* pp. 2124-2130. 2010. Available: http://dx.doi.org/10.1016/j.enbuild.2010.07.002.

[29] R. M. Dell and D. A. J. Rand. Energy storage-a key technology for global energy sustainability. *J. Power Sources 100(1-2),* pp. 2-17. 2001. Available: http://dx.doi.org/10.1016/S0378-7753(01)00894-1.

[30] M. Beaudin, H. Zareipour, A. Schellenberglabe and W. Rosehart. Energy storage for mitigating the variability of renewable electricity sources: An updated review. *Energy for Sustainable Development 14(4),* pp. 302-314. 2010.

[31] P. J. Hall and E. J. Bain. Energy-storage technologies and electricity generation. *Energy Policy 36(12),* pp. 4352-4355. 2008. Available: http://dx.doi.org/10.1016/j.enpol.2008.09.037.

[32] I. Hadjipaschalis, A. Poullikkas and V. Efthimiou. Overview of current and future energy storage technologies for electric power applications. *Renewable and Sustainable Energy Reviews 13(6-7),* pp. 1513-1522. 2009. Available: http://dx.doi.org/10.1016/j.rser.2008.09.028.

[33] Electricity Storage Association. *2012(08/19),* 2012. http://www.electricitystorage.org/.

[34] J. McDowall. Integrating energy storage with wind power in weak electricity grids. *J. Power Sources 162(2),* pp. 959-964. 2006. Available: http://dx.doi.org/10.1016/j.jpowsour.2005.06.034.

[35] J. O. G. Tande. Grid integration of wind farms. *Wind Energy 6(3),* pp. 281-295. 2003. Available: http://dx.doi.org/10.1002/we.91.

[36] B. W. Kennedy. Integrating wind power: Transmission and operational impacts. *Refocus 5(1),* pp. 36-37. 2004.

[37] S. Teleke, M. E. Baran, A. Q. Huang, S. Bhattacharya and L. Anderson. Control strategies for battery energy storage for wind farm dispatching. *IEEE Trans. Energy*

Convers. 24(3), pp. 725-732. 2009. Available: http://dx.doi.org/10.1109/TEC.2009.2016000.

[38] E. Ela and B. Kirby. ERCOT event on february 26, 2008: Lessons learned. NREL. 2008[Online]. Available: http://www.nrel.gov/docs/fy08osti/43373.pdf.

[39] Q. Li, S. S. Choi, Y. Yuan and D. L. Yao. On the determination of battery energy storage capacity and short-term power dispatch of a wind farm. *IEEE Transactions on Sustainable Energy 2(2),* pp. 148-58. 2011. Available: http://dx.doi.org/10.1109/TSTE.2010.2095434.

[40] A. Uehara, T. Senjyu, Y. Kikunaga, A. Yona, N. Urasaki, T. Funabashi and C. Kim. Study on optimum operation planning of wind farm/battery system using forecasted power data. Presented at 2009 International Conference on Power Electronics and Drive Systems, PEDS 2009, January 2, 2009 - January 5. 2009, Available: http://dx.doi.org/10.1109/PEDS.2009.5385766.

[41] T. K. A. Brekken, A. Yokochi, A. von Jouanne, Z. Z. Yen, H. M. Hapke and D. A. Halamay. Optimal energy storage sizing and control for wind power applications. *IEEE Transactions on Sustainable Energy 2(1),* pp. 69-77. 2011. Available: http://dx.doi.org/10.1109/TSTE.2010.2066294.

[42] D. Weisser and R. S. Garcia. Instantaneous wind energy penetration in isolated electricity grids: Concepts and review. *Renewable Energy 30(8),* pp. 1299-1308. 2005. Available: http://dx.doi.org/10.1016/j.renene.2004.10.002.

[43] M. Kohli. Average energy prices in new york-northern new jersey - july 2011. [Online]. 2011. Available: http://www.bls.gov/ro2/avgengny.pdf.

[44] D. Linden and T. Reddy, *Handbook of Batteries.* McGraw-Hill Professional, 2010.

[45] P. Ruetschi. Aging mechanisms and service life of lead-acid batteries. Presented at Eight Ulmer Electrochemische Tage, June 20, 2002 - June 21. 2004, Available: http://dx.doi.org/10.1016/j.jpowsour.2003.09.052.

[46] C. D. Parker. Lead–acid battery energy-storage systems for electricity supply networks. *J. Power Sources 100(1-2),* pp. 18-28. 2001.

[47] G. D. Rodriguez, W. C. Spindler and D. S. Carr. Operating the world's largest lead/acid battery energy storage system. Presented at International Conference on Lead/Acid Batteries: LABAT '89. 1990, Available: http://dx.doi.org/10.1016/0378-7753(90)80083-P.

[48] R. Wagner. Large lead/acid batteries for frequency regulation, load levelling and solar power applications. *J. Power Sources 67(1-2),* pp. 163-172. 1997.

[49] M. F. De Anda, J. D. Boyes and W. Torres. Lessons learned from the puerto rico battery energy sotrage system. SANDIA National Labratories. Albuquerque, New Mexico. 1999.

[50] J. Liu, D. Yang, L. Gao, X. Zhu, L. Li and J. Yang. Effect of iron doped lead oxide on the performance of lead acid batteries. *J. Power Sources 196(20),* pp. 8802-8808. 2011.

[51] L. Tang, A. Li, H. Chen, H. Li, Q. Chen, H. Zhou, W. Wei, W. Zhang, J. Hu, C. Dou, H. Wang and D. Finlow. The electrochemical performances of a novel lead–sodium binary grid alloy for lead-acid batteries. *Electrochim. Acta 56(12),* pp. 4566-4570. 2011.

[52] M. Cugnet and B. Y. Liaw. Effect of discharge rate on charging a lead-acid battery simulated by mathematical model. *J. Power Sources 196(7),* pp. 3414-3419. 2011.

[53] K. Siniard, M. Xiao and S. Choe. One-dimensional dynamic modeling and validation of maintenance-free lead-acid batteries emphasizing temperature effects. *J. Power Sources 195(20),* pp. 7102-7114. 2010.

[54] K. Mamadou, T. M. P. Nguyen, E. Lemaire-Potteau, C. Glaize and J. Alzieu. New accelerated charge methods using early destratification applied on flooded lead acid batteries. *J. Power Sources 196(8),* pp. 3981-3987. 2011.

[55] T. Ikeya, N. Sawada, S. Takagi, J. Murakami, K. Kobayashi, T. Sakabe, E. Kousaka, H. Yoshioka, S. Kato, M. Yamashita, H. Narisoko, Y. Mita, K. Nishiyama, K. Adachi and K. Ishihara. Multi-step constant-current charging method for electric vehicle, valve-regulated, lead/acid batteries during night time for load-levelling. *J. Power Sources 75(1),* pp. 101-7. 1998. Available: http://dx.doi.org/10.1016/S0378-7753(98)00102-5.

[56] J. Alzieu, H. Smimite and C. Glaize. Improvement of intelligent battery controller: State-of-charge indicator and associated functions. Presented at 5th European Lead Battery Conference. 1997, Available: http://dx.doi.org/10.1016/S0378-7753(97)02508-1.

[57] M. Colemn, C. B. Zhu, C. K. Lee and W. G. Hurley. A combined SOC estimation method under varied ambient temperature for a lead-acid battery. *Conference Proceedings - IEEE Applied Power Electronics Conference and Exposition - APEC 2*pp. 991-997. 2005. Available: http://dx.doi.org/10.1109/APEC.2005.1453110.

[58] J. Han, D. Kim and M. Sunwoo. State-of-charge estimation of lead-acid batteries using an adaptive extended kalman filter. *J. Power Sources 188(2),* pp. 606-612. 2009.

[59] J. F. A. Leao, L. V. Hartmann, M. B. R. Correa and A. M. N. Lima. Lead-acid battery modeling and state of charge monitoring. Presented at 2010 Twenty-Fifth Annual IEEE Applied Power Electronics Conference and Exposition - APEC 2010. 2010, Available: http://dx.doi.org/10.1109/APEC.2010.5433666.

[60] S. Piller, M. Perrin and A. Jossen. Methods for state-of-charge determination and their applications. Presented at Proceedings of the 22nd International Power Sources Symposium, April 9, 2001 - April 11. 2001, Available: http://dx.doi.org/10.1016/S0378-7753(01)00560-2.

[61] W. X. Shen. State of available capacity estimation for lead-acid batteries in electric vehicles using neural network. *Energy Conversion and Management 48(2),* pp. 433-442. 2007. Available: http://dx.doi.org/10.1016/j.enconman.2006.06.023.

[62] P. Bača, K. Micka, P. Křivík, K. Tonar and P. Tošer. Study of the influence of carbon on the negative lead-acid battery electrodes. *J. Power Sources 196(8),* pp. 3988-3992. 2011.

[63] K. R. Bullock. Carbon reactions and effects on valve-regulated lead-acid (VRLA) battery cycle life in high-rate, partial state-of-charge cycling. *J. Power Sources 195(14),* pp. 4513-4519. 2010.

[64] A. Czerwiński, S. Obrębowski, J. Kotowski, Z. Rogulski, J. Skowroński, M. Bajsert, M. Przystałowski, M. Buczkowska-Biniecka, E. Jankowska, M. Baraniak, J. Rotnicki and M. Kopczyk. Hybrid lead-acid battery with reticulated vitreous carbon as a carrier- and current-collector of negative plate. *J. Power Sources 195(22),* pp. 7530-7534. 2010.

[65] A. Kirchev, N. Kircheva and M. Perrin. Carbon honeycomb grids for advanced lead-acid batteries. part I: Proof of concept. *J. Power Sources 196(20),* pp. 8773-8788. 2011.

[66] D. Pavlov, P. Nikolov and T. Rogachev. Influence of carbons on the structure of the negative active material of lead-acid batteries and on battery performance. *J. Power Sources 196(11),* pp. 5155-5167. 2011.

[67] J. Furukawa, T. Takada, D. Monma and L. T. Lam. Further demonstration of the VRLA-type UltraBattery under medium-HEV duty and development of the flooded-type UltraBattery for micro-HEV applications. *J. Power Sources 195(4),* pp. 1241-1245. 2010.

[68] L. T. Lam, R. Louey, N. P. Haigh, O. V. Lim, D. G. Vella, C. G. Phyland, L. H. Vu, J. Furukawa, T. Takada, D. Monma and T. Kano. VRLA ultrabattery for high-rate partial-state-of-charge operation. *J. Power Sources 174(1),* pp. 16-29. 2007.

[69] P. T. Moseley, R. F. Nelson and A. F. Hollenkamp. The role of carbon in valve-regulated lead–acid battery technology. *J. Power Sources 157(1),* pp. 3-10. 2006.

[70] Y. Chen, B. Chen, L. Ma and Y. Yuan. Effect of carbon foams as negative current collectors on partial-state-of-charge performance of lead acid batteries. *Electrochemistry Communications 10(7),* pp. 1064-1066. 2008.

[71] D. G. Enos, T. H. Hund and R. Shane, "Understanding the function and performance of carbon-enhanced lead-acid batteries," Tech. Rep. SAND2011-3460, 2011.

[72] T. Okoshi, K. Yamada, T. Hirasawa and A. Emori. Battery condition monitoring (BCM) technologies about lead–acid batteries. *J. Power Sources 158(2),* pp. 874-878. 2006.

[73] B. Scrosati and J. Garche. Lithium batteries: Status, prospects and future. *J. Power Sources 195(9),* pp. 2419-2430. 2010. Available: http://dx.doi.org/10.1016/j.jpowsour.2009.11.048.

[74] M. Charkhgard and M. Farrokhi. State-of-charge estimation for lithium-ion batteries using neural networks and EKF. *IEEE Trans. Ind. Electron. 57(12),* pp. 4178-87. 2010. Available: http://dx.doi.org/10.1109/TIE.2010.2043035.

[75] S. Santhanagopalan and R. E. White. State of charge estimation using an unscented filter for high power lithium ion cells. *Int. J. Energy Res. 34(2),* pp. 152-63. 2010. Available: http://dx.doi.org/10.1002/er.1655.

[76] X. Hu, F. Sun and Y. Zou. Estimation of state of charge of a lithium-ion battery pack for electric vehicles using an adaptive luenberger observer. *Energies 3(9),* pp. 1586-1603. 2010. Available: http://dx.doi.org/10.3390/en3091586.

[77] S. N. Kong, Chin-Sien Moo, Yi-Ping Chen and Yao-Ching Hsieh. Enhanced coulomb counting method for estimating state-of-charge and state-of-health of lithium-ion batteries. *Appl. Energy 86(9),* pp. 1506-11. 2009. Available: http://dx.doi.org/10.1016/j.apenergy.2008.11.021.

[78] C. Vartanian and N. Bentley. A123 systems' advanced battery energy storage for renewable integration. Presented at 2011 IEEE/PES Power Systems Conference and Exposition (PSCE 2011). 2011, Available: http://dx.doi.org/10.1109/PSCE.2011.5772569.

[79] J. W. Fergus. Recent developments in cathode materials for lithium ion batteries. *J. Power Sources 195(4),* pp. 939-954. 2010.

[80] A. Ritchie and W. Howard. Recent developments and likely advances in lithium-ion batteries. *J. Power Sources 162(2),* pp. 809-812. 2006.

[81] R. J. Gummow, A. de Kock and M. M. Thackeray. Improved capacity retention in rechargeable 4 V lithium/lithium-manganese oxide (spinel) cells. *Solid State Ionics 69(1),* pp. 59-67. 1994.

[82] J. Hassoun, P. Reale and B. Scrosati. Recent advances in liquid and polymer lithium-ion batteries. *Journal of Materials Chemistry 17(35),* pp. 3668-3677. 2007. Available: http://dx.doi.org/10.1039/b707040n.

[83] M. Winter and J. O. Besenhard. Electrochemical lithiation of tin and tin-based intermetallics and composites. *Electrochim. Acta 45(1-2),* pp. 31-50. 1999.

[84] G. Derrien, J. Hassoun, S. Panero and B. Scrosati. Nanostructured Snâ€“C composite as an advanced anode material in high-performance lithium-ion batteries. *Adv Mater 19(17),* pp. 2336-2340. 2007. Available: http://dx.doi.org/10.1002/adma.200700748.

[85] Altair Nano. Altair nano website. *2011(08/31),* 2011. http://www.altairnano.com.

[86] J. Xu, J. Yang, Y. NuLi, J. Wang and Z. Zhang. Additive-containing ionic liquid electrolytes for secondary lithium battery. *J. Power Sources 160(1),* pp. 621-626. 2006.

[87] L. Damen, M. Lazzari and M. Mastragostino. Safe lithium-ion battery with ionic liquid-based electrolyte for hybrid electric vehicles. *J. Power Sources 196(20),* pp. 8692-8695. 2011.

[88] NGK Insulators. Sodium-sulfur batteries: NGK insulators website. *2011(08/31),* 2011. Available: http://www.ngk.co.jp/english/products/power/nas/index.html.

[89] R. Dufo-López, J. L. Bernal-Agustín and J. A. Domínguez-Navarro. Generation management using batteries in wind farms: Economical and technical analysis for spain. *Energy Policy 37(1),* pp. 126-139. 2009.

[90] NGK Insulators. NGK's sodium sulfur (NAS) battery the Vendor's perspective on barriers & issues encountered in U.S. deployment. [Online]. 2009. Available: http://www.energy.ca.gov/2009_energypolicy/documents/2009-04-02_workshop/presentations/2_2%20NGK-NAS%20-%20Harold%20Gotschall.pdf.

[91] A. Nourai. Installation of the first distributed energy storage system (DESS) at american electric power (AEP). SANDIA National Labratories. Albuquerque, New Mexico. 2007[Online]. Available: http://www.corrosionanalysisnetwork.org/portal/site/csc/Details/?vgnextoid=389cb87a13152210VgnVCM100000701e010aRCRD&campaign=recommends-personal.

[92] Z. Wen, J. Cao, Z. Gu, X. Xu, F. Zhang and Z. Lin. Research on sodium sulfur battery for energy storage. *Solid State Ionics 179(27-32),* pp. 1697-1701. 2008.

[93] R. M. Dell and P. T. Moseley. Beta-alumina electrolyte for use in sodium/sulphur batteries part 2. manufacture and use. *J. Power Sources 7(1),* pp. 45-63. 1982.

[94] Z. Wen, Z. Gu, X. Xu, J. Cao, F. Zhang and Z. Lin. Research activities in shanghai institute of ceramics, chinese academy of sciences on the solid electrolytes for sodium sulfur batteries. *J. Power Sources 184(2),* pp. 641-645. 2008.

[95] X. Lu, G. Xia, J. P. Lemmon and Z. Yang. Advanced materials for sodium-beta alumina batteries: Status, challenges and perspectives. *J. Power Sources 195(9),* pp. 2431-2442. 2010.

[96] C. Park, H. Ryu, K. Kim, J. Ahn, J. Lee and H. Ahn. Discharge properties of all-solid sodium–sulfur battery using poly (ethylene oxide) electrolyte. *J. Power Sources 165(1),* pp. 450-454. 2007.

[97] H. Ryu, T. Kim, K. Kim, J. Ahn, T. Nam, G. Wang and H. Ahn. Discharge reaction mechanism of room-temperature sodium–sulfur battery with tetra ethylene glycol dimethyl ether liquid electrolyte. *J. Power Sources 196(11),* pp. 5186-5190. 2011.

[98] S. Song, Z. Wen, Y. Liu, X. Wu and J. Lin. Bi-doped borosilicate glass as sealant for sodium sulfur battery. *J. Non Cryst. Solids 357(16-17),* pp. 3074-3079. 2011.

[99] S. Song, Z. Wen, Q. Zhang and Y. Liu. A novel bi-doped borosilicate glass as sealant for sodium sulfur battery. part 1: Thermophysical characteristics and structure. *J. Power Sources 195(1),* pp. 384-388. 2010.

[100] Prudent Energy. VRB battery system specifications. [Online]. 2011. Available: http://www.pdenergy.com/pdfs/datasheet_websalespacket.pdf.

[101] L. Li, S. Kim, W. Wang, M. Vijayakumar, Z. Nie, B. Chen, J. Zhang, G. Xia, J. Hu, G. Graff, J. Liu and Z. Yang. A stable vanadium redox-flow battery with high energy density for large-scale energy storage. *Advanced Energy Materials 1(3),* pp. 394-400. 2011. Available: http://dx.doi.org/10.1002/aenm.201100008.

[102] Smart Energy News. Prudent energy raises $29.5 million in venture capital

. *2011(12/14),* 2011. http://smartenergynews.net/2011/10/12/prudent-energy-raises-29-5-million/.

[103] Prudent Energy. VRB technology in japan. [Online]. 2011. Available: http://www.pdenergy.com/pdfs/casestudy_japan.pdf.

[104] C. Jia, J. Liu and C. Yan. A significantly improved membrane for vanadium redox flow battery. *J. Power Sources 195(13),* pp. 4380-3. 2010. Available: http://dx.doi.org/10.1016/j.jpowsour.2010.02.008.

[105] G. Hwang and H. Ohya. Preparation of cation exchange membrane as a separator for the all-vanadium redox flow battery. *J. Membr. Sci. 120(1),* pp. 55-67. 1996. Available: http://dx.doi.org/10.1016/0376-7388(96)00135-4.

[106] X. Li, H. Zhang, Z. Mai, H. Zhang and I. Vankelecom. Ion exchange membranes for vanadium redox flow battery (VRB) applications. *Energy and Environmental Science 4(4),* pp. 1147-1160. 2011. Available: http://dx.doi.org/10.1039/c0ee00770f.

[107] T. Sukkar and M. Skyllas-Kazacos. Membrane stability studies for vanadium redox cell applications. *J. Appl. Electrochem. 34(2),* pp. 137-145. 2004. Available: http://dx.doi.org/10.1023/B:JACH.0000009931.83368.dc.

[108] B. Tian, C. -. Yan and F. -. Wang. Modification and evaluation of membranes for vanadium redox battery applications. *J. Appl. Electrochem. 34(12),* pp. 1205-1210. 2004. Available: http://dx.doi.org/10.1007/s10800-004-1765-2.

[109] K. Huang, X. Li, S. Liu, N. Tan and L. Chen. Research progress of vanadium redox flow battery for energy storage in china. *Renewable Energy 33(2),* pp. 186-192. 2008.

[110] F. Rahman and M. Skyllas-Kazacos. Vanadium redox battery: Positive half-cell electrolyte studies. *J. Power Sources 189(2),* pp. 1212-1219. 2009. Available: http://dx.doi.org/10.1016/j.jpowsour.2008.12.113.

[111] X. Wu, S. Liu and K. Huang. Characteristics of CTAB as electrolyte additive for vanadium redox flow battery. *Wuji Cailiao Xuebao/Journal of Inorganic Materials 25(6),* pp. 641-646. 2010. Available: http://dx.doi.org/10.3724/SP.J.1077.2010.00641.

[112] Chen Mao-bin, Li Xiao-bing, Zhang Sheng-tao and L. Lian. The charge-discharge characteristics of vanadium redox flow battery. *Battery Bimonthly 38(1),* pp. 37-9. 2008.

[113] M. Skyllas-Kazacos and M. Kazacos. State of charge monitoring methods for vanadium redox flow battery control. *J. Power Sources 196(20),* pp. 8822-8827. 2011. Available: http://dx.doi.org/10.1016/j.jpowsour.2011.06.080.

[114] C. Blanc and A. Rufer. Modeling of a vanadium redox flow battery. Presented at International Exhibition & Conference for Power Electronics Intelligent Motion Power Quality 2007. 2007, .

[115] C. Blanc and A. Rufer. Optimization of the operating point of a vanadium redox flow battery. Presented at 2009 IEEE Energy Conversion Congress and Exposition, ECCE 2009, September 20, 2009 - September 24. 2009, Available: http://dx.doi.org/10.1109/ECCE.2009.5316566.

[116] D. You, H. Zhang, C. Sun and X. Ma. Simulation of the self-discharge process in vanadium redox flow battery. *J. Power Sources 196(3),* pp. 1578-85. 2011. Available: http://dx.doi.org/10.1016/j.jpowsour.2010.08.036.

[117] A123. A123 systems website. *2011(08/31),* 2011. http://www.a123systems.com/.

[118] J. P. Barton and D. G. Infield. Energy storage and its use with intermittent renewable energy. *IEEE Trans. Energy Convers. 19(2),* pp. 441-8. 2004. Available: http://dx.doi.org/10.1109/TEC.2003.822305.

[119] A. M. Genaidy, R. Sequeira, T. Tolaymat, J. Kohler and M. Rinder. An exploratory study of lead recovery in lead-acid battery lifecycle in US market: An evidence-based approach. *Sci. Total Environ. 407(1),* pp. 7-22. 2008. Available: http://dx.doi.org/10.1016/j.scitotenv.2008.07.043.

[120] EPRI-DOE. Handbook supplement of energy storage for grid connected wind generation applications. EPRI. Palo Alto, CA. 2004Available: http://www.sandia.gov/ess/publications/EPRI-DOE%20ESHB%20Wind%20Supplement.pdf.

[121] D. Connolly, H. Lund, B. V. Mathiesen and M. Leahy. A review of computer tools for analysing the integration of renewable energy into various energy systems. *Appl. Energy 87(4),* pp. 1059-1082. 2010. Available: http://dx.doi.org/10.1016/j.apenergy.2009.09.026.

[122] IESO. Market summaries. *2012(6/25),* 2012. http://www.ieso.ca/imoweb/marketdata/marketSummary.asp.

[123] M. Perrin, Y. Saint-Drenan, F. Mattera and P. Malbranche. Lead-acid batteries in stationary applications: Competitors and new markets for large penetration of renewable energies. Presented at Selected Papers from the Ninth European Lead Battery Conference, September 21, 2004 - September 24. 2005, Available: http://dx.doi.org/10.1016/j.jpowsour.2004.10.026.

[124] IESO. Smart meters and time-of-use rates. *2012(6/25),* 2012. http://www.ieso.ca/imoweb/siteshared/smart_meters.asp.

[125] Z. M. Fadlullah, M. M. Fouda, N. Kato, A. Takeuchi, N. Iwasaki and Y. Nozaki. Toward intelligent machine-to-machine communications in smart grid. *IEEE Communications Magazine 49(4),* pp. 60-65. 2011. Available: http://dx.doi.org/10.1109/MCOM.2011.5741147.

[126] L. G. Swan, V. I. Ugursal and I. Beausoleil-Morrison. Hybrid residential end-use energy and GHG emissions model – development and verification for canada. *Journal of Building Performance Simulation In-Press*2011.

[127] L. G. Swan, V. I. Ugursal and I. Beausoleil-Morrison. Occupant related household energy consumption in canada: Estimation using a bottom-up neural-network technique. *Energy Build. 43(2-3),* pp. 326-337. 2011. Available: http://dx.doi.org/10.1016/j.enbuild.2010.09.021.

[128] J. Clarke. *Energy Simulation in Building Design* (2nd ed.) 2001Available: http://www.sciencedirect.com/science/book/9780750650823.

[129] D. B. e. a. Crawley. EnergyPlus, an update in. Presented at Proceeding of SimBuild (IBPSA-USA). 2004, .

[130] M. M. Armstrong, M. C. Swinton, H. Ribberink, I. Beausoleil-Morrison and J. Millette. Synthetically derived profiles for representing occupant-driven electric loads in canadian housing. *Journal of Building Performance Simulation 2(1),* pp. 15-30. 2009. Available: http://dx.doi.org/10.1080/19401490802706653.

[131] N. Saldanha and I. Beausoleil-Morrison. Analysis of electrical loads of canadian residences at one-minute intervals. Presented at The 6th IBPSA Canada Conference. 2010, .

[132] T. Reddy. *Handbook of Batteries* (4th ed.) 2001.

[133] M. Safari and C. Delacourt. Aging of a commercial graphite/LiFePO4 cell. *J. Electrochem. Soc. 158(10),* pp. A1123-A1135. 2011. Available: http://dx.doi.org/10.1149/1.3614529.

[134] G. Sarre, P. Blanchard and M. Broussely. Aging of lithium-ion batteries. *J. Power Sources 127(1-2),* pp. 65-71. 2004.

[135] J. Tanimoto and A. Hagishima. Total utility demand prediction considering variation of occupants' behavior schedules applied to multi dwellings. *J. Environ. Eng. 76(660),* pp. 141-149. 2011. Available: http://dx.doi.org/10.3130/aije.76.141.

[136] C. Peabody and C. B. Arnold. The role of mechanically induced separator creep in lithium-ion battery capacity fade. *J. Power Sources 196(19),* pp. 8147-8153. 2011.

[137] T. Utsunomiya, O. Hatozaki, N. Yoshimoto, M. Egashira and M. Morita. Self-discharge behavior and its temperature dependence of carbon electrodes in lithium-ion batteries. *J. Power Sources 196(20),* pp. 8598-8603. 2011.

[138] Y. Ozawa, R. Yazami and B. Fultz. Self-discharge study of LiCoO2 cathode materials. *J. Power Sources 119–121(0),* pp. 918-923. 2003.

[139] F. Incropera, Dewitt, D.,Bergman, T and A. Lavine, *Introduction to Heat Transfer.* USA: John Wiley & Sons, 2007.

[140] HiPower New Energy Group Co. Ltd. HiPower LiFePO4 battery catalogue. *2012(07/18),* 2010. http://www.hipowergroup.com/products/LiFePO4%20batteries/2.html.

[141] J. Leadbetter and L. G. Swan, "Assessment of battery energy storage characteristics to perform residential peak demand shaving," in *Proceedings of eSim 2012,* 2012, pp. 366.

[142] V. Ramadesigan, P. W. C. Northrop, S. De, S. Santhanagopalan, R. D. Braatz and V. R. Subramanian. Modeling and simulation of lithium-ion batteries from a systems engineering perspective. *J. Electrochem. Soc. 159(3),* pp. R31-R45. 2012.

[143] L. G. Swan, V. I. Ugursal and I. Beausoleil-Morrison. A database of house descriptions representative of the canadian housing stock for coupling to building energy performance simulation. *Journal of Building Performance Simulation 2(2),* pp. 75-84. 2009. Available: http://dx.doi.org/10.1080/19401490802491827.

[144] S. Teleke, M. E. Baran, S. Bhattacharya and A. Q. Huang. Rule-based control of battery energy storage for dispatching intermittent renewable sources. *IEEE Transactions on Sustainable Energy 1(3),* pp. 117-124. 2010. Available: http://dx.doi.org/10.1109/TSTE.2010.2061880.

[145] L. Zhang and Y. Li. Optimal energy management of hybrid power system with two-scale dynamic programming. Presented at 2011 IEEE/PES Power Systems Conference and Exposition (PSCE 2011). 2011, Available: http://dx.doi.org/10.1109/PSCE.2011.5772607.

[146] M. -. Hessami and D. R. Bowly. Economic feasibility and optimisation of an energy storage system for portland wind farm (victoria, australia). *Appl. Energy 88(8),* pp. 2755-63. 2011. Available: http://dx.doi.org/10.1016/j.apenergy.2010.12.013.

[147] EPRI. Electric energy storage technology options: A white paper primer on applications, costs and benefits. EPRI. Palo Alto, CA. 2010.

APPENDIX A ELSEVIER COPYRIGHT RELEASE

The following copyright release statement was obtained from:

http://www.elsevier.com/wps/find/authorsview.authors/rights

The release pertaining to use in thesis is bolded and highlighted below.

Copyright
Intellectual property, in particular copyright (rights in editorial content), trademarks (rights in brands for services or journals), and database rights (rights in compilations of information), form the foundation of Elsevier's publishing services and communications businesses. We in Elsevier embrace the opportunities the digital environment offers for communication and access, while at the same time we recognize the new risks that this environment poses, that being the ease with which unauthorized copies can be made and distributed worldwide. Download your practical guide to Elsevier's copyright policy.

Our objective
We aim to manage digital rights and brands amidst the structural changes that the "information society" represents, while at the same time recognizing the shared goals we have with our customers and authors. These include providing the widest possible distribution of scientific and medical content and services in a financially sustainable business model.

Elsevier wants to ensure a proper balance between the scholarly rights which authors retain (or are granted/transferred back in some cases) and the rights granted to Elsevier that are necessary to support our mix of business models. We routinely analyse and modify our policies to ensure we are responding to authors' needs and concerns, and to the concerns in general of the research and scholarly communities.

What rights do I retain as a journal author*?

- the right to make copies (print or electronic) of the journal article for your own personal use, including for your own classroom teaching use;
- the right to make copies and distribute copies of the journal article (including via e-mail) to research colleagues, for personal use by such colleagues for scholarly purposes**;**
- the right to post a pre-print version of the journal article on Internet websites including electronic pre-print servers, and to retain indefinitely such version on such servers or sites for scholarly purposes***** (with some exceptions such as The Lancet and Cell Press. See also our information on electronic preprints for a more detailed discussion on these points)*;
- the right to post a revised personal version of the text of the final journal article (to reflect changes made in the peer review process) on your personal or institutional website or server for scholarly purposes*, incorporating the complete citation and with a link to the Digital Object Identifier (DOI) of the article (but not in subject-oriented or centralized repositories or institutional repositories with mandates for systematic postings unless there is a specific agreement with the publisher. Click here for further information);
- the right to present the journal article at a meeting or conference and to distribute copies of such paper or article to the delegates attending the meeting;
- for your employer, if the journal article is a 'work for hire', made within the scope of the author's employment, the right to use all or part of the information in (any version of) the journal article for other intra-company use (e.g. training);
- patent and trademark rights and rights to any process or procedure described in the journal article;

- **the right to include the journal article, in full or in part, in a thesis or dissertation;**
- the right to use the journal article or any part thereof in a printed compilation of your works, such as collected writings or lecture notes (subsequent to publication of the article in the journal); and
- the right to prepare other derivative works, to extend the journal article into book-length form, or to otherwise re-use portions or excerpts in other works, with full acknowledgement of its original publication in the journal.

***Commercial purposes and systematic distribution**
Authors of Elsevier-published articles may use them only for scholarly purposes as set out above and may not use or post them for commercial purposes or under policies or other mechanisms designed to aggregate and openly disseminate manuscripts or articles or to substitute for journal-provided services. This includes the use or posting of articles for commercial gain or to substitute for the services provided directly by the journal including the posting by companies of their employee-authored works for use by customers of such companies (e.g. pharmaceutical companies and physician-prescribers); commercial exploitation such as directly associating advertising with such postings; the charging of fees for document delivery or access; the systematic distribution to others via e-mail lists or list servers (to parties other than known colleagues), whether for a fee or for free; the posting of links to sponsored articles by commercial third parties including pharmaceutical companies; institutional, funding body or government manuscript posting policies or mandates that aim to aggregate and openly distribute the accepted, peer reviewed manuscripts or published journal articles authored by its researchers or funded researchers; and subject repositories that aim to aggregate and openly distribute accepted peer reviewed manuscripts or published journal articles authored by researchers in specific subject areas.

For a more detailed discussion of our article posting policies and the different stages of a journal article development that are relevant from a policy perspective, please see the Article Posting Policies information page.

When Elsevier changes its journal usage policies, are those changes also retroactive?
Yes, when Elsevier changes its policies to enable greater academic use of journal materials (such as the changes several years ago in our web-posting policies) or to clarify the rights retained by journal authors, Elsevier is prepared to extend those rights retroactively with respect to articles published in journal issues produced prior to the policy change.

We are pleased to confirm that, unless explicitly noted to the contrary, all policies apply retrospectively to previously published journal content. If, after reviewing the material noted above, you have any questions about such rights, please contact Global Rights.

How do I obtain a Journal Publishing Agreement?
You will receive a form automatically by post or e-mail once your article is received by Elsevier's Editorial-Production Department. View a generic example of the agreement. Some journals will use another variation of this form.

Why does Elsevier request transfer of copyright?
The research community needs certainty with respect to the validity of scientific papers, which is normally obtained through the editing and peer review processes. The scientific record must be clear and unambiguous. Elsevier believes that, by obtaining copyright transfer, it will always be clear to researchers that when they access an Elsevier site to review a paper, they are reading a final version of the paper which has been edited, peer-reviewed and accepted for publication in an appropriate journal. This eliminates any ambiguity or uncertainty about Elsevier's ability to distribute, sub-license and protect the article from unauthorized copying, unauthorized distribution, and plagiarism.

Can you provide me with a PDF file of my article?
Many Elsevier journals are now offering authors e-offprints – free electronic versions of published articles. E-offprints are watermarked PDF versions, and are usually delivered within 24 hours, much

APPENDIX B ISO-FAILURE SIZING PLOTS FOR ALL REGIONS

Atlantic:

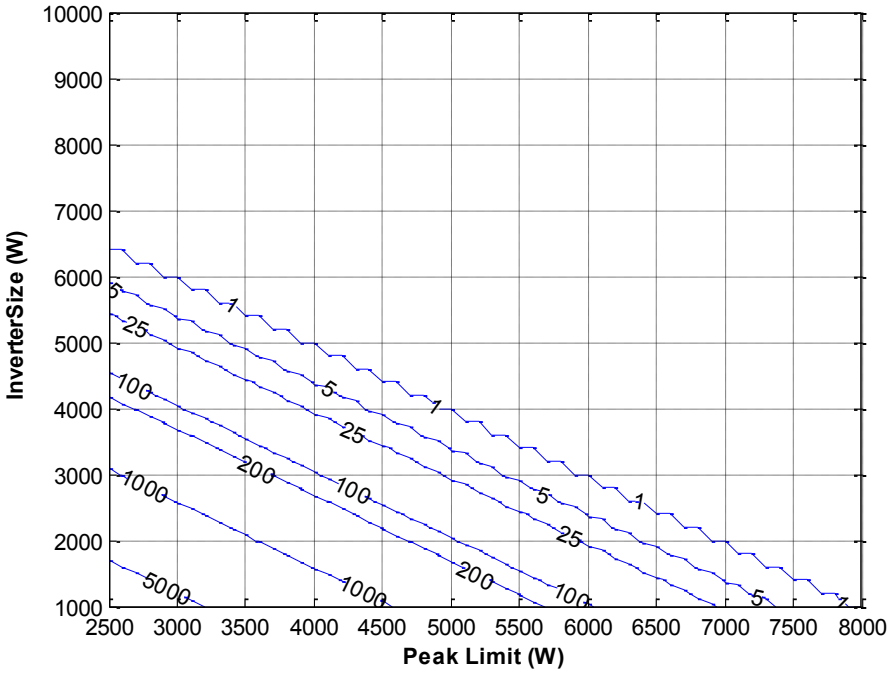

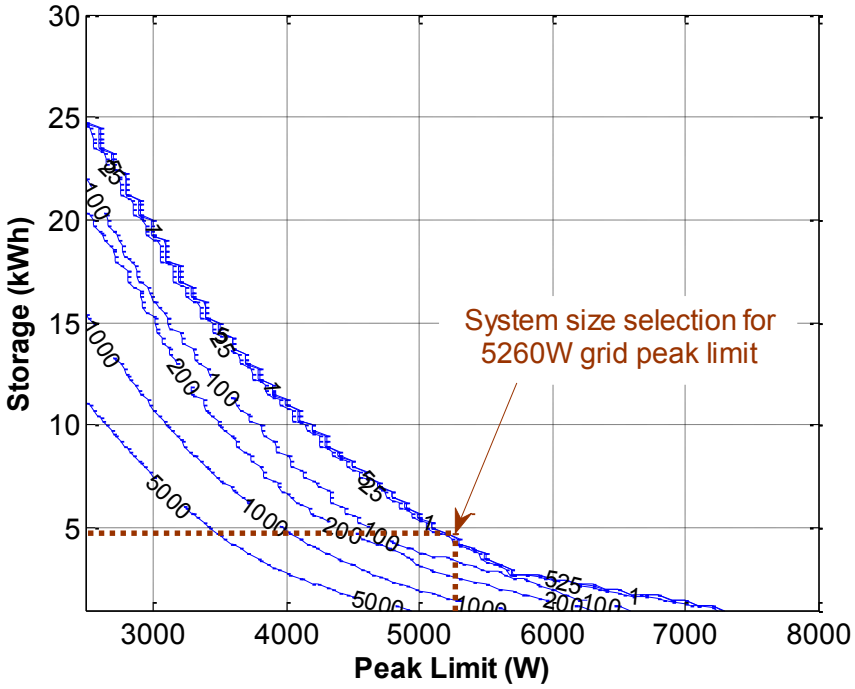

British Columbia:

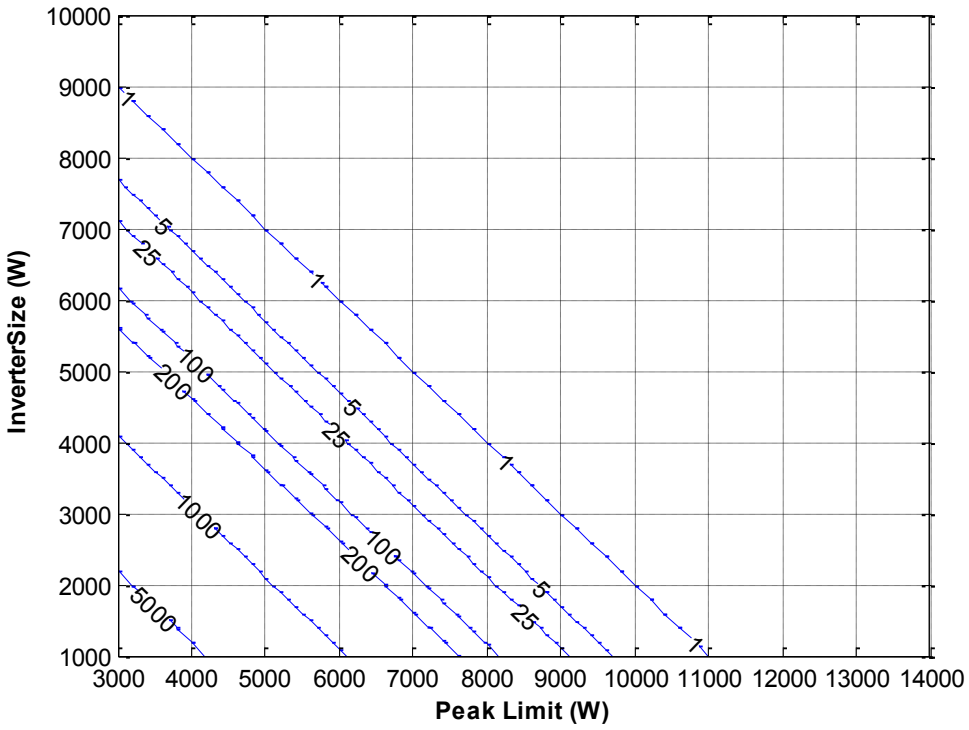

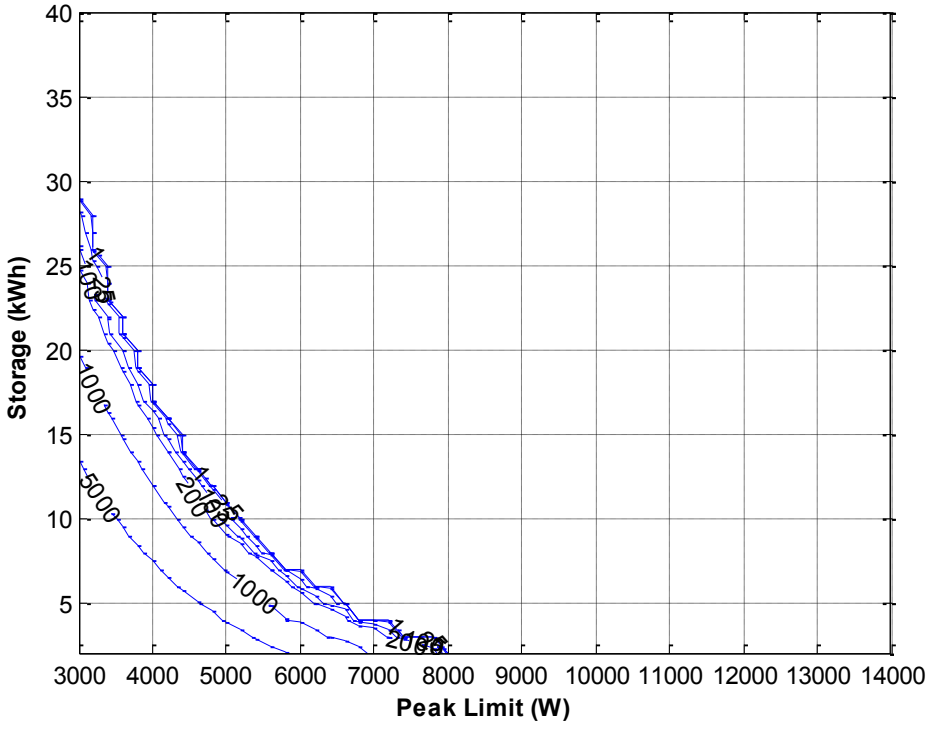

Ontario:

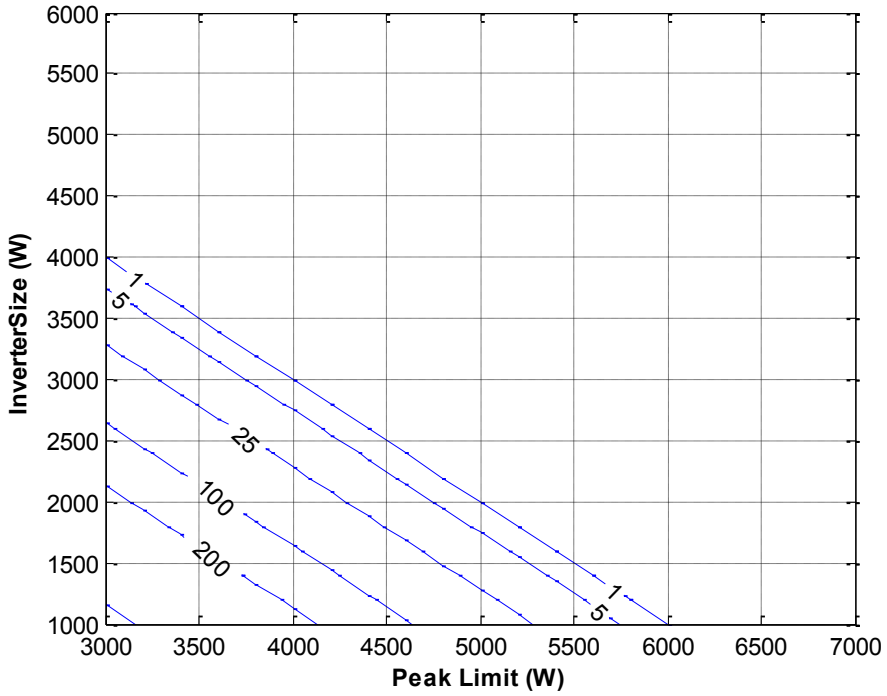
InverterSize (W)
Peak Limit (W)
6000
5500
5000
4500
4000
3500
3000
2500
2000
1500
1000
3000
3500
4000
4500
5000
5500
6000
6500
7000
1
5
25
100
200
1
5

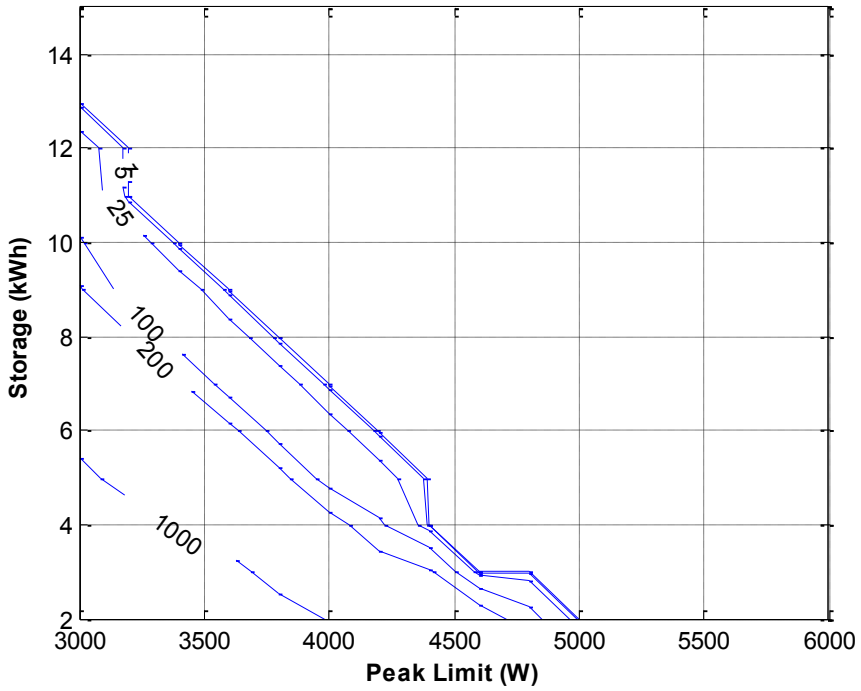
Storage (kWh)
Peak Limit (W)
14
12
10
8
6
4
2
3000
3500
4000
4500
5000
5500
6000
1
5
25
100
200
1000

Prairies:

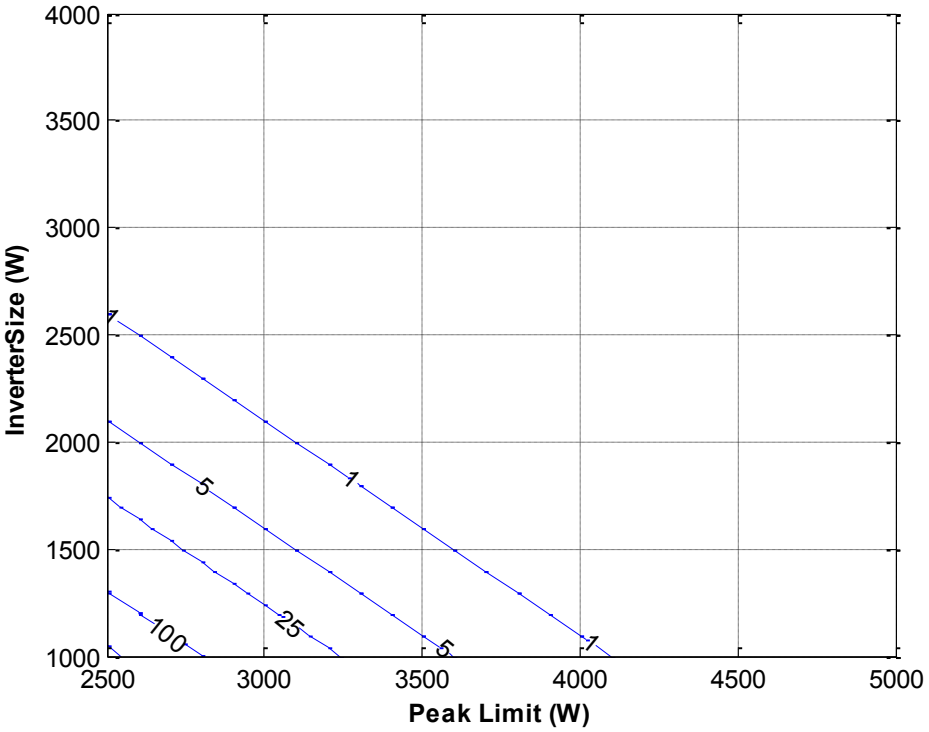
InverterSize (W)
Peak Limit (W)
4000
3500
3000
2500
2000
1500
1000
2500
3000
3500
4000
4500
5000
1
5
25
100

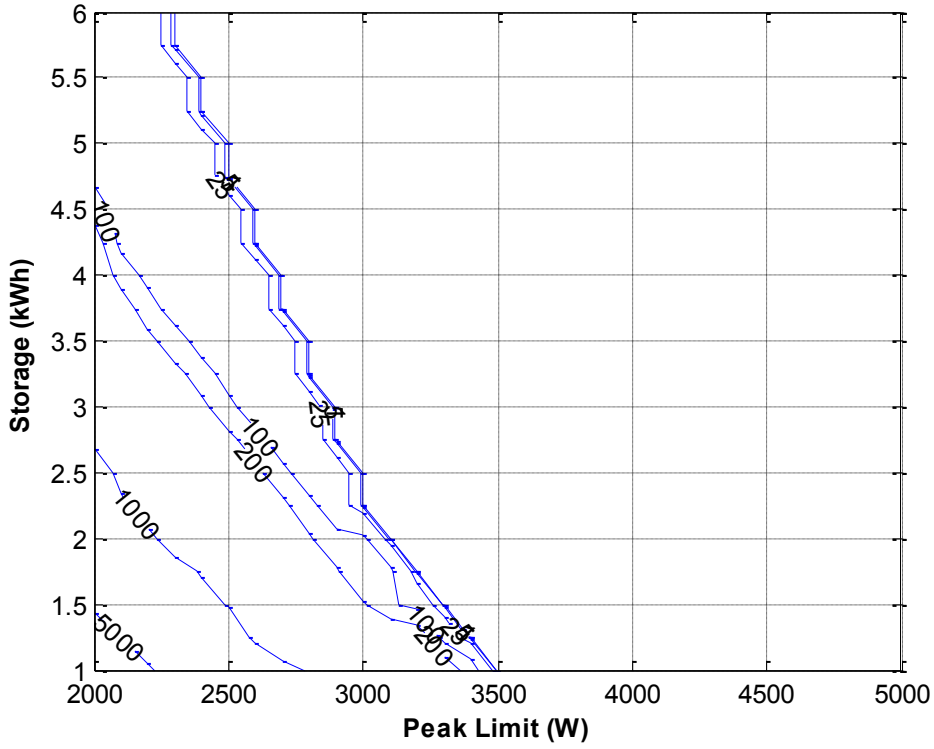
Storage (kWh)
Peak Limit (W)
6
5.5
5
4.5
4
3.5
3
2.5
2
1.5
1
2000
2500
3000
3500
4000
4500
5000
25
100
200
1000
5000

Quebec:

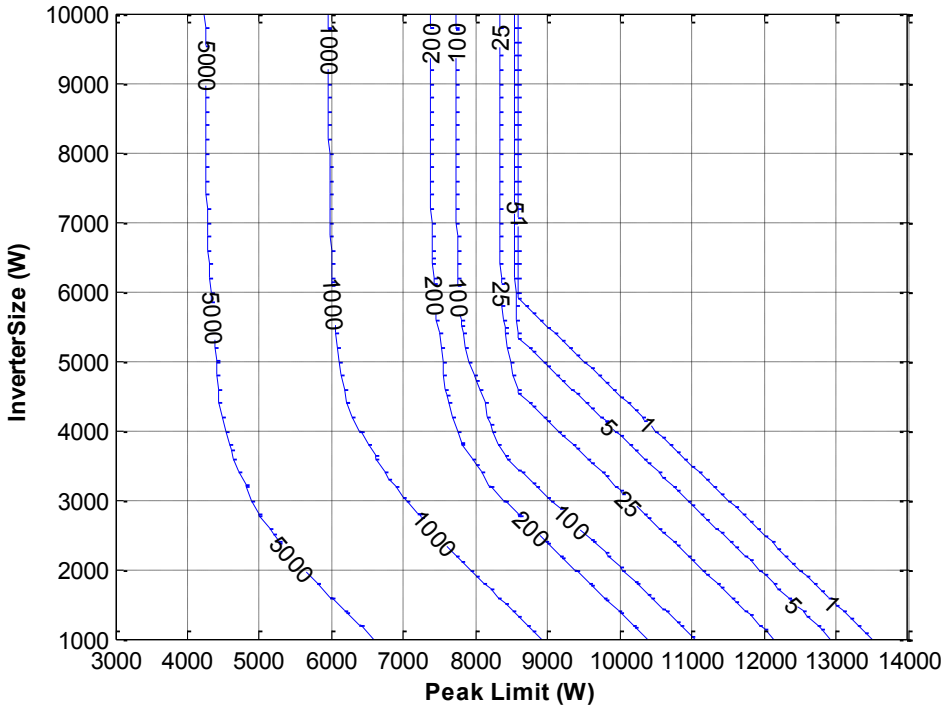
InverterSize (W)
Peak Limit (W)
10000
9000
8000
7000
6000
5000
4000
3000
2000
1000
3000 4000 5000 6000 7000 8000 9000 10000 11000 12000 13000 14000
5000
1000
200
100
25
5
1

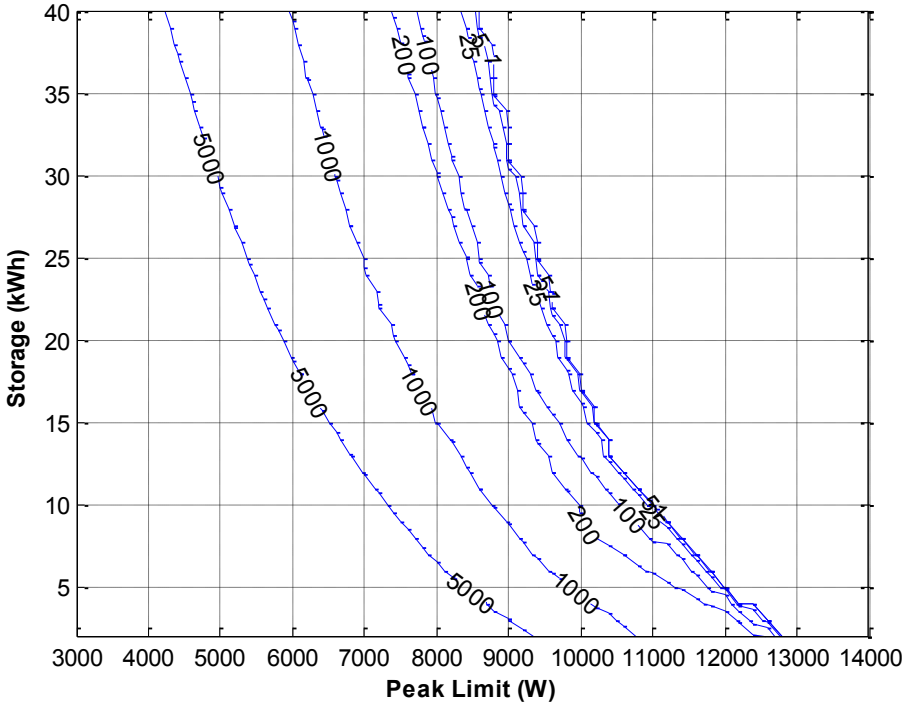
Storage (kWh)
Peak Limit (W)
40
35
30
25
20
15
10
5
3000 4000 5000 6000 7000 8000 9000 10000 11000 12000 13000 14000
5000
1000
200
100
25
5
1

APPENDIX C CR1000 POWER AND CURRENT CONTROL DISCHARGE AND FULL RECHARGE CODE

CRBasic Code:

```
'Power or Current specified discharge and full charge code

'Author: Jason Leadbetter
'For the 72V LiFePO4 battery bank used to run peak shaving and calibrate and validate a lithium iron phosphate model
'Date: July 24, 2012

‘To discharge input a CC value (in amps) if you want constant current discharge, or a DischargeP (in watts) value if you want a power discharge, these values can be changed at any point during discharge and the output will change on the next scan cycle (within one second). To activate the discharge once a CC or DischargeP value is set simply set Discharge = 1

‘To charge simply set Charge = 1. This will activate the stepped charge cycle to full charge

SequentialMode
'Declare Constants
Const cells=22
Const scantime = 1000

'Declare Public Variables
Public PTemp,batt_volt 'CR1000 vars
Public Vshunt,Volt(cells),DCA,DCAtemp,DCAh,DCEnergy,DCPower, DCPoweravg 'Shunt and cell voltages
Public Vtemp(cells+1), Vgnd 'temp vars to avoid bogus screen readout results, Vgnd accounts for Vdivider ground offset
Public Vmult(cells+1) =
{146.2854913,145.6141689,145.4054998,145.3972493,145.3252534,145.6553049,144.6608129,145.0598143,308.7397394,309.1669
432,309.0210906,309.0216273,309.1954143,309.1280000,308.7927795,308.674955,451.6407431,451.9609533,452.95000,453.31148
87,453.1732231,453.450917,453.1935739} 'Vdiv multipliers
Public MUXS0,MUXS1,MUXS2 'variables to set MUX signal states
Public MUXCH(8,3) = {0,0,0, 1,0,0, 0,1,0, 1,1,0, 0,0,1, 1,0,1, 0,1,1, 1,1,1} 'where MUXCH(channel desired 1-8 but MUX is 0-7, S0 S1 S2) '18 was .884,
Public VACa,AACa,VACb,AACb,PACa,PACb,EACa,EACb,VACavg,AACtotal,PACtotal,EACtotal 'WN volt and current readouts (AC side)
Public MCstart = 0,MCkey = 0,MCaccel = 0 'Motor Controller (MC) control variables. Start then pause then key then control acceleration
Public ACplug(4) 'AC box charger plugs control
Public NEXa,NEXb 'NEXTEC charger controls, both off = ramp down, one on = stay the same, both on = ramp up current
Public WTN_Response = 0
Public WTN_Reset = 0
Public EShutdown = 0
Public IO16Status, AO4Status
Public IO16ports(8),AO4ports(4)
Public IO16portdirectionset(16) = {0,0,0,0,0,0,0,0,1,1,1,1,1,1,1,1} '0 is output, 1 is input
Public usemodbus = 1
Public Vpack, Vcellavg(cells),Vmax(2),Vmin(2),Vminavg
Public Charge,Chargestage = 1, Rcount, Icount, skip 'Charge controls whether charging is active or not, Rcount is reduction count, I count is increase count, skip is to adjust for delay in V reading reduction becuase of averaging and 4*scan issues
Public Discharge, DischargeP, Setdischarge, Seek, change, tempDP, ChgC, CC, DCAavg, Vmaxavg, 'Discharge controls whether discahrge is active or not, DischargeP is the desired output power from the batteries, Set discharge is a flag to allow the throttle function to set the MCaccel variable based on DischargeP value,
'Seek is a flag that triggers throttle tuning to activate, change prevents a sudden change in voltage due to on/off  from creating false voltages readings that shut the system down, tempDP assists in determining change, ChgC is the constant current level above which the nextec charger "holds steady" until the votlage limit is reached after which ChgC is decreased
'CC is the varible to set the desired constant current output level,
Public tcs = 4 , w
Public T(4),tch,Tmax(2)


'Declare Other Variables
'Example:
'Dim Counter
Dim m=0
Dim n=0
```

```
Dim p=0

'Define Data Tables
DataTable (LithiumReadings,1,-1)
	DataInterval(0,scantime*3,mSec,-1)
	Average(1,Vpack,FP2,False)
	Average(1,Tmax,FP2,False)
	Average(1,DCA,FP2,False)
	Sample(1,DCAh,FP2)
	Average(1,DCPower,FP2,False)
	Sample(1,DCEnergy,FP2)
	Sample(1,MCaccel,FP2)
	Maximum(1,Vmax(1),FP2,False,False)
	Minimum(1,Vmin(1),FP2,False,False)
	Average(22,Volt(),FP2,False)


EndTable

'Define Subroutines
'Sub
	'EnterSub instructions here
'EndSub

'Main Program
BeginProg

 ModBusMaster (WTN_Response, Com4, 19200, 1, 06, 50, 1604, 1, 1, 20) 'Current transformer Amps Phase A
	ModBusMaster (WTN_Response, Com4, 19200, 1, 06, 50, 1605, 1, 1, 20) 'Current transformer Amps Phase B

 SDMIO16 (IO16portdirectionset,IO16Status,1,96,0,0,0,0,1,0)

 'SCAN START ------------------------------------------------------------------------
	Scan (scantime,mSec,0,0)
		PanelTemp (PTemp,250)
		Battery (batt_volt)

		'Voltage readings ------------------------------------------------------------------------

		VoltDiff(DCAtemp,1,mV250,3,False,0,_60Hz,-3,0)

		DCAtemp = ABS(DCAtemp)

		'done to prevent false voltage readings that shutdown the system
		If DCAtemp < (ABS(DCA) - 3) OR DCAtemp > (ABS(DCA) + 3)
		change = 2
		EndIf

		VoltDiff(DCA,1,mV250,3,False,0,_60Hz,-3,0)
		DCAh = DCAh + (DCA)/(3600*1000/scantime)

		If change <> 0
		change = change - 1
		EndIf

		'cell temperatures
		TCSe(T(),4,mV2_5C,7,TypeT,PTemp,True,0,_60Hz,1,0)

		MaxSpa(Tmax(),4,T)

		'overtemp protection
		If Tmax(1) > 40
		Charge = 0
		Discharge = 0
		EndIf

		'change = 0 means there wasn't a recent sharp change in desired current or power that will result in incorrect
voltage readings causing system shutdown for safety reasons
		If change = 0
```

```
VoltSe(Vgnd,1,mV2_5,4,False,0,_60Hz,1,0)

'cycle through and measure all voltages, based on voltage diveder setup and MUX channel codes specified
earlier
For m = 1 To 8

 MUXS0 = MUXCH(m,1)
 MUXS1 = MUXCH(m,2)
 MUXS2 = MUXCH(m,3)

 PortSet(4,MUXS0)
 PortSet(5,MUXS1)
 PortSet(6,MUXS2)

 If m < 8
 VoltSe(Vtemp(8-m),1,mV250,1,False,0,_60Hz,1,-Vgnd)
 EndIf

 VoltSe(Vtemp(16-m),1,mV250,2,False,0,_60Hz,1,-Vgnd)

 VoltSe(Vtemp(24-m),1,mV250,3,False,0,_60Hz,1,-Vgnd)

 Next

'Voltage calculations----------------------------------------------------------



For n = 1 To (cells+1)
  Vtemp(n) = Vtemp(n) * Vmult(n) /1000
Next

'For n = 1 To 23
'               Vpack(n) = Vtemp(n)
'Next

Vpack = Vtemp(cells+1)

Volt(1) = Vtemp(1)

For p = 2 To 11
  Volt(p) = Vtemp(p) - Vtemp(p-1)
Next

Volt(12) = Vtemp(13) - Vtemp(12)

For p = 14 To 23
  Volt(p-1) = Vtemp(p) - Vtemp(p-1)
Next

'AvgRun(Vcellavg(),cells,Volt(),2)

EndIf ' change = 0 if

MaxSpa(Vmax(),cells,Volt) 'Checks highest cell voltage
MinSpa(Vmin(),22,Volt) 'Checks lowest cell voltage
AvgRun(Vmaxavg,1,Vmax,4)
AvgRun(Vminavg,1,Vmin,4)

If Vmaxavg > 3.74
NEXa = 0
NEXb = 0
ACplug(1) = 0
ACplug(2) = 0
ACplug(3) = 0
ACplug(4) = 0
Charge = 0
EndIf
```

```
'Power/energy code ------------------------------------------------

DCPower = DCA * Vpack
AvgRun(DCPoweravg,1,DCPower,5)
AvgRun(DCAavg,1,DCA,5)
DCEnergy = DCEnergy + DCA * Vpack /(3600*1000/scantime)

'Discharging Code ----------------------------------------------------------------------------------------

If Discharge = 1

If MCkey = 0
Charge = 0 ' done to prevent simultaneous charge/discharge
MCkey = 1
skip = 6
EndIf

If MCkey = 1 AND MCstart = 0 AND skip = 0
MCstart = 1
'skip included to allow time to turn on MC
skip = 7
Setdischarge = 1
EndIf

If CC > 0
DischargeP = CC * 71
EndIf

If tempDP <> DischargeP
Setdischarge = 1
EndIf

tempDP = DischargeP

'Set discharge code ---

If Setdischarge = 1 AND skip = 0

If DischargeP <=50
MCaccel = 0
ElseIf DischargeP < 165
MCaccel = (DischargeP + 149.583)/0.29678
ElseIf DischargeP >= 165
MCaccel = (1.45963 + SQR(2.13052 - (.0060672 * (-87.392 - DischargeP))))/0.00303362
EndIf

Setdischarge = 0
Seek = 1
skip = 5/(scantime/1000)

EndIf ' skip = 0 AND setdischarge endif

'Constant current discharge code and throttle tuning----

If CC > 0

If Seek = 1 AND -DCA < (CC - 1.2) AND skip = 0
MCaccel = MCaccel + 3
skip = 5/(scantime/1000)
EndIf

If Seek = 1 AND -DCA > (CC + 1.2) AND skip = 0
MCaccel = MCaccel - 3
skip = 5/(scantime/1000)
EndIf

If Seek = 1 AND -DCA < (CC + 1.2) AND -DCA > (CC - 1.2)
Seek = 2
skip = 5/(scantime/1000)
EndIf
```

```
If Seek = 2 AND skip = 0

 If -DCAavg < (CC - .08)
 MCaccel = MCaccel + 1
 skip = 5/(scantime/1000)
 EndIf

 If -DCAavg > (CC + .1)
 MCaccel = MCaccel - 1
 skip = 5/(scantime/1000)
 EndIf

 If -DCAavg > (CC + 1.2) OR -DCAavg < (CC - 1.2)
 Seek = 1
 skip = 3/(scantime/1000)
 EndIf

EndIf ' seek = 2 endif

EndIf ' CC > 0 endif


'Power specified discharge code and throttle tuning --------

If CC = 0

If Seek = 1 AND -DCPower < (DischargeP - 30) AND skip = 0
MCaccel = MCaccel + 3
skip = 3/(scantime/1000)
EndIf

If Seek = 1 AND -DCPower > (DischargeP + 30) AND skip = 0
MCaccel = MCaccel - 3
skip = 3/(scantime/1000)
EndIf

If Seek = 1 AND -DCPoweravg < (DischargeP + 30) AND -DCPoweravg > (DischargeP - 30)
Seek = 2
skip = 5/(scantime/1000)
EndIf

If Seek = 2 AND skip = 0

 If -DCPoweravg < (DischargeP - 6)
 MCaccel = MCaccel + 1
 skip = 5/(scantime/1000)
 EndIf

 If -DCPoweravg > (DischargeP + 8)
 MCaccel = MCaccel - 1
 skip = 5/(scantime/1000)
 EndIf

EndIf

EndIf ' CC = 0 endif


If skip <> 0
skip = skip -1
EndIf

EndIf 'discharge = 0 endif



'discharge shutoff conditions check

If Discharge = 0
```

```
MCaccel = 0
MCkey = 0
MCstart = 0
EndIf

If Vminavg < 2.6 ' undervoltage protection and discharge shutoff
MCaccel = 0
Discharge = 0
skip = 0
seek = 0
EndIf


'Charging Code ----------------------------------------------------------------------------------

If Charge = 1

If Chargestage = 1

Discharge = 0 ' simultaneous charge/discharge prevention
ACplug(1) = 1
ACplug(2) = 1
ACplug(3) = 1
ACplug(4) = 1
NEXa = 1
NEXb = 1
Icount = 28/(scantime/1000)
Chargestage = 2
skip = 4
EndIf

If Chargestage = 2
NEXa = 1

If Icount = 0
NEXb = 0
Else
  NEXb = 1
  Icount = Icount - 1
EndIf

If Vmax(1) > 3.68 AND skip = 0
Chargestage = 3
'Icount = 28/(scantime/1000)
skip = 3/(scantime/1000)
'ChgC = 8
EndIf

If skip <> 0
skip = skip - 1
EndIf

EndIf



If Chargestage = 3

'If ACplug(4) = 1
'ACplug(4) = 0
If ACplug(3) = 1
  ACplug(3) = 0
  Chargestage = 2
  ElseIf ACplug (2) = 1
    ACplug(2) = 0
    Chargestage = 2
    Else
      Chargestage = 4
                                    'Icount = 28/(scantime/1000)
                                    skip = 6/(scantime/1000)
```

```
                                        ChgC = 8
                                ACplug(2)=0
                                        ACplug(3)=0
                                        ACplug(4)=0
endif

Endif ' chargestage 3 endif


If Chargestage = 4

If skip = 0

If Vmax > 3.68

If ChgC = 8
ChgC = 4
Rcount = 5/(scantime/1000)
Chargestage = 5
ElseIf ChgC = 4
        ChgC = 3
        Rcount = 5/(scantime/1000)
        Chargestage = 5
        ElseIf ChgC = 3
                ChgC = 2
                Rcount = 5/(scantime/1000)
                Chargestage = 5
                ElseIf ChgC = 2
                        ChgC = 1
                        Rcount = 5/(scantime/1000)
                        Chargestage = 5
                        ElseIf ChgC = 1
                                ChgC = .5
                                Rcount = 5/(scantime/1000)
                                Chargestage = 5
                                Else
                                        Charge = 0
EndIf

EndIf ' vmax > # endif
EndIf 'skip = 0 endif

If skip <> 0
skip = skip - 1
EndIf

EndIf ' Chargestage 4 endif



If Chargestage = 5

If Rcount <> 0
NEXa = 0
NEXb = 0
EndIf

If Rcount = 0

If DCA < ChgC
NEXa = 1
NEXb = 1
Else
        NEXa = 1
        NEXb = 0
        Chargestage = 4
        skip = 3/(scantime/1000)
EndIf

Endif ' Rcount = 0 endif
```

```
If Rcount <> 0
Rcount = Rcount - 1
EndIf

EndIf ' chargestage 5 endif



EndIf ' charge = 1 endif

If Charge = 0
Chargestage = 1
ACplug(1) = 0
ACplug(2) = 0
ACplug(3) = 0
ACplug(4) = 0
NEXa = 0
NEXb = 0
EndIf



'Wattnode Readings---------------------------------------------------

"If usemodbus = 1
"ModBusMaster (WTN_Response, Com4, 19200, 1, 04, VACa, 1019, 1, 1, 20) 'Phase A AC voltage (V-rms)
"ModBusMaster (WTN_Response, Com4, 19200, 1, 04, VACb, 1021, 1, 1, 20) 'Phase B AC voltage (V-rms)
'ModBusMaster (WTN_Response, Com4, 19200, 1, 04, AACa, 1163, 1, 1, 20) 'Phase B AC current (A-rms)
'ModBusMaster (WTN_Response, Com4, 19200, 1, 04, AACb, 1165, 1, 1, 20) 'Phase B AC current (A-rms)
"ModBusMaster (WTN_Response, Com4, 19200, 1, 04, PACa, 1011, 1, 1, 20) 'Phase A AC discharge power
(W)
"ModBusMaster (WTN_Response, Com4, 19200, 1, 04, PACb, 1013, 1, 1, 20) 'Phase B AC discharge power
(W)
'ModBusMaster (WTN_Response, Com4, 19200, 1, 04, EACa, 1101, 1, 1, 20) 'Phase A Energy (kWh)
'ModBusMaster (WTN_Response, Com4, 19200, 1, 04, EACb, 1103, 1, 1, 20) 'Phase B Energy (kWh)
'ModBusMaster (WTN_Response, Com4, 19200, 1, 04, EACtotal, 1001, 1, 1, 20) 'Total AC energy (kWh)
"EndIf


If WTN_Reset = 1 Then
        ModBusMaster (WTN_Response, Com4, 19200, 1, 06, 1, 1620, 1, 1, 1) 'Reset the WattNode energy
registers
        EACa = 0
        EACb = 0
        EACtotal = 0
        WTN_Reset = 0 'Put reset back to zero as operation is complete
EndIf

'SDM port controls ----------------------------------------

IO16ports(1) = MCkey
IO16ports(2) = MCstart
IO16ports(3) = ACplug(1)
IO16ports(4) = ACplug(2)
IO16ports(5) = ACplug(3)
IO16ports(6) = ACplug(4)
IO16ports(7) = NEXa
IO16ports(8) = NEXb
AO4ports(1) = MCaccel 'AO4 uses units mV as input unit, not volts


SDMIO16(IO16Ports,IO16Status,1,94,0,0,0,0,1,0)
SDMAO4(AO4ports,1,0)

'SDMIO16 is at SDM address 1
'SDMAO4 is at ADM address 0

If Status.WatchdogErrors <> 0 Then
        Discharge = 0
```

```
                Charge = 0
        EndIf

        CallTable LithiumReadings
        NextScan
        'EndSequence


EndProg
```

APPENDIX D BESS OPERATION CODE FOR LIFEPO4 MODEL VALIDATION

CRBasic Code:

```
‘To operate simply input Discharge = 1, this will take the discharge through 5 minute discharges of power levels specified in the schedule(75) variable

SequentialMode
'Declare Constants
Const cells=22
Const scantime = 1000

'Declare Public Variables
Public PTemp,batt_volt 'CR1000 vars
Public Vshunt,Volt(cells),DCA,DCAtemp,DCAh,DCEnergy,DCPower, DCPoweravg 'Shunt and cell voltages
Public Vtemp(cells+1), Vgnd 'temp vars to avoid bogus screen readout results, Vgnd accounts for Vdivider ground offset
Public Vmult(cells+1) =
{146.2854913,145.6141689,145.4054998,145.3972493,145.3252534,145.6553049,144.6608129,145.0598143,308.7397394,309.1669
432,309.0210906,309.0216273,309.1954143,309.1280000,308.7927795,308.674955,451.6407431,451.9609533,452.95000,453.31148
87,453.1732231,453.450917,453.1935739} 'Vdiv multipliers
Public MUXS0,MUXS1,MUXS2 'variables to set MUX signal states
Public MUXCH(8,3) = {0,0,0, 1,0,0, 0,1,0, 1,1,0, 0,0,1, 1,0,1, 0,1,1, 1,1,1} 'where MUXCH(channel desired 1-8 but MUX is 0-7, S0 S1 S2) '18 was .884,
Public VACa,AACa,VACb,AACb,PACa,PACb,EACa,EACb,VACavg,AACtotal,PACtotal,EACtotal 'WN volt and current readouts (AC side)
Public MCstart = 0,MCkey = 0,MCaccel = 0 'Motor Controller (MC) control variables. Start then pause then key then control acceleration
Public ACplug(4) 'AC box charger plugs control
Public NEXa,NEXb 'NEXTEC charger controls, both off = ramp down, one on = stay the same, both on = ramp up current
Public WTN_Response = 0
Public WTN_Reset = 0
Public EShutdown = 0
Public IO16Status, AO4Status
Public IO16ports(8),AO4ports(4)
Public IO16portdirectionset(16) = {0,0,0,0,0,0,0,0,1,1,1,1,1,1,1,1} '0 is output, 1 is input
Public usemodbus = 1
Public Vpack, Vcellavg(cells),Vmax(2),Vmin(2),Vminavg
Public Charge,Chargestage = 1, Rcount, Icount, skip 'Rcount is reduction count, I count is increase count, skip is to adjust for delay in V reading reduction becuase of averaging and 4*scan issues
Public Discharge, DischargeP, Setdischarge, Seek, change, tempDP, ChgC, CC, DCAavg, Vmaxavg, SDcount
Public tcs = 4 , w
Public T(4),tch,Tmax(2)
Public waitcount, DCAhdiff, stop, dischargestep, chargestep
Public schedule(75) =
{561.7197,768.6299,757.7402,831.5498,979.1699,882.3701,0,0,0,0,0,0,0,0,0,0,0,0,2047.6001,1979.8398,1832.2197,0,0,0,0,0,883.580
1,172.4902,0,0,0,0,0,0,0,0,0,0,0,0,0,0,0,0,1475.27,1378.4702,1184.8701,1176.3999,1108.6401,1203.02,1130.4199,0,0,1106.2202,1578.
1201,1930.23,1822.54,1896.3501,1898.77,2443.27,313.6699,305.2002,92.2402,0,0,0,0,0,0,683.9302,673.04,746.8501,398.3701,0,0,0
}
Public peakshave, tick, schplace

'Declare Other Variables
'Example:
'Dim Counter
Dim m=0
Dim n=0
Dim p=0

'Define Data Tables
DataTable (LithiumReadings,1,-1)
        DataInterval(0,scantime*3,mSec,-1)
        'Minimum(1,batt_volt,FP2,0,False)
        'Sample(1,PTemp,FP2)
        'Sample(1,Vpack),FP2)
```

```
            Average(1,Vpack,FP2,False)

            Average(1,Tmax,FP2,False)

            'Sample(1,DCA,FP2)
            Average(1,DCA,FP2,False)

            Sample(1,DCAh,FP2)
            'Sample(1,DCPower,FP2)
            Average(1,DCPower,FP2,False)

            Sample(1,DCEnergy,FP2)

            'Sample(1,change,FP2)

            'Sample(1,ChgC,FP2)

            'Sample(1,Charge,Boolean)
            'Sample(1,Discharge,Boolean)
            'Sample(1,DischargeP,FP2)

            Sample(1,MCaccel,FP2)

            'Sample(1,ACplug(1),Boolean)
            'Sample(1,ACplug(2),Boolean)
            'Sample(1,ACplug(3),Boolean)

            'Sample(1,Chargestage,FP2)
            'Sample(1,Rcount,FP2)
            'Sample(1,Icount,FP2)
            'Sample(1,skip,FP2)

            Maximum(1,Vmax(1),FP2,False,False)
            Minimum(1,Vmin(1),FP2,False,False)

            'Sample(1,NEXa,FP2)
            'Sample(1,NEXb,FP2)

            'Average(22,Volt(),FP2,False)

            'Sample(22,Vcellavg(),FP2)
            'Sample(1,MCkey,FP2)
            'Sample(1,MCStart,FP2)

EndTable

'Define Subroutines
'Sub
            'EnterSub instructions here
'EndSub

'Main Program
BeginProg

  ModBusMaster (WTN_Response, Com4, 19200, 1, 06, 50, 1604, 1, 1, 20) 'Current transformer Amps Phase A
            ModBusMaster (WTN_Response, Com4, 19200, 1, 06, 50, 1605, 1, 1, 20) 'Current transformer Amps Phase B

  SDMIO16 (IO16portdirectionset,IO16Status,1,96,0,0,0,0,1,0)
  stop = 1
  tick = 299
  schplace = 0

  'SCAN START ------------------------------------------------------------------------
            Scan (scantime,mSec,0,0)
                        PanelTemp (PTemp,250)
                        Battery (batt_volt)

                        'Voltage readings ------------------------------------------------------------------------

                        VoltDiff(DCAtemp,1,mV250,3,False,0,_60Hz,-3,0)
```

```
DCAtemp = ABS(DCAtemp)

If DCAtemp < (ABS(DCA) - 3) OR DCAtemp > (ABS(DCA) + 3)
change = 2
EndIf

VoltDiff(DCA,1,mV250,3,False,0,_60Hz,-3,0)
DCAh = DCAh + (DCA)/(3600*1000/scantime)



If peakshave = 1

 tick = tick + 1

 Discharge = 1

 If DischargeP = 0
 Discharge = 0
 EndIf

 If tick = 300

  tick = 1

  schplace = schplace + 1

  If schplace = 76
   schplace = 75
   peakshave = 0
   Discharge = 0
  EndIf

  DischargeP = schedule(schplace)

 EndIf

EndIf




If dischargestep = 1

DCAhdiff = DCAhdiff + ABS((DCA)/(3600*1000/scantime))

If DCAhdiff > 5
Discharge = 0
waitcount = 10800
DCAhdiff = 0
EndIf

If waitcount > 0
waitcount = waitcount - 1
EndIf

If waitcount = 0 AND stop = 0
Discharge = 1
EndIf

EndIf



If chargestep = 1
```

```
DCAhdiff = DCAhdiff + ABS((DCA)/(3600*1000/scantime))

If DCAhdiff > 5
Charge = 0
waitcount = 10800
DCAhdiff = 0
EndIf

If waitcount > 0
waitcount = waitcount - 1
EndIf

If waitcount = 0 AND stop = 0
Charge = 1
EndIf

EndIf




If change <> 0
change = change - 1
EndIf

TCSe(T(),4,mV2_5C,7,TypeT,PTemp,True,0,_60Hz,1,0)

MaxSpa(Tmax(),4,T)

If Tmax(1) > 42
Charge = 0
Discharge = 0
EndIf


If change = 0

VoltSe(Vgnd,1,mV2_5,4,False,0,_60Hz,1,0)

For m = 1 To 8

  MUXS0 = MUXCH(m,1)
  MUXS1 = MUXCH(m,2)
  MUXS2 = MUXCH(m,3)

  PortSet(4,MUXS0)
  PortSet(5,MUXS1)
  PortSet(6,MUXS2)

  If m < 8
  VoltSe(Vtemp(8-m),1,mV250,1,False,0,_60Hz,1,-Vgnd)
  EndIf

  VoltSe(Vtemp(16-m),1,mV250,2,False,0,_60Hz,1,-Vgnd)

  VoltSe(Vtemp(24-m),1,mV250,3,False,0,_60Hz,1,-Vgnd)

  Next

'Voltage calculations-------------------------------------------------------



For n = 1 To (cells+1)
  Vtemp(n) = Vtemp(n) * Vmult(n) /1000
Next
```

```
'For n = 1 To 23
'               Vpack(n) = Vtemp(n)
'Next

Vpack = Vtemp(cells+1)

Volt(1) = Vtemp(1)

For p = 2 To 11
  Volt(p) = Vtemp(p) - Vtemp(p-1)
Next

Volt(12) = Vtemp(13) - Vtemp(12)

For p = 14 To 23
  Volt(p-1) = Vtemp(p) - Vtemp(p-1)
Next

'AvgRun(Vcellavg(),cells,Volt(),2)

EndIf ' change = 0 if

MaxSpa(Vmax(),cells,Volt) 'Checks highest cell voltage
MinSpa(Vmin(),22,Volt) 'Checks lowest cell voltage
AvgRun(Vmaxavg,1,Vmax,4)
AvgRun(Vminavg,1,Vmin,4)

If Vmaxavg > 3.74
NEXa = 0
NEXb = 0
ACplug(1) = 0
ACplug(2) = 0
ACplug(3) = 0
ACplug(4) = 0
Charge = 0
stop = 1
chargestep = 0
EndIf


'Power/energy code ------------------------------------------------

DCPower = DCA * Vpack
AvgRun(DCPoweravg,1,DCPower,5)
AvgRun(DCAavg,1,DCA,5)
DCEnergy = DCEnergy + DCA * Vpack /(3600*1000/scantime)

'Discharging Code ---------------------------------------------------------------------------------------

If Discharge = 1

'dischargestep = 1
'stop = 0

If MCkey = 0
Charge = 0 ' done to prevent simultaneous charge/discharge
MCkey = 1
skip = 3
EndIf

If MCkey = 1 AND MCstart = 0 AND skip = 0
MCstart = 1
skip = 3
Setdischarge = 1
EndIf

If CC > 0
DischargeP = CC * 71
EndIf
```

```
If tempDP <> DischargeP
Setdischarge = 1
EndIf

tempDP = DischargeP

If Setdischarge = 1 AND skip = 0

If DischargeP <=50
MCaccel = 0
ElseIf DischargeP < 165
MCaccel = (DischargeP + 149.583)/0.29678
ElseIf DischargeP >= 165
MCaccel = (1.45963 + SQR(2.13052 - (.0060672 * (-87.392 - DischargeP))))/0.00303362
EndIf

Setdischarge = 0
Seek = 1
skip = 5/(scantime/1000)

EndIf ' skip = 0 AND setdischarge endif


If CC > 0

If Seek = 1 AND -DCA < (CC - 1.2) AND skip = 0
MCaccel = MCaccel + 3
skip = 5/(scantime/1000)
EndIf

If Seek = 1 AND -DCA > (CC + 1.2) AND skip = 0
MCaccel = MCaccel - 3
skip = 5/(scantime/1000)
EndIf

If Seek = 1 AND -DCA < (CC + 1.2) AND -DCA > (CC - 1.2)
Seek = 2
skip = 5/(scantime/1000)
EndIf

If Seek = 2 AND skip = 0

 If -DCAavg < (CC - .08)
 MCaccel = MCaccel + 1
 skip = 5/(scantime/1000)
 EndIf

 If -DCAavg > (CC + .1)
 MCaccel = MCaccel - 1
 skip = 5/(scantime/1000)
 EndIf

 If -DCAavg > (CC + 1.2) OR -DCAavg < (CC - 1.2)
 Seek = 1
 skip = 3/(scantime/1000)
 EndIf

EndIf ' seek = 2 endif

EndIf ' CC > 0 endif


If CC = 0

If Seek = 1 AND -DCPower < (DischargeP - 30) AND skip = 0
MCaccel = MCaccel + 4
skip = 3/(scantime/1000)
EndIf

If Seek = 1 AND -DCPower > (DischargeP + 30) AND skip = 0
```

```
MCaccel = MCaccel - 4
skip = 3/(scantime/1000)
EndIf

If Seek = 1 AND -DCPoweravg < (DischargeP + 30) AND -DCPoweravg > (DischargeP - 30)
Seek = 2
skip = 5/(scantime/1000)
EndIf

If Seek = 2 AND skip = 0

 If -DCPoweravg < (DischargeP - 6)
 MCaccel = MCaccel + 2
 skip = 5/(scantime/1000)
 EndIf

 If -DCPoweravg > (DischargeP + 8)
 MCaccel = MCaccel - 2
 skip = 5/(scantime/1000)
 EndIf

EndIf

EndIf ' CC = 0 endif


If skip <> 0
skip = skip -1
EndIf

EndIf 'discharge = 0 endif




If Discharge = 0
MCaccel = 0
MCkey = 0
MCstart = 0
EndIf

If Vminavg < 2.6 ' undervoltage protection and discharge shutoff
MCaccel = 0
Discharge = 0
skip = 0
Seek = 0
DCAhdiff = 0
stop = 1
dischargestep = 0
EndIf
```

----------CODE WAS TRUNCATED AFTER THIS POINT AS IT IS IDENTICAL TO THE CC or power code ----------

APPENDIX E PEAK SHAVING MODEL MATLAB CODE FOR ATLANTIC REGION USING THE DEVELOPED LIFEPO4 BATTERY MODEL

The following MatLab code calls on several csv files which are save in the Renewable Energy Storage Lab dropbox repository and are available on request.

```
%  Inverter and BESS capacity sizing for residential peak shaving system

clear all, close all, fclose all;

%%%%%%%%%%%%%%%%%%%%%%%%%%%%%%%%%%%%%%%%%%%%%%%%%%%%%%%%%%%%%%%%%%%%%%%%%%%%%%%
%%%%%%%%%%%%%%%%%%%%%%%%JASON PEAK SHAVING CODE %%%%%%%%%%%%%%%%%%%%%%%%%%%%%%%
%%%%%%%%%%%%%%%%%%%%%%%%%%%%%%%%%%%%%%%%%%%%%%%%%%%%%%%%%%%%%%%%%%%%%%%%%%%%%%%


%for p = 1:5
    %p=1;
p = 1; %Atlantic region only so only p = 1
clear ElecLoad BatteryOptions InverterSize PeakOptions Failures StoredEn

if p==1
m=1;
n=2;
o=3;
region='AT';
ElecLoad = csvread('ATelectotal.csv');
PeakSelection=5260;
end

%if p==2

    %p=3;

%m=4;
%n=5;
%o=6;
%region='QC';
%ElecLoad = csvread('QCelectotal.csv');
%PeakSelection=10910;
%end

if p==2
m=7;
n=8;
o=9;
region='OT';
ElecLoad = csvread('OTelectotal.csv');
PeakSelection=2870;
end

if p==3
m=10;
n=11;
o=12;
region='OT-AC';
ElecLoad = csvread('OTACelectotal.csv');
PeakSelection=3790;
end

if p==4
m=13;
n=14;
```

```
o=15;
region='PR';
ElecLoad = csvread('PRelectotal.csv');
PeakSelection=2600;
end

if p==5
m=16;
n=17;
o=18;
region='BC';
ElecLoad = csvread('BCelectotal.csv');
PeakSelection=6630;
end


%length(ATload)
time = 0 : 5 : 525595;
hour = csvread('hours.csv');


%clear BatteryOptions InverterSize PeakOptions Failures StoredEn


  % Battsize vs. Inverter Size @ 98.5%tile
  % Cap Dispatchable Generation:
  Dispatch        = ElecLoad;
  NightStart      = 1;
  NightEnd        = 6;

  %% bat,inv

  BatteryOptions  = 2:1:9;
  InverterSize    = 2800:400:6000;
  PeakOptions     = PeakSelection;

  yeardischargeenergy = 0;
  yearchargeenergy = 0;

  %Failures  = zeros(length(BatteryOptions), length(InverterSize));
  %PowerFailures = zeros(length(BatteryOptions), length(InverterSize));

  Failures  = zeros(length(BatteryOptions), length(InverterSize));
  Efficiency = zeros(length(BatteryOptions), length(InverterSize));



    %% bat,peak

  BatteryOptions  = 1:1:20;
  InverterSize    = 15000;
  PeakOptions     = 2000:200:8000;

  yeardischargeenergy = 0;
  yearchargeenergy = 0;

  %Failures  = zeros(length(BatteryOptions), length(InverterSize));
  %PowerFailures = zeros(length(BatteryOptions), length(InverterSize));

  Failures  = zeros(length(BatteryOptions), length(PeakOptions));
  Efficiency = zeros(length(BatteryOptions), length(PeakOptions));

  for IS  = 1 : length(InverterSize)
      InvCap  = InverterSize(IS);

  for BB = 1 : length(BatteryOptions)
      %disp(['Working on Battery option ' num2str(BB) ' of '
num2str(length(BatteryOptions))])
      StorCap   = BatteryOptions(BB);%*.7; %Allows for 15 - 85% SOC operation
      StorCap
```

```
  for MP = 1 : length(PeakOptions)
      MaxPeak = PeakOptions(MP);
      MaxPeak




      DOD = zeros(size(Dispatch));
      StoredEn = zeros(size(Dispatch));
      StoredEn(1) = StorCap;
      DOD(1) = 0.15;

      for t = 2 : length(StoredEn)
        % night check for charging
        if hour(t) >= NightStart && hour(t) < NightEnd
          %set to prevent skipping if its fully charged
          DOD(t) = DOD(t-1);
          if DOD(t-1) > .15
          % Charge
          Power = 0;
          [DOD1,EnStored,Vpack1,ReqCurrent1,Ah] = lithiumcharge(StorCap,DOD(t-1),Power,-
1);%-1 to indicate charge

          DOD(t) = DOD1;
          %StoredEn(t) = EnStored1;
          yearchargeenergy = yearchargeenergy + (Vpack1 * -ReqCurrent1)/12;%energy per
timestep (/12 ofor 5 min timesteps)
          end
          % Ensure it doesn't "overcharge"
          %if DOD(t) < 0;
          %    DOD(t) = 0;
          %end

        else%if hour(t) < NightStart || hour(t) >= NightEnd

        if DOD(t-1) > .85
            Failures(BB,MP) = Failures(BB,MP) + 1;
            DOD(t) = DOD(t-1);
        %    StoredEn(t) = 0;
        % Check if over peak value
        elseif Dispatch(t) < MaxPeak
          % Do Nothing
          DOD(t) = DOD(t-1);
        elseif Dispatch(t) > MaxPeak
          % discharge to peak shave
          % check to ensure not over inverter size
          if InvCap < (Dispatch(t) - MaxPeak)

            Power = InvCap;
            [DOD1,EnStored,Vpack1,ReqCurrent1,Ah] = lithiumcharge(StorCap,DOD(t-
1),Power,0);
            DOD(t) = DOD1;
            yeardischargeenergy = yeardischargeenergy + Power/12;

            Failures(BB,MP) = Failures(BB,MP) + 1;

          else
            Power = Dispatch(t) - MaxPeak;
            [DOD1,EnStored,Vpack1,ReqCurrent1,Ah] = lithiumcharge(StorCap,DOD(t-
1),Power,0);
            DOD(t) = DOD1;
            yeardischargeenergy = yeardischargeenergy + Power/12;
          end
        end
        end
      end

      Efficiency(BB,MP) = yeardischargeenergy/yearchargeenergy;
      yeardischargeenergy = 0;
```

```
      yearchargeenergy = 0;

  end
  end
  %'done'
  %pause(inf)

  figure(n)
  subplot(1,1,1)
%  [C, h] = contour(InverterSize, BatteryOptions, Failures, ...
%    'b', 'LineWidth', 1);
  [C, h] = contour(PeakOptions, BatteryOptions, Failures, ...
    [1 5 25 100 200 1000 5000], 'b', 'LineWidth', 1);
  set(h,'ShowText', 'on', 'TextStep', get(h,'LevelStep')*1)
  %set(gca, 'ylim', [0 10])
  xlabel('Peak Limit (W)', 'FontWeight', 'Bold')
  ylabel('Storage Capacity (kWh)', 'FontWeight', 'Bold')
  %title(['Battery Storage (kWh): ',int2str(StorCap/.7)], 'FontWeight', 'Bold')
  set(n,'Name',region)
  grid on

  hold on

  end



  for MP = 1 : length(PeakOptions)
      MaxPeak = PeakOptions(MP);
      %MP=1

  for BB = 1 : length(BatteryOptions)
      %disp(['Working on Battery option ' num2str(BB) ' of '
num2str(length(BatteryOptions))])
    StorCap   = BatteryOptions(BB);%*.7; %Allows for 15 - 85% SOC operation
    StorCap

  for IS  = 1 : length(InverterSize)
      InvCap  = InverterSize(IS);
      InvCap

      DOD = zeros(size(Dispatch));
      StoredEn = zeros(size(Dispatch));
      StoredEn(1) = StorCap;
      DOD(1) = 0.15;

      for t = 2 : length(StoredEn)
        % night check for charging
        if hour(t) >= NightStart && hour(t) < NightEnd
          %set to prevent skipping if its fully charged
          DOD(t) = DOD(t-1);
          if DOD(t-1) > .15
          % Charge
          Power = 0;
          [DOD1,EnStored,Vpack1,ReqCurrent1,Ah] = lithiumcharge(StorCap,DOD(t-1),Power,-
1);%-1 to indicate charge

          DOD(t) = DOD1;
          %StoredEn(t) = EnStored1;
          yearchargeenergy = yearchargeenergy + (Vpack1 * -ReqCurrent1)/12;%energy per
timestep (/12 ofor 5 min timesteps)
          end
          % Ensure it doesn't "overcharge"
          %if DOD(t) < 0;
          %    DOD(t) = 0;
          %end

        else%if hour(t) < NightStart || hour(t) >= NightEnd

        if DOD(t-1) > .85
            Failures(BB,IS) = Failures(BB,IS) + 1;
```

```
            DOD(t) = DOD(t-1);
        %    StoredEn(t) = 0;
        % Check if over peak value
        elseif Dispatch(t) < MaxPeak
          % Do Nothing
          DOD(t) = DOD(t-1);
        elseif Dispatch(t) > MaxPeak
          % discharge to peak shave
          % check to ensure not over inverter size
          if InvCap < (Dispatch(t) - MaxPeak)

            Power = InvCap;
            [DOD1,EnStored,Vpack1,ReqCurrent1,Ah] = lithiumcharge(StorCap,DOD(t-
1),Power,0);
            DOD(t) = DOD1;
            yeardischargeenergy = yeardischargeenergy + Power/12;

            Failures(BB,IS) = Failures(BB,IS) + 1;

          else
            Power = Dispatch(t) - MaxPeak;
            [DOD1,EnStored,Vpack1,ReqCurrent1,Ah] = lithiumcharge(StorCap,DOD(t-
1),Power,0);
            DOD(t) = DOD1;
            yeardischargeenergy = yeardischargeenergy + Power/12;
          end
        end
        end
      end

      Efficiency(BB,IS) = yeardischargeenergy/yearchargeenergy;
      yeardischargeenergy = 0;
      yearchargeenergy = 0;

  end
  end
  %'done'
  %pause(inf)

  figure(m)
  subplot(1,1,1)
%  [C, h] = contour(InverterSize, BatteryOptions, Failures, ...
%    'b', 'LineWidth', 1);
  [C, h] = contour(InverterSize, BatteryOptions, Failures, ...
    [1 5 25 100 200 1000 5000], 'b', 'LineWidth', 1);
  set(h,'ShowText', 'on', 'TextStep', get(h,'LevelStep')*1)
  %set(gca, 'ylim', [0 10])
  xlabel('InverterSize (W)', 'FontWeight', 'Bold')
  ylabel('Storage Capacity (kWh)', 'FontWeight', 'Bold')
  %title(['Battery Storage (kWh): ',int2str(StorCap/.7)], 'FontWeight', 'Bold')
  set(m,'Name',region)
  grid on

  hold on

  end
```

APPENDIX F CALIBRATED LIFEPO4 BATTERY MODEL CODE

MatLab Code:

```
Calibrated lithium model code
%%%%%%%%%%%%%%%%%%%%%%%%%%%%%%%%%%%%%%%%%%%%%%%%%%%%%%%%%%%%%%%%%%%%%%%%%%%%%%%
%%%%%%%%%%%%%%%%%%%%%%%%%%JASONS LITHIUM MODEL CODE %%%%%%%%%%%%%%%%%%%%%%%%%%%
%%%%%%%%%%%%%%%%%%%%%%%%%%%%%%%%%%%%%%%%%%%%%%%%%%%%%%%%%%%%%%%%%%%%%%%%%%%%%%%

%%%%Adapted from Gao Model%%%%

function [DOD1,EnStored,Vpack1,ReqCurrent1,Ah] =
lithiumcharge(refcapkwh,DOD0,Power,Current)

%battery model parameters:
%refcurrent = 7 %A
%refcap = 83.9; %Ah
alphacurrent = [1 15 25 35 45 55];

%alpha = [1 1 1 1 1];

alpha = [1.05 1.035 1.0121 1 0.985 0.967];
cellvolts = 3.43;
cells = 22;

battvolts = cellvolts * cells;

err = 50;

low = .062;

refcap = refcapkwh*1000/72;

Power = Power/0.93; % 93% discharge eff in power elecs

if (Power == 0) && (Current == 0)
    Vpack1 = 50;
    DOD1 = DOD0;
    ReqCurrent1 = 0;
    EnStored = refcap;
    Ah = 0;
    return
end



if (Power > 0) || (Current > 0)

    if Current == 0 %power input code
    easy = 0;

    ReqCurrentavg = Power/(battvolts-5);
    alphaavg = interp1(alphacurrent,alpha,ReqCurrentavg,'spline');
    n=0;

    while (abs(err) > .2)

    if n > 0
    ReqCurrentavg = ReqCurrent2;
    alphaavg = interp1(alphacurrent,alpha,ReqCurrentavg,'spline');
    end

    DOD1 = DOD0 + ReqCurrentavg*(5/60)/(refcap*alphaavg);

    if DOD1 > 1.05
        DOD1 = 1.01;
        EnStored = 0;
```

```
        Vpack1 = 72;
        ReqCurrent1 = 0;
        Ah = 0;
        return
    end

    if ReqCurrentavg < 20
        Res1 = .0625;
    elseif ReqCurrentavg >= 20 && ReqCurrentavg < 35
        Res1 = .059;
    elseif ReqCurrentavg >= 35
        Res1 = low;
    end

    Respack = Res1; % *cells

    Vdroppackcurrentavg = (ReqCurrentavg - 35) * Respack;

    DODavg = (DOD0 + DOD1)/2;

    OCVavg = -79.76*DODavg^6 +178.6*DODavg^5 - 145.3*DODavg^4 + 50.72*DODavg^3 -
12.35*DODavg^2 - 0.9733*DODavg + 70.92;

    OCVpackavg = OCVavg; % * cells
    Vpackavg = OCVpackavg - Vdroppackcurrentavg;

    ReqCurrent2 = Power/Vpackavg;
    err = (ReqCurrentavg - ReqCurrent2)/ReqCurrent2*100;

    n=n+1;

    end %while end


    else %current input code
    ReqCurrentavg = Current;
    easy = 1;
    err = 50;
    alphaavg = interp1(alphacurrent,alpha,ReqCurrentavg,'spline');
    DOD1 = DOD0 + ReqCurrentavg*(5/60)/(refcap*alphaavg);
    end % current = 0 if



    if (abs(err) < .2)

    OCV1 = -79.76*DOD1^6 +178.6*DOD1^5 - 145.3*DOD1^4 + 50.72*DOD1^3 - 12.35*DOD1^2 -
0.9733*DOD1 + 70.92;
    OCVpack1 = OCV1; % * cells;

    if ReqCurrentavg < 20
        Res1 = .0625;
    elseif ReqCurrentavg >= 20 && ReqCurrentavg < 35
        Res1 = .059;
    elseif ReqCurrentavg >= 35
        Res1 = low;
    end

    Respack1 = Res1; % * cells;

    Vpack1 = ((OCVpack1+35*Respack1) + (sqrt((OCVpack1+35*Respack1)^2-
4*Respack1*Power)))/2;

    ReqCurrent1 = Power/Vpack1;

    EnStored = refcap * (1 - DOD1);
    Ah = ReqCurrentavg/12;

    end %if abserr2 final calculations end

    %n=n+1;
```

```
    if (easy == 1) %easy becuase have current as input

        OCV1 = -79.76*DOD1^6 +178.6*DOD1^5 - 145.3*DOD1^4 + 50.72*DOD1^3 - 12.35*DOD1^2 -
0.9733*DOD1 + 70.92;
        OCVpack1 = OCV1; % * cells;

    if ReqCurrentavg < 20
        Res1 = .0625;
    elseif ReqCurrentavg >= 20 && ReqCurrentavg < 35
        Res1 = .059;
    elseif ReqCurrentavg >= 35
        Res1 = low;
    end


    Respack1 = Res1; % * cells;

    Vpack1 = OCVpack1 - (ReqCurrentavg-35) * Respack1;
    ReqCurrent1 = ReqCurrentavg;
    EnStored = refcap * (1 - DOD1);
    Ah = Current/12;
    end


else % charge else

    depletion = refcap * (DOD0);

    if DOD0 > -.025

        if depletion > 19.1
            ReqCurrent1 = - 33.85;
            DOD1 = DOD0 + 0.977 * ReqCurrent1*(5/60)/(refcap);
            EnStored = refcap * (1 - DOD1);
            En = refcap * DOD1;
            Ah = ReqCurrent1/12;
            chargepower = 0.0239 * En^2 - 4.9829 * En + 2742.8;
            Vpack1 = chargepower/-ReqCurrent1;
            ReqCurrent1 = - 33.85; %95% charge eff in power elecs
        else
            ReqCurrent1 = - 20.80;
            DOD1 = DOD0 + 0.977 * ReqCurrent1*(5/60)/(refcap);
            EnStored = refcap * (1 - DOD1);
            En = refcap * DOD1;
            Ah = ReqCurrent1/12;
            chargepower = 0.1769 * En^2 - 9.8522 * En + 1727.9;
            Vpack1 = chargepower/-ReqCurrent1;
            ReqCurrent1 =  - 20.80/0.95; %95% charge eff in power elecs
        end

    else
        ReqCurrent1 = 0;
        DOD1 = DOD0;
        EnStored = refcap;
        Ah = 0;
        OCV1 = 19.93*DOD1^5 - 55.59*DOD1^4 + 46.27*DOD1^3 - 18.25*DOD1^2 +1.745*DOD1 +
72.93;
        Vpack1 = OCV1;

    end

end



end %function end
```